



## Durham E-Theses

---

### *Investigations into Radical Reactions Facilitated by $\eta^6$ -Ruthenium Intermediate Complexes*

BRADLEY, DAVID

#### How to cite:

---

BRADLEY, DAVID (2019) *Investigations into Radical Reactions Facilitated by  $\eta^6$ -Ruthenium Intermediate Complexes*, Durham theses, Durham University. Available at Durham E-Theses Online: <http://etheses.dur.ac.uk/13362/>

#### Use policy

---

The full-text may be used and/or reproduced, and given to third parties in any format or medium, without prior permission or charge, for personal research or study, educational, or not-for-profit purposes provided that:

- a full bibliographic reference is made to the original source
- a [link](#) is made to the metadata record in Durham E-Theses
- the full-text is not changed in any way

The full-text must not be sold in any format or medium without the formal permission of the copyright holders.

Please consult the [full Durham E-Theses policy](#) for further details.



**Investigations into Radical Reactions  
Facilitated by  $\eta^6$ -Ruthenium Intermediate  
Complexes**

**David Bradley**

A thesis submitted for the degree of Master of Science

Department of Chemistry

**October 2019**

# Abstract

$\eta^6$ -Coordination of arenes to transition metals results in a significant alteration of arene properties. While reactions incorporating stoichiometric metals are common, those that proceed by transient  $\pi$ -coordination are less so. A recently developed hydrodeiodination protocol is believed to react *via*  $\eta^6$ -arene intermediate ruthenium complexes, and this offers the opportunity to develop new reactions that are mediated by this type of coordination bonding.

Firstly, an intramolecular radical cyclisation reaction was investigated. Initially tested under optimised hydrodeiodination conditions, purification was difficult and so a better solvent alternative was found. Optimisation of base, catalyst, solvent, time, and temperature returned a maximum yield of only 8% with  $[\text{RuCp}]^+$  catalyst, mainly as a result of large amounts of alkene hydrogenation and isomerisation occurring in very short reaction times. Synthesis of sterically hindered alkenes showed that trisubstituted alkenes were significantly more resistant to these reactions.

Secondly, a ruthenium-catalysed iodide to bromide halogen exchange protocol is described. Optimisations found  $[\text{RuCp}^*]^+$  as the best catalyst, with yields of 51% for unsubstituted iodobenzene. Electron deficient arenes were tolerated better, with a yield of 57% for the formation of 4-bromoacetophenone. The reaction mechanism remains unclear, with evidence suggesting that it might proceed *via* an oxidative addition or  $\text{S}_{\text{N}}\text{Ar}$ -type mechanism.

# Statement of Copyright

The copyright of this thesis rests with the author. No quotation from it should be published without the author's prior written consent and information derived from it should be acknowledged.

# Acknowledgements

First and foremost, I would like to thank Dr James W. Walton for his expertise, assistance and guidance over the past year, and for allowing me to carry out this project in his group. Secondly, I want to thank all the current and past members of the Walton, McGonigal and Avestro groups that I have had the pleasure of knowing. Finally, I want to thank my Mam, Dad and brothers for being so supportive.

# Abbreviations

2-MeTHF	2-methyltetrahydrofuran
AIBN	azobisisobutyronitrile
b.p	boiling point
CDCl <sub>3</sub>	deuterated chloroform
CH <sub>2</sub> Cl <sub>2</sub>	dichloromethane
CMD	concerted metalation deprotonation
COSY	correlation spectroscopy
Cp	cyclopentadienyl
Cp*	pentamethylcyclopentadienyl
d	doublet
DABCO	1,4-diazabicyclo[2.2.2]octane
DBU	1,8-Diazabicyclo[5.4.0]undec-7-ene
dd	doublet of doublets
ddq	doublet of doublets of quartets
DDQ	2,3-dichloro-5,6-dicyano-1,4-benzoquinone
ddt	doublet of doublets of triplets
δ	delta
DMA	N,N-dimethylacetamide
DMF	N,N-dimethylformamide
dq	doublet of quartets
dt	doublet of triplets of triplets
equiv	equivalents
ESI-MS	electrospray ionisation – mass spectrometry
Et	ethyl

Et <sub>2</sub> O	diethylether
EtOAc	ethyl acetate
GCMS	gas chromatography – mass spectrometry
HMBC	hetronuclear multiple bond correlation
HOMO	highest occupied molecular orbital
HSQC	heteronuclear single quantum coherence
LUMO	lowest unoccupied molecular orbital
m	multiplet
m/z	mass/charge
Me	methyl
MeCN	acetonitrile
MW	microwave
NBS	N-bromosuccinimide
NMR	nuclear magnetic resonance
<i>o</i>	<i>ortho</i>
<i>p</i>	<i>para</i>
Ph	phenyl
q	quartet
s	singlet
S <sub>E</sub> Ar	electrophilic aromatic substitution
sept.	septet
SET	single electron transfer
S <sub>N</sub> Ar	nucleophilic aromatic substitution
td	triplet of doublets
tdt	triplet of doublets of triplets
TEMPO	(2,2,6,6-tetramethylpiperidin-1-yl)oxyl

THF	tetrahydrofuran
UV	ultraviolet
VE	valence electrons
$\eta$	eta
$\pi$	pi

# Contents

1.	Introduction .....	8
1.1	$\pi$ -Arene Complexes .....	8
1.1.1	C-H Activation <i>via</i> $\pi$ -Arene Complexes.....	9
1.1.2	Nucleophilic Transformations <i>via</i> $\pi$ -Coordination.....	13
1.1.3	Reductive Dehalogenation mediated by $\pi$ -Coordination to Metals.....	20
1.2	Arene Exchange.....	21
1.2.1	Arene Exchange Mechanism .....	21
1.2.2	Transformations <i>via</i> Transient $\pi$ -Coordination of Arenes to Metals.....	24
1.2.3	Hydrodeiodination .....	27
1.3	Project Aims .....	29
2.	Radical Cyclisation <i>via</i> $\eta^6$ -Coordinated Intermediates.....	31
2.1	Introduction .....	31
2.1.1	Ruthenium-Catalysed Radical Cyclisation .....	32
2.2	Results and Discussion .....	34
2.2.1	Initial Results.....	34
2.2.2	Alkene Hydrogenation and Isomerism .....	41
2.2.3	Synthesis of a Hindered Alkene .....	47
2.3	Conclusions and Future Work .....	50
3.	Ruthenium-Catalysed Aromatic Halogen Exchange .....	51
3.1	Introduction .....	51
3.1.1	Transition Metal-Catalysed Halogen Exchange .....	52
3.1.2	Ruthenium-Catalysed Halogen Exchange .....	54
3.2	Results and Discussion .....	55
3.2.1	Initial Optimisations .....	55
3.2.2	Mechanistic Studies .....	61
3.3	Conclusions and Future Work .....	67
4.	Conclusions and Future Work .....	69
5.	Experimental.....	72
5.1	Experimental Procedures .....	72
5.1.1	General Procedures.....	72
5.2	Synthetic Procedures .....	72
6.	References .....	78



# 1. Introduction

## 1.1 $\pi$ -Arene Complexes

The discovery and structural determination of ferrocene in the mid-1900s ushered in a new era of chemistry that deals with the synthesis and reactivity of so called “sandwich” complexes.<sup>1-5</sup> Over the subsequent decades, these complexes have found wide-ranging applications, including molecular electronics, bioinorganic chemistry and catalysis.<sup>6,7</sup>

In contrast to the ionic cyclopentadienyl ligands of metallocenes, sandwich complexes can also be synthesised with neutral ligands such as benzene. Benzene can act as a 6-electron donor when bonding to metals through its  $\pi$ -system, as shown by E. O. Fisher in 1955 with the synthesis of the 18 electron complex bis(benzene)chromium.<sup>8</sup> This type of bonding is relatively strong and can be explained by molecular orbital interactions with metal d orbitals (Figure 1.1). The  $\pi$ -system of benzene has 6 molecular orbitals, 3 bonding, which are filled, and 3 antibonding. When bonding to metals through  $\eta^6$ -coordination, benzene forms a strong  $\sigma$ -interaction with the metal  $d_{z^2}$  orbital and weaker  $\pi$ -interactions between its HOMOs and metal  $d_{zx}$  and  $d_{yz}$ . In addition, backbonding from the metal into the LUMOs of benzene creates a  $\delta$ -interaction.

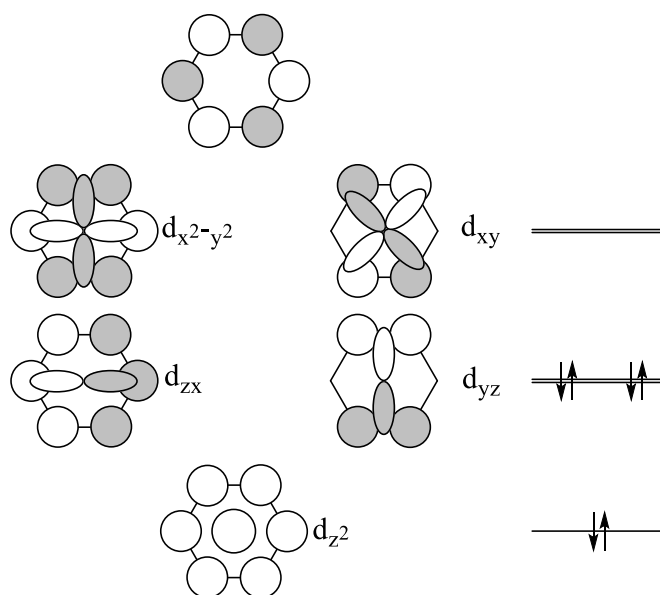


**Figure 1.1** Molecular orbitals of the  $\pi$  system in benzene and their interactions with metal d-orbitals.

Upon binding to metals through their  $\pi$ -system, arenes undergo significant changes in their reactivity (Figure 1.2). The electron-withdrawing effect of metals makes bound arenes relatively electron deficient, comparable to the arene having 1, 2 or 3 nitro groups.<sup>9</sup> As a result, the acidity of aryl and benzylic protons increases when arenes are coordinated. In addition, nucleophilic substitution on the ring is enhanced due to the increased electrophilicity of aromatic carbons, and for the same reason they are deactivated towards electrophilic aromatic substitutions. The bound metal also acts as a directing group, blocking approach from one face of the arene, offering the potential to control stereoselectivity. As a result, coordination can facilitate C-H activation, nucleophilic aromatic substitution ( $S_NAr$ ) and dehalogenation on the aromatic ring.

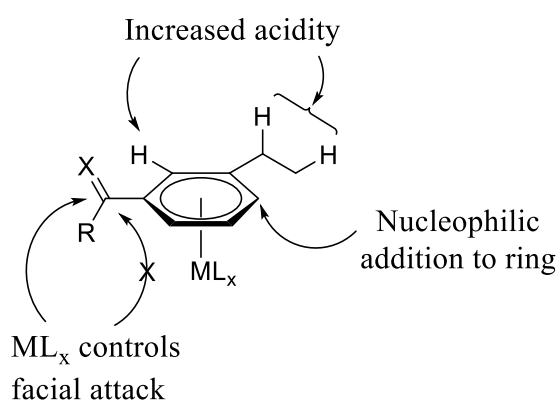
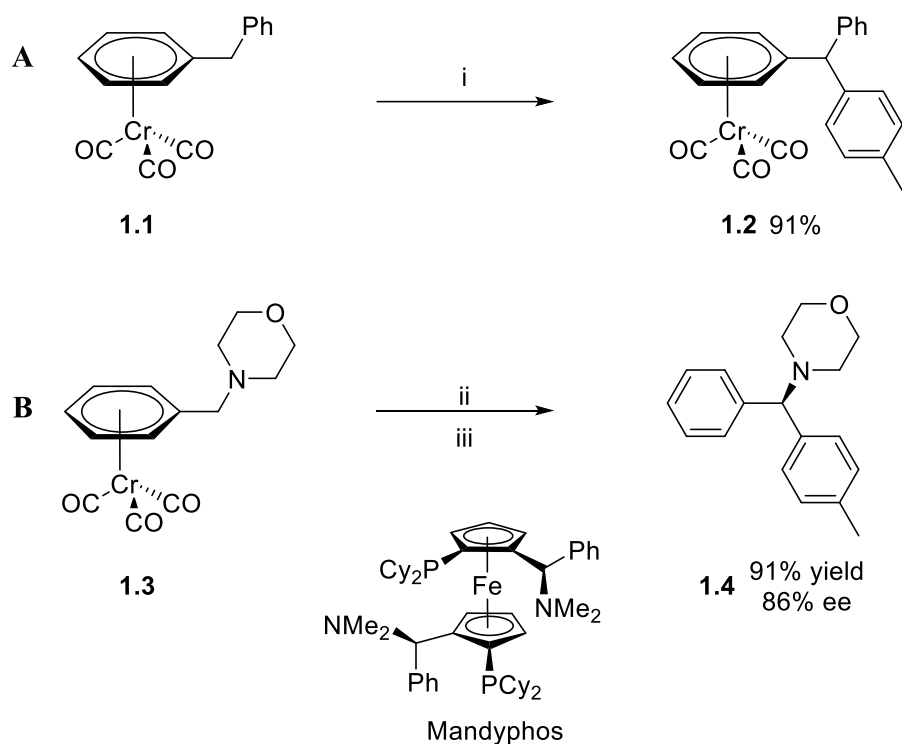


**Figure 1.2** Reactivity changes upon  $\eta^6$ -coordination of arenes to metals.

### 1.1.1 C-H Activation *via* $\pi$ -Arene Complexes

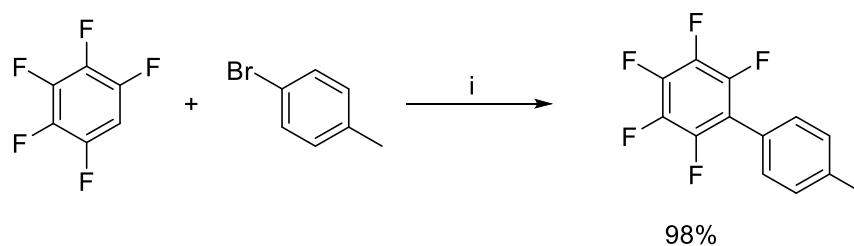
The electron withdrawing effect of chromium on  $\pi$ -coordinated arenes has been shown to increase benzylic C-H acidity.<sup>10</sup> In 2010, Walsh and co-workers exploited this reactivity to demonstrate palladium-catalysed cross-coupling of diphenylmethane tricarbonylchromium (**1.1**) with bromotoluene (Scheme 1.1 A).<sup>11</sup> Typically, synthesis of polyarylmethanes is achieved *via* Friedel-Crafts-type electrophilic aromatic substitutions, however this method is limited by the need for highly nucleophilic arenes. The use of a moderate base activates benzylic protons of  $[(\eta^6\text{-arene})\text{Cr}(\text{CO})_3]$  complexes, allowing oxidative addition of the complex to palladium. Building on these results, in 2012 the same research group published a palladium-catalysed asymmetric cross-coupling of  $\eta^6$ -coordinated benzylamines with aryl triflates (Scheme 1.1 B).<sup>12</sup> Benzylamine complex **1.3**, in the presence of a palladium catalyst and base, undergoes benzylic C-H activation with 4-bromotoluene. Dynamic kinetic resolution is achieved through a diastereoselective transmetalation step, which affords

enantioenriched arylated  $[(\eta^6\text{-benzylamine})\text{Cr}(\text{CO})_3]$  complex. Exposing a solution of product to air oxidises the complex, yielding free arylated benzylamine product (**1.4**).



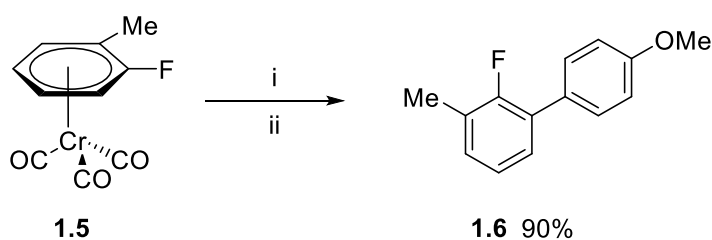
**Scheme 1.1 A** Synthesis of polyarylmethanes via chromium-mediated benzylic C-H activation. **B** Asymmetric cross-coupling of  $\pi$ -coordinated benzylamines with 4-bromotoluene. Reagents and conditions: (i)  $[\text{PdCl}_2(\text{PPh}_3)_2]$  (3 mol%) / 4-bromotoluene /  $\text{LiN}(\text{SiMe}_3)_2$  (1.5 equiv) / THF / 55 - 60 °C / 0.75 h; (ii)  $[\{\text{PdCl}(\text{allyl})\}_2]$  (4 mol%) / 4-bromotoluene /  $\text{LiN}(\text{SiMe}_3)_2$  (4 equiv) / Cy-Mandyphos (10 mol%) tol/THF/PhCl (40:60:2) / 24 °C / 12 h; (iii) hv / air.

Fagnou and co-workers showed that highly electron deficient arenes undergo C-H functionalisation *via* a concerted metalation deprotonation (CMD) mechanism and used this reaction to produce new C-C bonds (Scheme 1.2).<sup>13</sup> They showed that the acidity of the C-H bond is an important parameter in the C-H activation step. Evidence of this came from assessing the regioselectivity of C-H arylations, which showed that arylation occurs preferentially at positions that are *ortho* to fluorine atoms. In addition, competition studies between less- and more-substituted fluoroarenes revealed that those with more fluorine substitution are more reactive.



**Scheme 1.2** Pd-catalysed C-H activation of electron-deficient arenes via CMD-type mechanism. Reagents and conditions: (i)  $\text{Pd}(\text{OAc})_2$  (1-5 mol%) /  $\text{P}^t\text{Bu}_2\text{Me-HBF}_4$  (2-10 mol%) /  $\text{K}_2\text{CO}_3$  (1.1 equiv) / DMA / 120 °C.

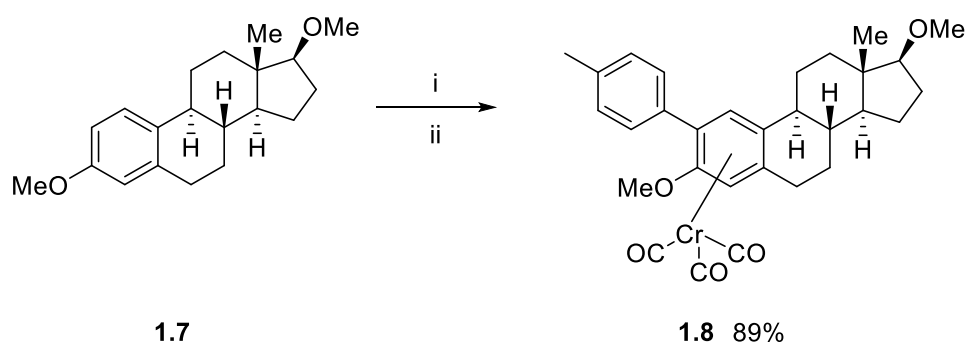
In 2013, Larrosa and co-workers reported the first example of  $\text{Cr}(\text{CO})_3$  as a reactivity enhancer for the aromatic Pd-catalysed C-H activation of monofluoroarenes (Scheme 1.3).<sup>14</sup> In competition experiments, they found that  $[(\eta^6\text{-2-fluorotoluene})\text{Cr}(\text{CO})_3]$  (**1.5**) is 6.7 times more reactive towards C-H activation than 1,3,5-trifluorobenzene and has a similar reactivity to pentafluorobenzene. The fluoroarene complex (**1.5**) is arylated *ortho* to the fluoro group in yields of up to 90% after oxidation by  $\text{MnO}_2$ , generating unbound product (**1.6**). In addition, they demonstrated that the product complex can be functionalised further by  $\text{S}_{\text{N}}\text{Ar}$  at the fluorine with a variety of nucleophiles. In attempts to arylate  $[(\eta^6\text{-benzene})\text{Cr}(\text{CO})_3]$ , they observed a yield of 42%, showing that even less electron-deficient arenes can undergo C-H activation upon  $\pi$ -coordination. However, calculations concluded that enhanced reactivity of  $\pi$ -complexes was due to bending of the C-H bond in rather than a direct result of increased acidity.



**Scheme 1.3** Chromium-mediated *ortho*-C-H arylation of fluoroarenes. Reagents and conditions: (i)  $\text{Pd}(\text{PPh}_3)_4$  (5 mol%) /  $\text{K}_2\text{CO}_3$  (2 equiv) /  $\text{Ag}_2\text{CO}_3$  (0.75 equiv) / 1- $\text{AdCO}_2\text{H}$  (0.5 equiv) / 4-iodoanisole (1.5 equiv) /  $\text{PhCH}_3$  / 60 °C / 24 h; (ii)  $\text{MnO}_2$  (3 equiv) /  $\text{AcOH}$  / RT / 30 min.

Following this, Larrosa extended the arylation scope to the more electron-rich anisoles.<sup>15</sup> Binding of the anisole to  $\text{Cr}(\text{CO})_3$  affords favourable properties for the arylation for two reasons: lower electron density of the arene disables  $\text{S}_{\text{E}}\text{Ar}$  pathways, and enhanced reactivity in CMD-type reactions as a result of out-of-plane C-H bending. Anisole derivatives are arylated *ortho* to alkoxy groups with excellent selectivity and yields of 64-93% for those

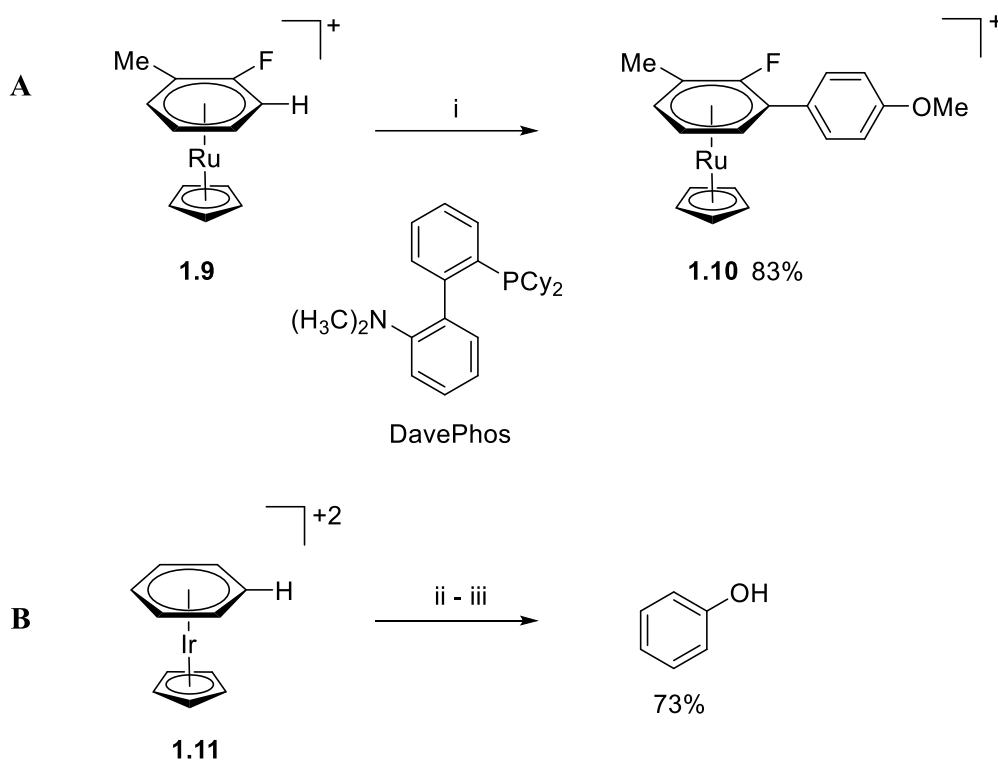
unaffected by steric hindrance. Additionally, electron-rich and electron-poor aryl iodides were tolerated to yield biaryls in excellent yields. Moreover, this arylation proceeds under mild conditions, offering the potential for late-stage functionalisations, as demonstrated by the arylation of  $[(\eta^6\text{-dimethylestrone})\text{Cr}(\text{CO})_3]$  (**1.7**) which achieved *ortho*-arylated product (**1.8**) in 89% yield (Scheme 1.4). In addition, rather than oxidising the complex, further transformations can be employed such as the Walsh benzylic C-H arylation. This was attempted, affording arylated product in 3:1 diastereomeric ratio and 57% yield. A significant drawback of this arylation procedure is that long reaction times (48 hours) are required.



**Scheme 1.4** *Ortho-arylation of  $[(\eta^6\text{-dimethylestrone})\text{Cr}(\text{CO})_3]$ . Reagents and conditions: (i)  $\text{Cr}(\text{CO})_6$  (1.3 equiv) /  $\text{Bu}_2\text{O}$  /  $\text{THF}$ ; (ii)  $\text{Pd}(\text{PPh}_3)_4$  (5 mol%) /  $\text{K}_2\text{CO}_3$  (2.5 equiv) /  $\text{Ag}_2\text{CO}_3$  (0.75 equiv) /  $1\text{-AdCO}_2\text{H}$  (0.5 equiv) /  $4\text{-iodotoluene}$  (1.5 equiv) /  $\text{PhCH}_3$  /  $60\text{ }^\circ\text{C}$  / 48 h.*

Chromium, while desirable for its ability to render  $\pi$ -coordinated arenes electrophilic, has the specific disadvantage that oxidation is required to cleave the  $\eta^6$ -arene-chromium bond, which leads to stoichiometric chromium waste product. Ruthenium-arene complexes have also been used to activate arenes through  $\pi$ -coordination, however after reaction they can be photolysed, offering the opportunity to regenerate the active ruthenium species.<sup>16</sup> Compared to chromium, ruthenium also offers increased arene electrophilicity upon  $\pi$ -coordination and can enhance Pd-catalysed aromatic C-H activations as shown by Walton and co-workers in 2017 (Scheme 1.5 A).<sup>17</sup>  $[(\eta^6\text{-2-Fluorotoluene})\text{RuCp}]^+$  (**1.9**) is arylated in 83% yield, forming  $\pi$ -coordinated product (**1.10**). They demonstrated photolysis of the product complex in acetonitrile, generating free biaryl product and  $[\text{RuCp}(\text{NCMe})_3]\text{PF}_6$  which is the ruthenium species that the starting complex was synthesised from. This represents a promising development towards C-H activation reactions that are catalytic in ruthenium. Similarly, Ritter and co-workers showed that arenes can undergo C-H nucleophilic functionalisation upon  $\pi$ -coordination to an iridium(III) fragment (Scheme 1.5 B).<sup>18</sup> In this case,  $\pi$ -coordinated

benzenes (**1.11**) are electrophilic enough to be attacked by nucleophiles such as NaClO<sub>2</sub> and peroxides forming η<sup>5</sup>-phenoxo coordinated intermediates under mild conditions. Subsequent treatment with acid in acetonitrile dissociates the product arene, yielding hydroxylated product and regenerating [(MeCN)<sub>3</sub>IrCp\*]<sup>2+</sup>. Despite the promising prospect of an arene exchange type mechanism, incompatibilities between the nucleophiles and acid mean this is not possible.



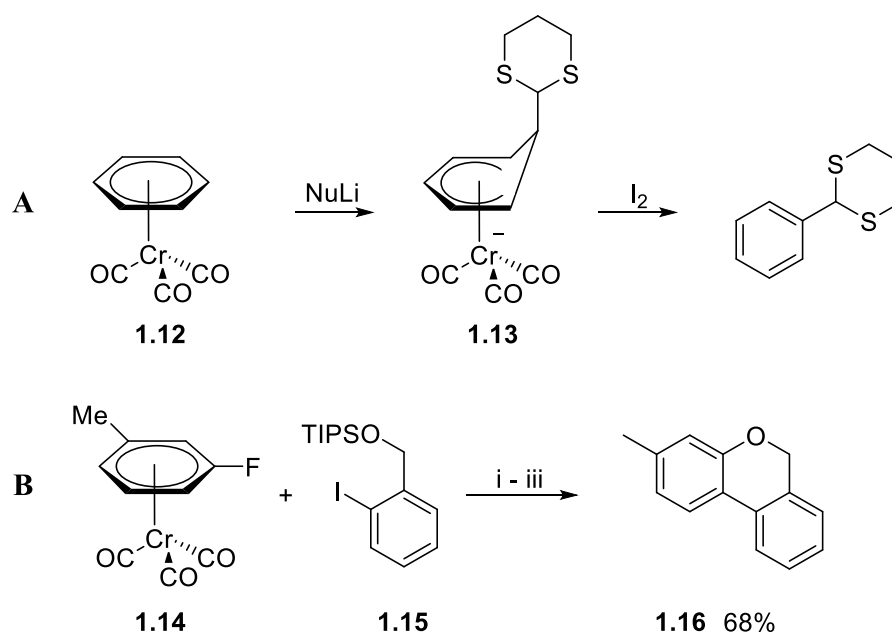
**Scheme 1.5** **A** Ruthenium-mediated *ortho*-C-H activation. **B** Iridium-mediated nucleophilic hydroxylation. Reagents and conditions: (i) Pd(OAc)<sub>2</sub> (10 mol%) / DavePhos (20 mol%) / Ag<sub>2</sub>CO<sub>3</sub> (2 equiv) / 1-AdCO<sub>2</sub>H (0.5 equiv) / TMP (1.5 equiv) / 1,2-DCE / 120 °C / 18 h; (ii) NaClO<sub>2</sub> / 2-*me-but-2-ene* / MeCN / 23 °C; (iii) HBF<sub>4</sub>·OEt<sub>2</sub> / MeCN / 80 °C.

### 1.1.2 Nucleophilic Transformations *via* π-Coordination

In order for arenes to undergo nucleophilic aromatic substitution (S<sub>N</sub>Ar), they must contain electron withdrawing groups to stabilise the negatively charged Meisenheimer intermediate. Typically, this is achieved by incorporating covalently bound nitro or cyano groups *ortho* and/or *para* to the leaving group. [(η<sup>6</sup>-Arene)M] complexes, as a result of the metals electron withdrawing effect, can increase the electrophilicity of the bound arene and stabilise negatively charged intermediates, as well as further polarising aryl C-X bonds. Together,

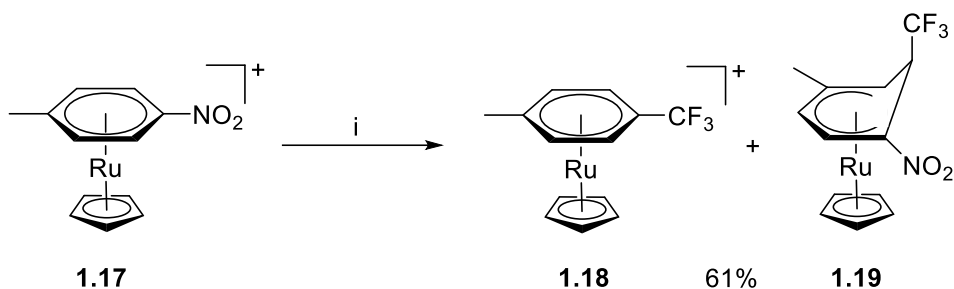
these factors mean  $\pi$ -coordination can facilitate nucleophilic aromatic substitution.  $\pi$ -Coordination thus avoids the need for covalently bound electron withdrawing groups, which could be undesirable in the final product.

This concept has been used to introduce reactive carbanions such as alkyl, vinyl and aryl lithium reagents to arene-chromium complexes.<sup>19</sup> Semmelhack *et al.* showed in 1979 that  $\eta^5$ -coordinated chromium intermediates (**1.13**) are formed upon nucleophilic attack of 2-lithio-1,3-dithiane to benzene-chromium complexes (**1.12**) and can even be analysed *via* X-ray diffraction (Scheme 1.6 A).<sup>20</sup> Subsequent oxidation of the intermediate leads to arene dissociation. It has also been demonstrated that chromium-mediated  $S_NAr$  can be used in conjunction with C-H activation in the synthesis of medium sized rings, as shown by Larrosa and co-workers (Scheme 1.6 B).<sup>21</sup> Synthesis of  $[(\eta^6\text{-3-fluorotoluene})\text{Cr}(\text{CO})_3]$  (**1.14**) followed by a Pd-catalysed cross-coupling with nucleophilic-pendant-containing iodoarene (**1.15**) yields  $\eta^6$ -biaryl-chromium complex. Subsequent cyclisation *via*  $S_NAr$  with the nucleophilic pendant and fluoroarene affords tricyclic complex. Oxidation with  $\text{MnO}_2$  then dissociates the product (**1.16**).



**Scheme 1.6 A** Nucleophilic substitution of  $\pi$ -coordinated arenes via  $\eta^5$ -Meisenheimer intermediates. **B** *ortho*-C-H arylation followed by  $S_NAr$  to synthesise tricyclic structures. Reagents and conditions: (i)  $\text{Pd}(\text{PPh}_3)_4$  (5 mol%) /  $\text{K}_2\text{CO}_3$  (2 equiv) /  $\text{AdCO}_2\text{H}$  (0.5 equiv) /  $\text{Ag}_2\text{CO}_3$  (1 equiv) /  $\text{H}_2\text{O}$  (2 equiv) /  $\text{PhCH}_3$  /  $70^\circ\text{C}$  / 16 h; (ii) TBAF (1.5 equiv) / THF / RT / 3 h; (iii)  $\text{MnO}_2$  / AcOH / RT / 3 h.

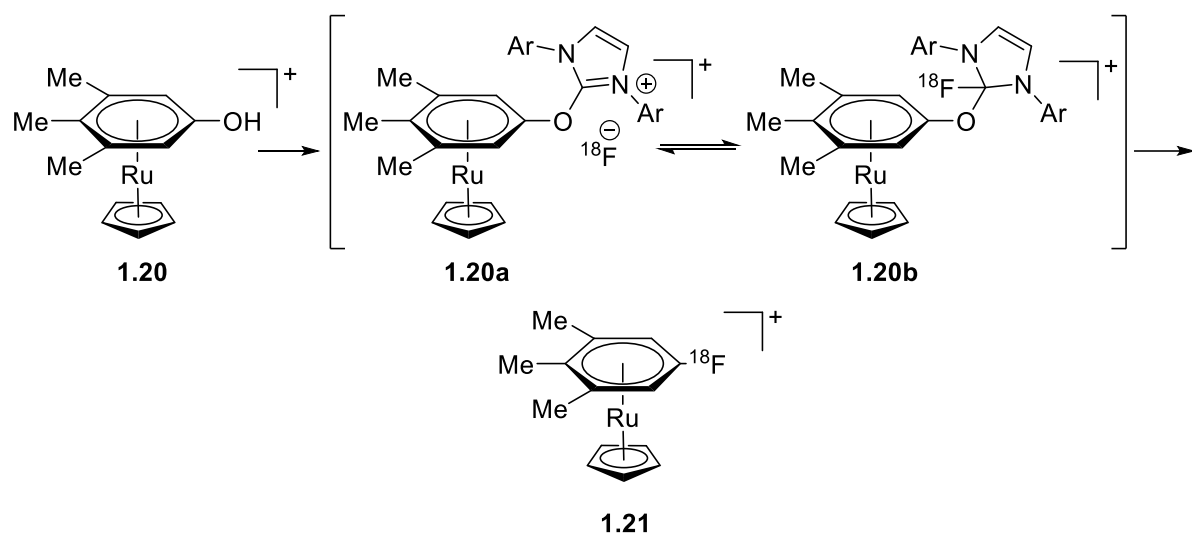
Ruthenium can also facilitate  $S_NAr$ , as demonstrated by Walton and Pike with their nucleophilic trifluoromethylation protocol mediated by  $\pi$ -arene complexation (Scheme 1.7).<sup>22</sup> With  $Me_3SiCF_3$  and  $KF$ , mild conditions allow nucleophilic substitution of  $[(\eta^6\text{-4-nitrotoluene})RuCp]^+$  (**1.17**) affording two products in 61% conversion with a 50:50 ratio. One product is from the direct substitution of the nitro group by  $CF_3$ , forming  $[(\eta^6\text{-trifluoromethylbenzene})RuCp]^+$  (**1.18**). The other product is from nucleophilic attack *ortho* to the nitro group to give the Meisenheimer complex  $[(\eta^5\text{-1-nitro-2-fluoromethyl-cyclohexadienyl})RuCp]^+$  (**1.19**), with selectivity for *endo* attack as a result of  $[RuCp]^+$  steric block. The use of other substituent groups, such as chloride, cyanide and methyl, leads to formation of only the Meisenheimer intermediate. Irradiation of trifluoromethylbenzene complex with 365 nm light in acetonitrile led to decomplexation and regeneration of the active  $[CpRu(NCMe)_3]PF_6$  catalyst. Whereas treatment of  $\eta^5$ -Meisenheimer complex with an oxidant (DDQ) rearomatizes and triggers decomplexation of 1-nitro-2-trifluoromethylbenzene. The mild conditions may allow for applications of this trifluoromethylation in late-stage functionalisation of pharmaceuticals.



**Scheme 1.7** Nucleophilic trifluoromethylation of  $[(\eta^6\text{-trifluoromethylbenzene})RuCp]^+$ . Reagents and conditions: (i)  $MeSiCF_3/KF/DMF/0\text{ }^\circ\text{C}/8\text{ h}$ .

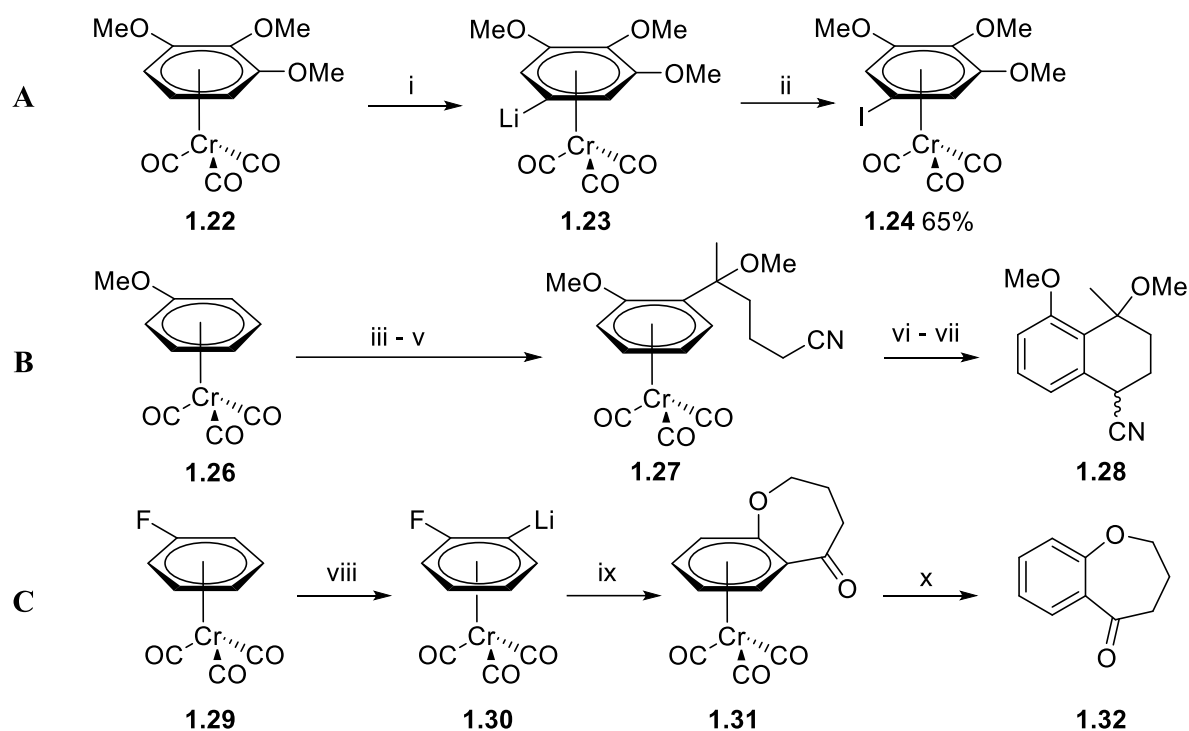
At around the same time, Ritter and co-workers developed a deoxyfluorination protocol which proceeds through an  $S_NAr$  mechanism.<sup>23</sup> Useful as a tracer in positron emission tomography (PET),  $^{18}\text{F}$  labelling allows the study of drug disposition and biochemical interactions.<sup>24</sup> The key problem with deoxyfluorination of unbound electron-rich arenes is that the equilibrium of intermediates lies to the unreacted side, which leads to detrimental side reactions of the free  $^{18}\text{F}$  anion.  $\pi$ -Coordination of 3,4,5-trimethylphenol to ruthenium (**1.20**), due to its reduced electron density, results in a shift in equilibrium to the fluorinated product (**1.20b**), thus generating fluorinated complex **1.21** with fewer side products (Scheme 1.8).





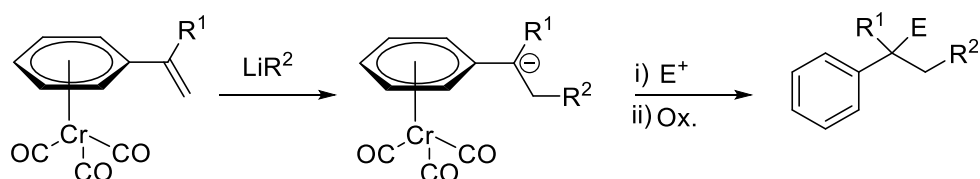
**Scheme 1.8** Deoxyfluorination of phenols via Ru  $\pi$ -complexes.

$[(\eta^6\text{-Arene})\text{M}]$  complexes typically do not undergo electrophilic aromatic substitutions due to their significantly lessened electron density. However, the high relative acidity of their aromatic protons allows these complexes to be lithiated and to participate in nucleophilic attack from the arene and has this been achieved with a variety of electrophiles.<sup>9</sup> Rose and co-workers demonstrated this with  $\pi$ -arene trimethoxybenzene complexes (**1.22**), lithiation generates lithiated complex **1.23** prior to treatment with electrophilic halogens, such as  $\text{I}_2$ , forming iodinated complexes (**1.24**). (Scheme 1.9 A).<sup>25</sup> This reactivity was also exploited by Semmelhack *et al.* in a two-step synthesis of a cyclised tetralin derivative (Scheme 1.9 B).<sup>26</sup> The starting material,  $[(\eta^6\text{-anisole})\text{Cr}(\text{CO})_3]$  (**1.26**), is *ortho*-lithiated by *n*-butyllithium and subsequent treatment with an electrophilic carbonyl species yields the *ortho*-substituted product (**1.27**). The pendant nitrile is lithiated and nucleophilic attack of the electron-deficient arene followed by oxidation with  $\text{I}_2$  affords free, unbound product (**1.28**). In the same publication, Semmelhack reports a similar procedure but with the use of  $[(\eta^6\text{-fluorobenzene})\text{Cr}(\text{CO})_3]$  (**1.29**, Scheme 1.9 C). Initial lithiation of the arene generates the *ortho*-lithiated intermediate (**1.30**) which ring-opens a  $\gamma$ -butyrolactone electrophile. The alkoxide spontaneously ring closes upon  $\text{S}_{\text{N}}\text{Ar}$  of the fluoride (**1.31**). Oxidation by  $\text{I}_2$  results in arene dissociation, yielding unbound product (**1.32**).



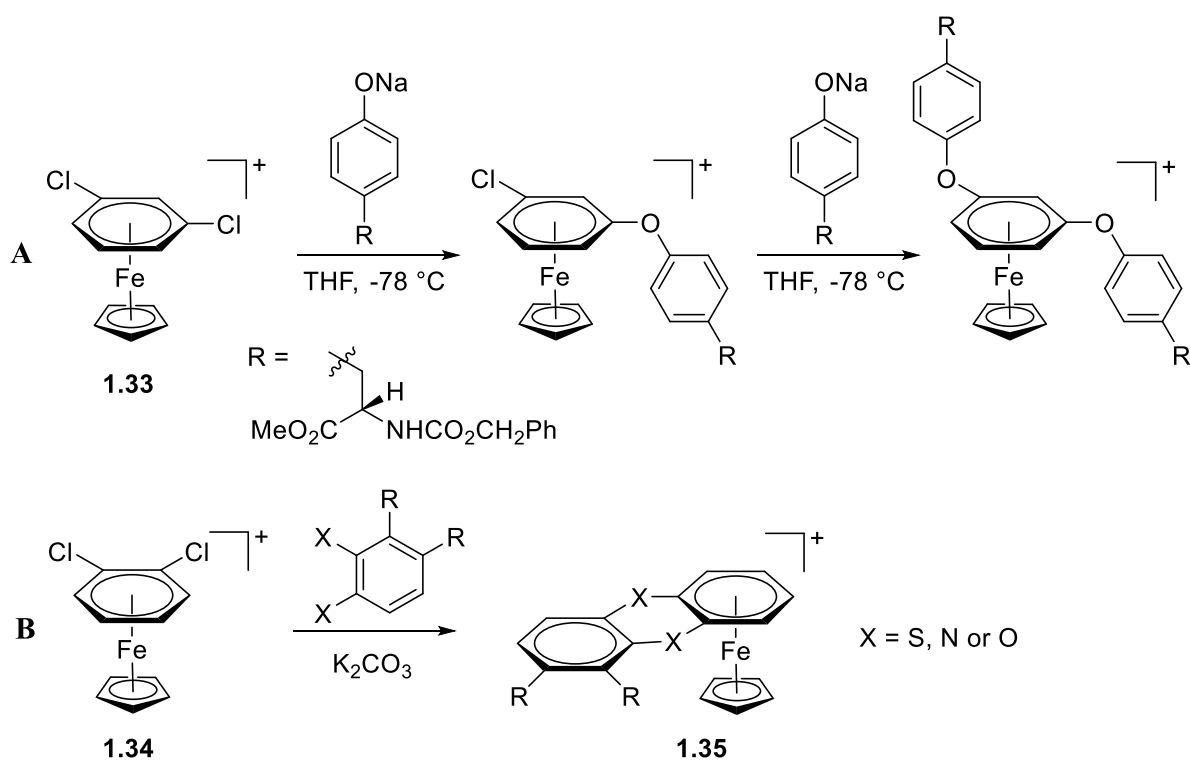
**Scheme 1.9** **A** Electrophilic iodination of  $[(\eta^6\text{-}1,2,3\text{-trimethoxybenzene})\text{Cr}(\text{CO})_3]$ . **B** Synthesis of tetralin derivative via ortho lithiation of  $[(\eta^6\text{-methoxybenzene})\text{Cr}(\text{CO})_3]$ . **C** Ortho lithiation of electron-deficient arenes to form bicyclic structures. Reagents and conditions: (i) LiTMP; (ii)  $\text{I}_2$ ; (iii) *n*-BuLi; (iv)  $\text{CH}_3\text{CO}(\text{CH}_2)_3\text{CN}$  (v)  $\text{CH}_3\text{I}$ ; (vi) LDA; (vii)  $\text{I}_2$ ; (viii) *n*-BuLi; (ix)  $\gamma$ -butyrolactone; (x)  $\text{I}_2$ .

In a similar vein to Walsh's benzylic C-H activation, distal carbons that are not directly bound to the metal are still affected by their electron-withdrawing nature.  $\eta^6$ -Styrene chromium complexes had previously been investigated for their ability to accept nucleophiles at the  $\beta$ -position, generating a stabilised benzyl anion, however yields with phenyllithium and methylolithium nucleophiles were low, at 30% and 7%, respectively.<sup>27</sup> Semmelhack *et al.* expanded on the scope and limitations of this type of nucleophilic attack, demonstrating that treatment with 2-lithio-2-methylpropionitrile achieves the adduct in 92% yield after acidic workup.<sup>28</sup> With the exclusion of acidic workup, electrophiles were added showing the ability to form two new carbon-carbon bonds with a range of electrophiles, as shown in a general scheme in Scheme 1.10.



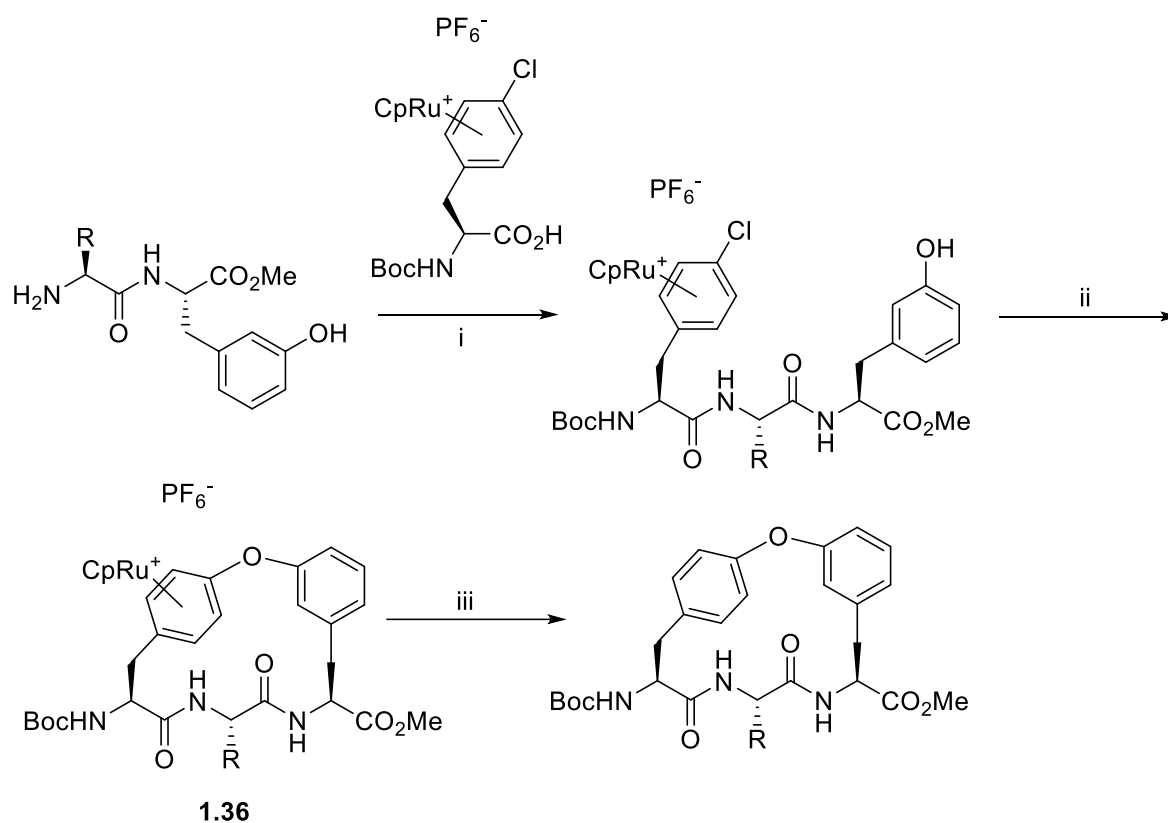
**Scheme 1.10** Nucleophilic addition to  $\eta^6$ -styrene chromium complex.

Like ruthenium  $\eta^6$ -complexes, the analogous iron complexes typically contain the  $\eta^5$ -cyclopentadienyl ligand. Pearson *et al.* reported the synthesis aryl ethers mediated by  $\eta^6$ -coordination of 1,3-dichlorobenzene to  $[\text{FeCp}]^+$  (**1.33**, Scheme 1.11 A).<sup>29</sup> In a double  $\text{S}_{\text{N}}\text{Ar}$  reaction, phenoxides displace the aromatic chlorides at  $-78\text{ }^\circ\text{C}$  in THF in 87% yield. Upon irradiation with light in acetonitrile at room temperature, the product arene is dissociated from the  $[\text{FeCp}]^+$  unit. Using the similar  $\eta^6$ -1,2-dichlorobenzene-iron complex (**1.34**), Pearson and Lee demonstrated the formation of nitrogen, oxygen and sulfur-containing heterocycles (**1.35**) in another double- $\text{S}_{\text{N}}\text{Ar}$  reaction (Scheme 1.11 B).<sup>30</sup> Yields of which were 23% to 82%, the best being the sulfur-containing heterocycle. Opting for pyrolytic sublimation rather than photolysis, yields were generally successful apart from nitrogen-containing heterocycles.



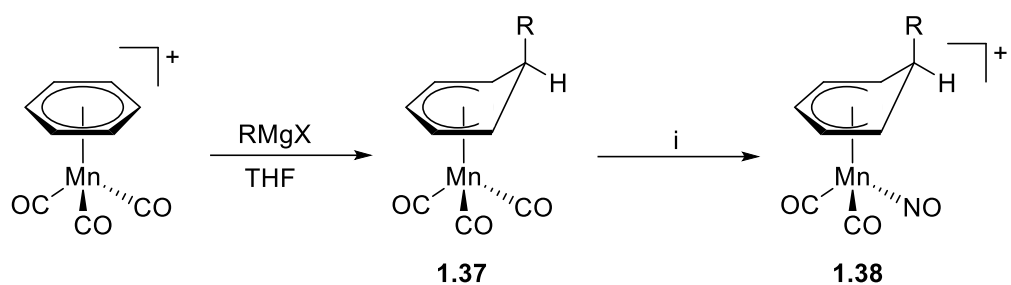
**Scheme 1.11** **A** Synthesis of arylethers via double  $\text{S}_{\text{N}}\text{Ar}$  of  $\eta^6$ -bound 1,3-dichlorobenzene. **B** Synthesis of cyclic arylethers via double  $\text{S}_{\text{N}}\text{Ar}$  of  $\eta^6$ -bound 1,2-dichlorobenzene.

Janetka and Rich employed a similar approach for a total synthesis of the natural product K-13.<sup>31</sup> Opting for ruthenium rather than an iron-mediated process, they used a Pearson-type intramolecular cyclisation forming a cyclic aryl ether (**1.36**, Scheme 1.12). This procedure offered a significant improvement over previous syntheses, with this  $\text{S}_{\text{N}}\text{Ar}$  pathway affording K-13 in seven steps compared to over 19 steps.



**Scheme 1.12** Synthesis of *K-13* model systems. Reagents and conditions: (i) EDCl / HOBt / DMF / 0 °C; (ii) Sodium 2,6-di-*t*-Bu-phenoxide / THF / 24 h / 0.002 M; (iii) *hν* (350 nm) / MeCN / RT / 24 h.

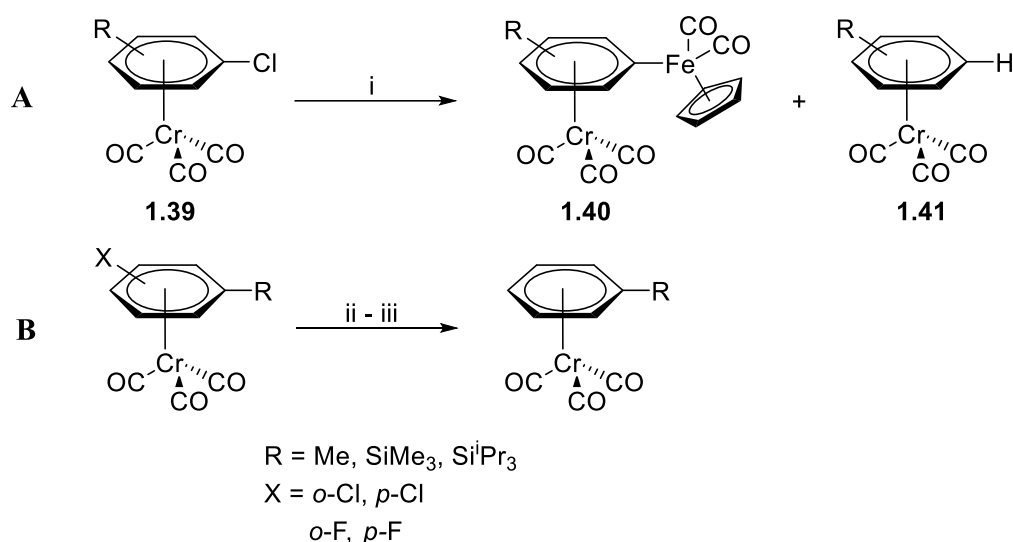
Similar to chromium, manganese- $\eta^6$ -arene complexes can be prepared and can also be activated towards nucleophilic attack. Mn(I) arene complexes are more reactive than their neutral chromium counterparts, due to the enhanced electrophilicity of the positively charged manganese metal. Consequently, they can undergo nucleophilic attack even by Grignard reagents, to generate  $\eta^5$ -Meisenheimer complexes (**1.37**), as demonstrated by Sweigart and co-workers (Scheme 1.13).<sup>32</sup> Treatment with NOPF<sub>6</sub> forms the charged  $\eta^5$ -Meisenheimer complex (**1.38**), making it further susceptible to nucleophilic attack, such that addition of NaBH<sub>4</sub> reduces the arene to  $\eta^4$ -cyclohexadienes. Furthermore,  $\eta^5$ -Meisenheimer complexes can be rearomatized with strong oxidising agents, such as DDQ in MeCN.<sup>33</sup> This also leads to ligand dissociation.



**Scheme 1.13** Nucleophilic attack of  $[(\eta^6\text{-benzene})\text{Mn}(\text{CO})_3]^+$  by Grignard reagents, forming  $\eta^5$ -Meisenheimer complex. Reagents and conditions: (i)  $\text{NOPF}_6 / \text{CH}_2\text{Cl}_2$ .

### 1.1.3 Reductive Dehalogenation mediated by $\pi$ -Coordination to Metals

An interesting example, albeit a rare one, is the reductive dehalogenation of  $\eta^6$ -coordinated arenes. In 1988, Heppert and co-workers were investigating  $\text{S}_{\text{N}}\text{Ar}$  of  $\eta^6$ -arylchloride-chromium (**1.39**) by nucleophilic  $[\text{FeCp}(\text{CO})_2]^-$  and while they observed the expected substitution product (**1.40**), they also observed the formation of dehalogenated arene complex (**1.41**, Scheme 1.14 A). It was identified that the arene functional groups had a significant effect on the distribution of substituted versus dehalogenated products. When a methoxy substitution is added *para* to the chloride, the product distribution is 88% dehalogenated and 12% substituted. Whereas the *meta* substituted analogue distribution is 19% dehalogenated and 81% substituted. The electron-withdrawing trifluoromethyl group resulted in a 92% preference for substitution in both the *para* and *meta* positions. In addition, steric factors were found to influence the product distribution with the *ortho*-substituted dichloro and methoxy functionalities favouring reductive dehalogenation. Unsurprisingly, the more electronegative halides show preference for nucleophilic substitution in the order of  $\text{F} > \text{Cl} > \text{I}$ . Rose and co-workers also demonstrated that of  $\eta^6$ -coordinated arylhalides to a chromiumtricarbonyl unit undergo reductive dehalogenation upon treatment of hydrides, such as  $\text{Et}_3\text{BHLi}$  (Scheme 1.14 B).<sup>34,35</sup>



**Scheme 1.14** **A** Dehalogenation with nucleophilic  $[FeCp(CO)_2]$  complex. **B** Hydrodehalogenation with a hydride source via  $Cr(CO)_3$  mediated complexes. Reagents and conditions: (i)  $[CpFe(CO)_2]$  / THF; (ii)  $Et_3BHLi$ ; (iii)  $H^+$ .

## 1.2 Arene Exchange

### 1.2.1 Arene Exchange Mechanism

Many examples exist in literature of reactions mediated by  $\pi$ -complexation to transition metals. The obvious drawback to these is that stoichiometric metal is required, and while there are several examples of product dissociation to regenerate catalyst, the ideal solution is to have reactions that proceed *via* transient  $\pi$ -coordination. A simplified mechanism of this system is shown in Figure 1.3. The starting arene undergoes a reaction whilst bonded to the active metal fragment, subsequent arene exchange replaces the product arene with another starting arene, thus releasing free product. The main challenge with this approach is that the arene exchange step must be compatible with reaction conditions.

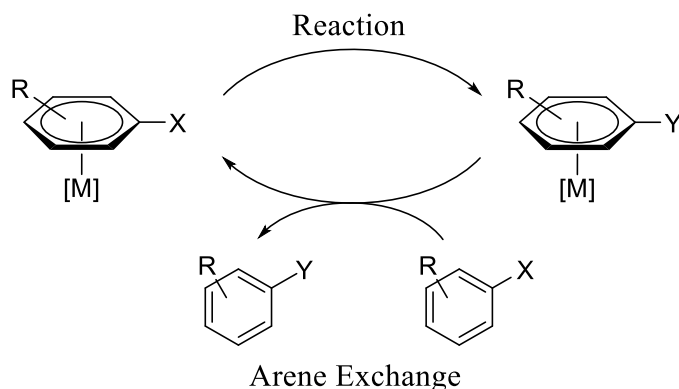


**Figure 1.3** General mechanism for a catalytic reaction via an arene exchange.

Interest in arene exchange has been around since the 1960s and many mechanisms have been hypothesised.<sup>36</sup> Initial kinetic studies by Traylor *et al.* in 1984 led to the proposed “unzipping” mechanism for  $[(\eta^6\text{-arene})\text{Cr}(\text{CO})_3]$  complexes (**1.42**, Figure 1.4).<sup>37–39</sup> In the first step, which is also the slowest step, the bound arene changes its coordination to chromium from  $\eta^6$  to  $\eta^4$  (**1.42a**). As a result of this change, the arene ligand becomes a 4-electron donor making the destabilised 16 valence electron (VE) intermediate. Subsequent fast  $\eta^2$ -coordination of incoming arene leads to an 18 VE complex (**1.42b**). Next, the coordination of the outgoing arene switches from  $\eta^4$  to  $\eta^2$  and the coordination of the incoming arene switches from  $\eta^2$  to  $\eta^4$  (**1.42c**). Finally, the incoming arene coordinates  $\eta^6$  to chromium forming the product 18 VE complex (**1.43**).

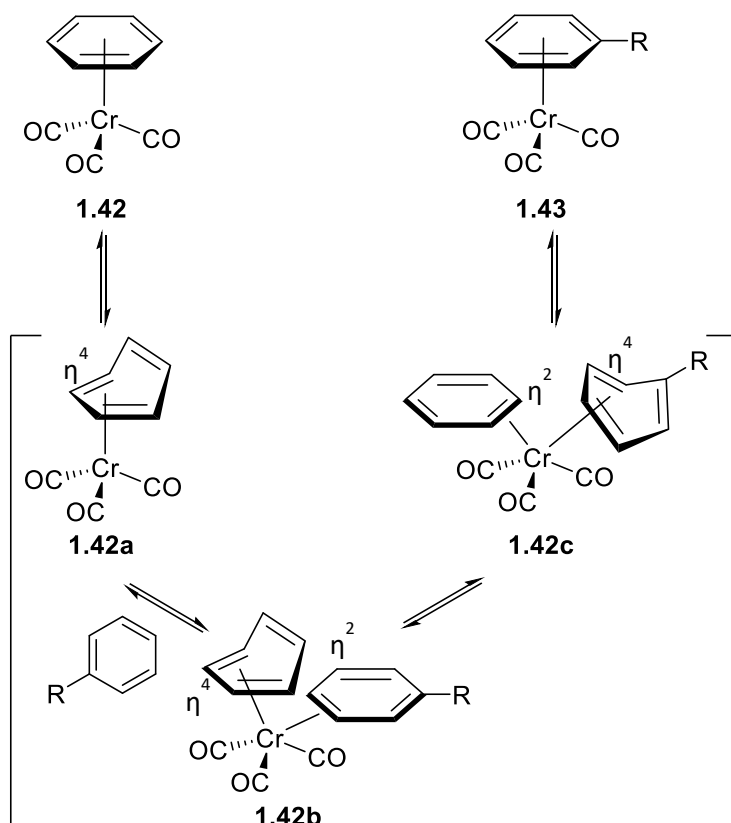
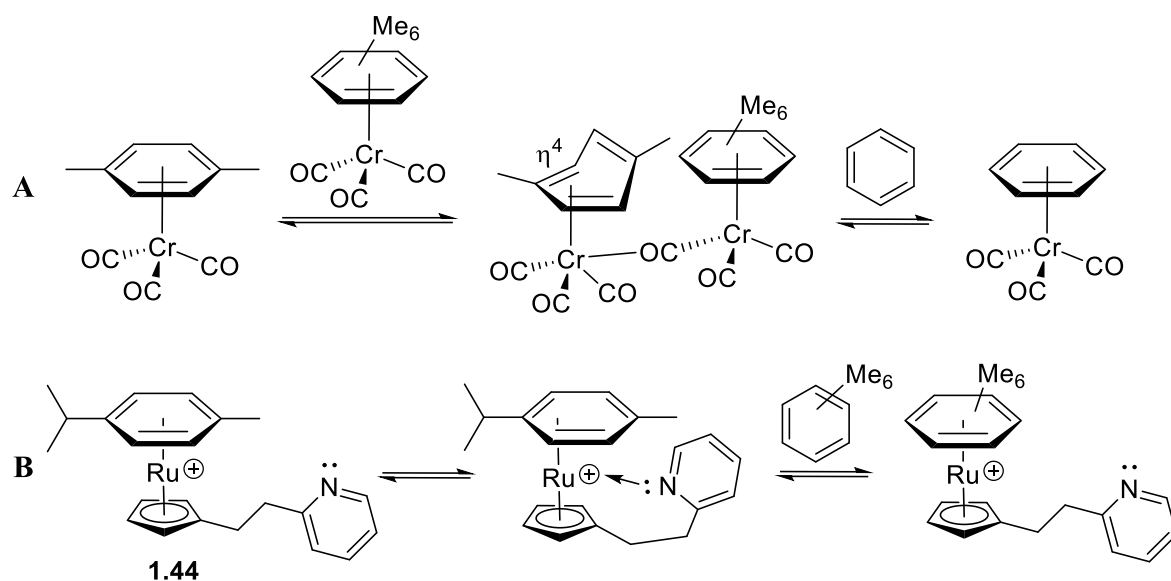


**Figure 1.4** “Unzipping” mechanism of arene exchange on a  $\text{Cr}(\text{CO})_3$  complex.

The change from  $\eta^6$  to  $\eta^4$ -coordination of the initial arene is unfavourable and is the rate determining step. In order to stabilise this intermediate, weakly-coordinating species can be added to generate the 18 VE intermediate thus catalysing arene exchange.<sup>36</sup> In 1986, Traylor also observed that addition of  $[(\text{arene})\text{Cr}(\text{CO})_3]$  complex catalyses arene exchange of another  $(\text{arene})\text{Cr}(\text{CO})_3$  complex, which was as a result of carbonyl coordination to the 16 VE intermediate (Scheme 1.15 A).<sup>39</sup> Similarly, coordinating solvents can accelerate arene exchange.<sup>40</sup> Walton and Williams investigated the addition of coordinating tethers on a ruthenium-catalysed  $\text{S}_{\text{N}}\text{Ar}$  reaction.<sup>40</sup> While arene exchange of  $[(\text{arene})\text{Cr}(\text{CO})_3]$  complexes is well studied, ruthenium<sup>II</sup>( $\eta^6$ -arene) complexes are not, although the mechanism is assumed to be the same. The incorporation of ester, amide, pyridine or ketone tethers onto a ruthenium cyclopentadienyl ligand provided increased rates of arene exchange (*p*-cymene to hexamethylbenzene) compared to the standard  $[\text{RuCp}]^+$  unit (Scheme 1.15 B). The most significant of which was the pyridine tether (**1.44**) in both cyclohexanone and 1-octanol, with an increased conversion of 62% and 8% respectively after 16 hours when compared to the analogous complex without tether.





**Scheme 1.15** **A** Arene exchange catalysed by another  $[\text{Cr}(\text{CO})_3(\eta^6\text{-arene})]$  complex. **B** Tether-assisted arene exchange.

In addition to the previous parameters, another factor that would affect arene exchange is the electronic nature of the ingoing and outgoing arenes. The order of thermodynamic stabilities of  $\pi$ -arene chromium complexes are shown in Figure 1.5.<sup>41</sup> Electron rich arenes bind to chromium more strongly than electron poor arenes, which highlights a particular challenge in catalytic  $\text{S}_{\text{N}}\text{Ar}$  reactions: that the product arene complex is usually more thermodynamically stable than ones that are activated towards  $\text{S}_{\text{N}}\text{Ar}$ .

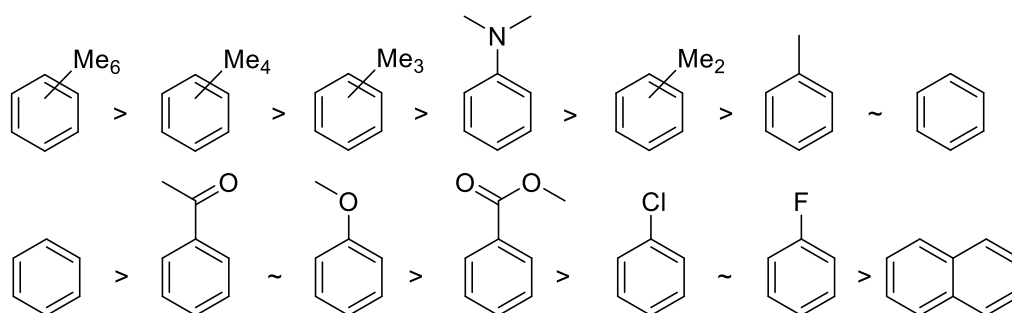


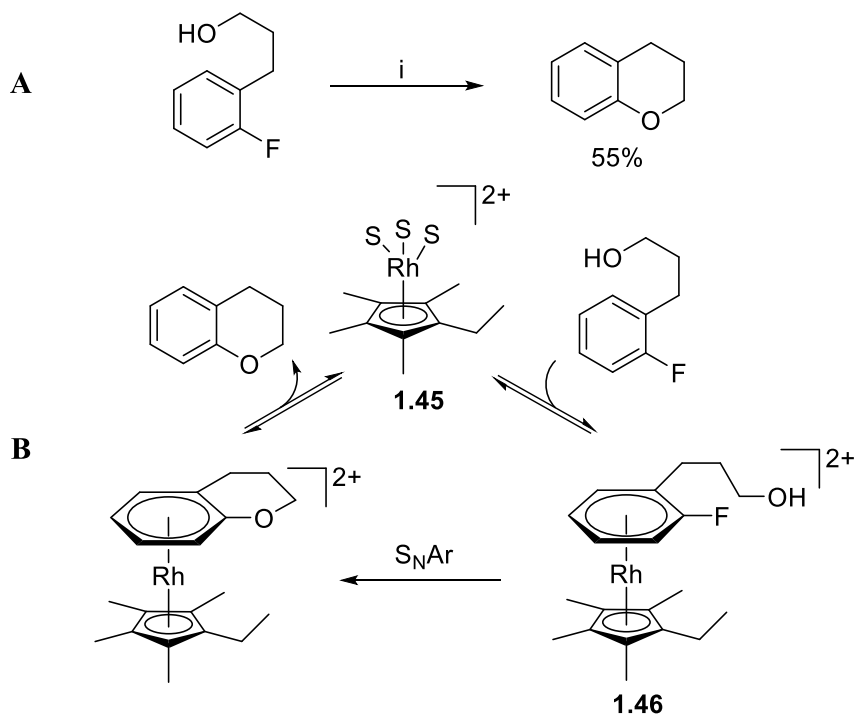
**Figure 1.5** Relative stabilities of  $[(\text{arene})\text{Cr}(\text{CO})_3]$  complexes.

## 1.2.2 Transformations *via* Transient $\pi$ -Coordination of Arenes to Metals

Although reactions to arenes bound to metals are well reported, reactions that proceed *via* an arene exchange mechanism are rare. This is due to the mechanism as discussed in Section 1.2.1, in which the bound arene changes from  $\eta^6$  to  $\eta^4$  coordination. Moreover, some

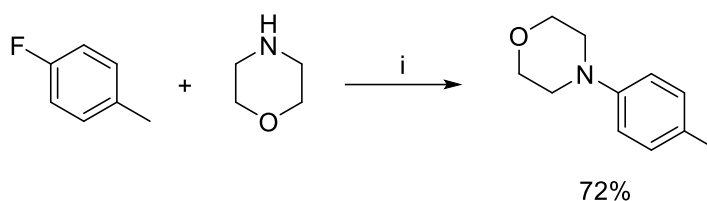
complexes require specific conditions to facilitate arene dissociation, which can lead to incompatibilities with reagents.

In 1980, Houghton and Voyle demonstrated the first example of an  $S_NAr$  reaction catalysed by transient  $\pi$ -coordination of arenes to metals: an intramolecular cyclisation to form chromans.<sup>42,43</sup> Chromium  $\pi$ -arene complexes of the starting fluoroalcohol were found to readily undergo cyclisation upon treatment with potassium *tert*-butoxide at room temperature in 75% yield, however the requirement for complex oxidation limits the potential for a process that is catalytic in metal. The use of an  $[(\eta^6\text{-C}_6\text{H}_6)\text{Rh}(\eta^5\text{-C}_5\text{Me}_4\text{Et})]^{2+}$  catalyst was found to avoid this problem, providing forming chroman product after 24 hours at room temperature (Scheme 1.16 A). Additionally, the catalyst counterion was found to have a significant effect on conversions, with the hexafluorophosphate salt and tetrafluoroborate returning conversions of 55% and 30% respectively. Nitro-substituted arenes (*para* to F) were not tolerated in the reaction, while methoxy-substituted arenes proceeded to give a conversion of 35%. They attributed that this difference was due to the equilibrium between solvated catalyst (**1.45**) and  $\pi$ -arene coordinated complex (**1.46**), with the former being favoured with nitroarenes and the latter with methoxyarenes. The proposed mechanism is shown in Scheme 1.16 B.



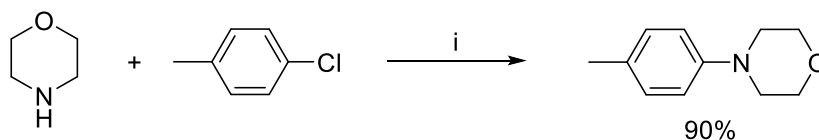
**Scheme 1.16** A Rh-catalysed intramolecular  $S_NAr$ . B Mechanism for Rh-catalysed intramolecular  $S_NAr$ . Reagents and conditions: (i)  $[(\text{C}_6\text{H}_6)\text{Rh}(\text{C}_5\text{Me}_4\text{Et})](\text{PF}_6)_2$  (23 mol%) /  $\text{MeNO}_2$ :acetone (4:1) /  $80^\circ\text{C}$  / 24 h.

A novel  $S_NAr$  of unactivated fluoroarenes was reported by Shibata and co-workers in 2010.<sup>44</sup> Optimisation studies of a morpholine substitution of 4-fluorotoluene were carried out, which returned yields of 72% (Scheme 1.17). Electron-rich arenes, while typically unreactive towards  $S_NAr$ , were tolerated with moderate yields, as demonstrated by reported 30%, 58% and 38% yields for *para*, *meta*, and *ortho*-methoxyfluorobenzene respectively. Evidence of Ru  $\eta^6$ -arene complex intermediates was obtained by synthesis of the deuterated fluorobenzene complex with ruthenium, followed by addition of morpholine. The resulting complex was observed by  $^{31}P$ -NMR and was confirmed to be that of the morpholine-substituted product, suggesting that  $S_NAr$  was proceeding while fluorobenzene is bound to ruthenium. Building on this, they then developed a more facile protocol using  $[Ru(\text{benzene})Cl_2]_2$  as the catalyst.<sup>45</sup>



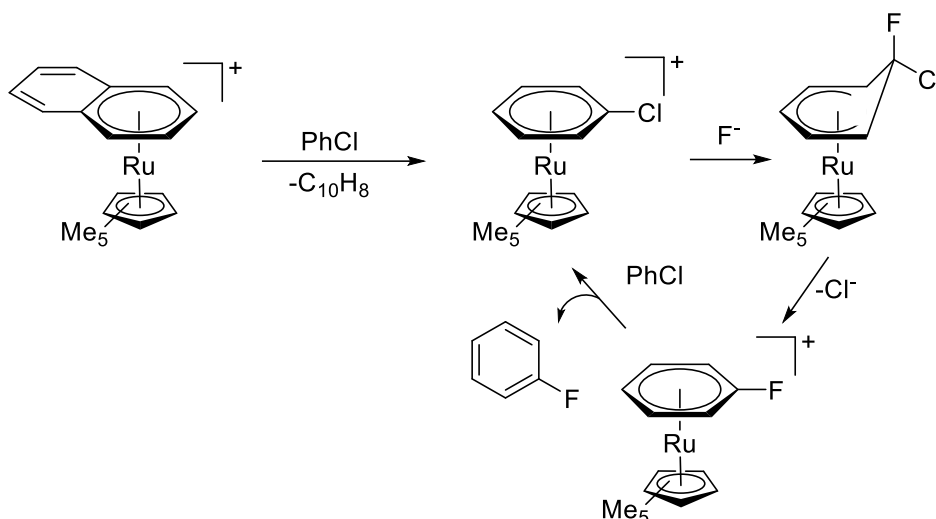
**Scheme 1.17** Ruthenium-catalysed  $S_NAr$  of 4-fluorotoluene with morpholine. Reagents and conditions: (i)  $Ru(cod)(2\text{-methylallyl})_2$  (5 mol%) /  $DPPent$  (7 mol%) /  $TfOH$  (10 mol%) /  $Et_3N$  (1 equiv) /  $Et_3SiH$  (1 equiv) / dioxane / reflux / 24 h.

$S_NAr$  of aromatics are typically limited by the need for covalently bound electron withdrawing groups to stabilise the Meisenheimer intermediate. Although fluorobenzene readily undergoes  $S_NAr$  with strong alkoxide nucleophiles,<sup>46</sup> chlorobenzene requires strong electron withdrawing groups. Ruthenium has previously been reported to mediate  $S_NAr$  reactions with stoichiometric metal.<sup>22</sup> Recently, Walton and Williams reported a catalytic  $S_NAr$  of unactivated aryl chlorides (Scheme 1.18).<sup>40</sup> This reaction proceeds *via* an arene exchange mechanism to achieve yields of up to 90%, albeit with high temperatures and long reaction times.



**Scheme 1.18** Catalytic  $S_NAr$  of unactivated 4-chlorotoluene with morpholine. Reagents and conditions: (i)  $[CpRu(p\text{-cymene})]PF_6$  (10 mol%) / 1-octanol / 180 °C / 14 days.

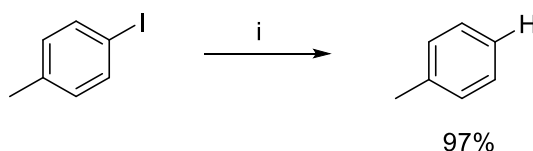
Soon after, Grushin reported the first ruthenium-catalysed nucleophilic fluorination of unactivated aryl halides.<sup>47</sup> The reaction itself proceeds *via*  $\pi$ -coordinated arylchloride intermediates, which generate  $\eta^5$ -Meisenheimer intermediates after nucleophilic addition of fluoride. Subsequent loss of chloride and rearomatisation affords  $\eta^6$ -fluoroarene complex (Scheme 1.19).



**Scheme 1.19** Catalytic nucleophilic fluorination of unactivated aryl chlorides via arene exchange mechanism.

### 1.2.3 Hydrodeiodination

An excellent example of ruthenium catalysis *via* transient arene  $\eta^6$ -coordination is the recently developed hydrodeiodination in the Walton group.<sup>48</sup> In unpublished data, aryl iodides are hydrodeiodinated with excellent functional group tolerance and selectivity. In optimised conditions, 4-iodotoluene is converted to toluene with a 97% conversion (Scheme 1.20). Other halides are not affected by the reaction conditions and electron-withdrawing/donating groups have minimal effect on conversions, other than nitro and amino-containing arenes which have 0% conversion.



**Scheme 1.20** Catalytic hydrodeiodination of 4-iodotoluene to toluene. Reagents and conditions: (i)  $[RuCp(NCMe)_3]PF_6$  (10 mol%) / DBU / 1-octanol / 180 °C (MW) / 3 h.

A detailed mechanistic investigation was conducted after evidence suggested that it might be proceeding *via*  $\pi$ -arene intermediates. First, alkyl iodides show no hydrodeiodination under optimised conditions, possibly because they do not coordinate to  $[\text{RuCp}]^+$  like aryl iodides. Next,  $[(\eta^6\text{-4-iodotoluene})\text{RuCp}]\text{PF}_6$  leads to the formation of the  $\eta^6$ -toluene complex upon hydrodeiodination conditions, with retention of the  $\pi$ -arene-metal bond, suggesting that hydrodeiodination is occurring while arene is bound to ruthenium. Kinetic studies revealed similar rate constants between hydrodeiodination and arene exchange between toluene and hexamethylbenzene, suggesting that arene exchange is rate-limiting in the hydrodeiodination reaction. Moreover, evidence that the reaction was proceeding *via* radical intermediates was observed upon the addition of radical trapping agents. Two equivalents of TEMPO reduced conversions from >99% to 77%, suggesting hydrodeiodination was being suppressed. Similarly,  $\alpha$ -methylstyrene was added and LC-MS revealed the formation of radical-trapped products.

Collating this evidence, the mechanism in Figure 1.6 is proposed. The reaction is triggered by arene exchange from the catalyst resting state (**1.47**), followed by single electron transfer (SET) from DBU to  $[(\eta^6\text{-4-iodotoluene})\text{RuCp}]^+$  (**1.48**) to form radical complex **1.49**. Subsequent loss of iodide leads to formation of an aryl radical intermediate (**1.50**). Abstraction of a H atom from deprotonated solvent affords  $\pi$ -coordinated toluene complex (**1.47**). The location of the radical in **1.49** is unknown, however Houk and co-workers showed that upon addition of  $\text{CH}_3$  radicals to  $[(\eta^6\text{-benzene})\text{Cr}(\text{CO})_3]$  complexes, the radical character is transferred to the metal fragment.<sup>49</sup> Additionally, calculations confirmed that radical addition to arenes is stabilised by  $\pi$ -coordination in chromium complexes and this hydrodeiodination reaction is the first example of radical addition to  $\pi$ -arene ruthenium complexes.

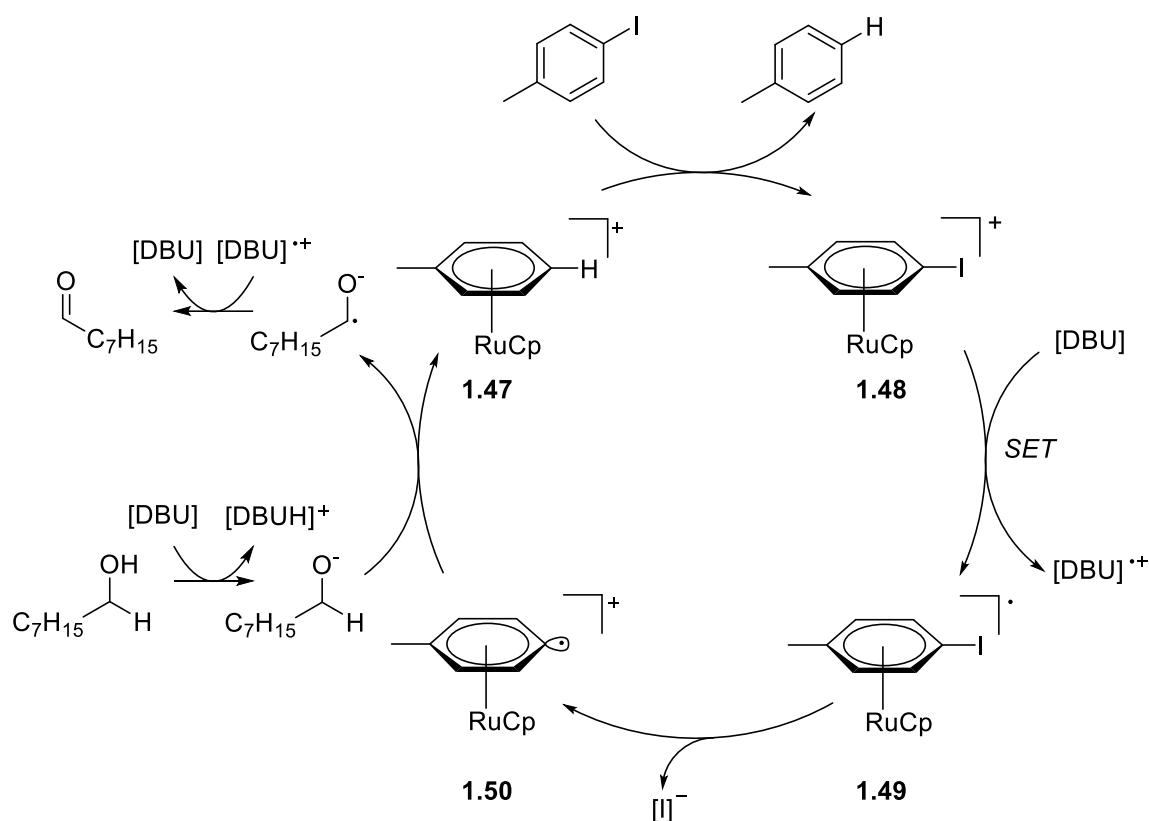


**Figure 1.6** Proposed reaction mechanism for ruthenium-catalysed hydrodeiodination.

### 1.3 Project Aims

Following the recently developed hydrodeiodination protocol, the potential for new ruthenium-catalysed reactions became apparent. If the mechanism in Figure 1.26 is correct, hydrodeiodination proceeds *via*  $\eta^6$ -radical intermediate complexes. It may be possible to trap the radical intermediate, generating new functionalised arenes *via* new carbon-carbon bonds or carbon-halide bonds. In addition, the cyclopentadienyl ligand acts as a directing group, blocking approach from one face of the arene, which allows stereochemical control. Reactions that proceed by arene exchange mechanisms are rare in literature, and this provides an opportunity to develop new transformations that are mediated by  $\pi$ -arene complex intermediates.

The exact aims of this work are as follows:

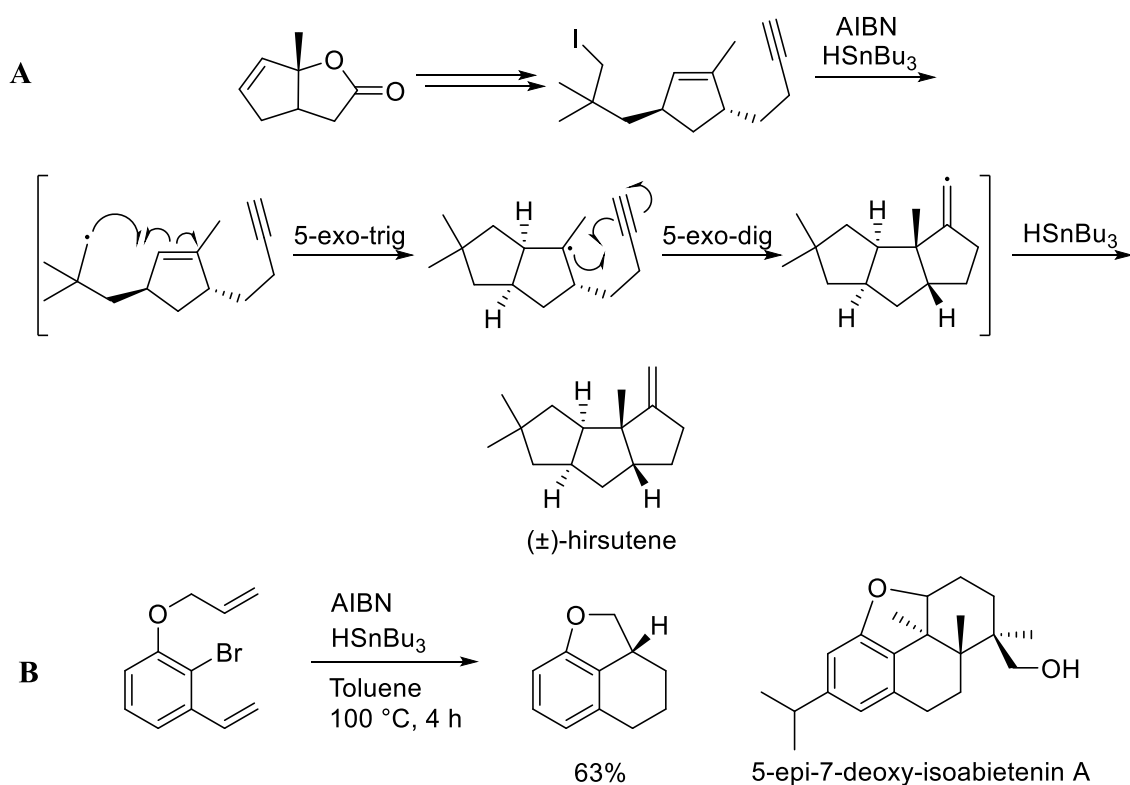
1. Develop an intramolecular radical cyclisation protocol
  - a. Synthesise alkene-containing iodoarene capable of intramolecular cyclisation
  - b. Test for radical cyclisation and optimise reaction conditions
2. Investigate a potential radical halogen-exchange reaction

- a. Test iodobenzene under hydrodeiodination conditions with N-bromosuccinimide to see if halogen exchange occurs
- b. Optimise halogen exchange
- c. Synthesise  $[(\eta^6\text{-arene})\text{RuCp}^*]^+$  complex and test under optimised conditions
- d. Perform tests to establish a mechanism

## 2. Radical Cyclisation *via* $\eta^6$ -Coordinated Intermediates

### 2.1 Introduction

Radical species can act as intermediates towards fundamental structural components of many widely used compounds. Notably, their ability to partake in cyclisations has resulted in their use in natural product syntheses *via* radical cascade reactions, such as Curran's synthesis of hirsutene in 1985 (Scheme 2.1, A).<sup>50</sup> After initiation, a radical cascade leads to 5-exo-trig then 5-exo-dig cyclisations to afford hirsutene product. More recently, Zhang reported the synthesis of 5-epi-7-deoxy-isoabietenin A *via* tandem radical cyclisations.<sup>51</sup> They recognised 6/6/5 fused tricyclic frameworks as a prevalent component of natural products so they developed a radical cascade reaction as shown in Scheme 2.1 B. After abstraction of the bromine atom, 5-exo-trig followed by 6-endo trig cyclisations form the tricyclic framework. They then applied their optimised conditions to the synthesis of the natural product 5-epi-7-deoxy-isoabietenin A.



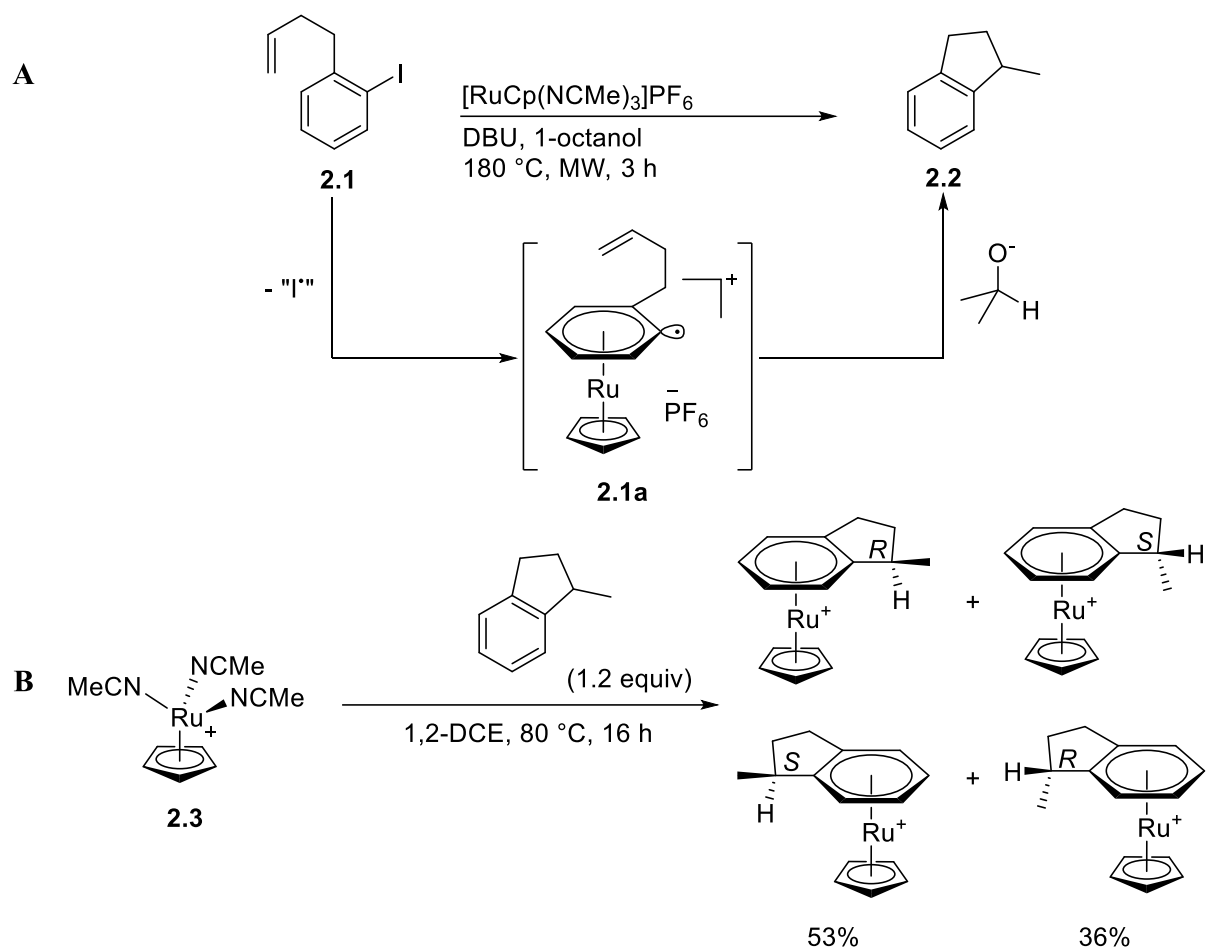
**Scheme 2.1** **A** Synthesis of hirsutene *via* radical cascade cyclisation reactions. **B** Zhang's tandem radical cyclisation, optimised for the synthesis of 5-epi-7-deoxy-isoabietenin A.



Common to both these examples are the use of radical initiators. One such initiator, azobisisobutyronitrile (AIBN), forms two 2-cyanoprop-2-yl radicals upon heating. These radicals can abstract a hydrogen atom from tributyltin hydride, which allows the resulting tin radical to abstract a halogen atom from the starting compound. The radical intermediate formed can then react with radical acceptors such as alkenes and alkynes.<sup>52</sup> However, this method of initiation has two disadvantages: elevated temperatures for radical formation may be undesirable and they offer limited selectivity, which is especially an issue for complex syntheses.<sup>53</sup> Therefore, it would be necessary to develop initiation methods that are highly selective.

### 2.1.1 Ruthenium-Catalysed Radical Cyclisation

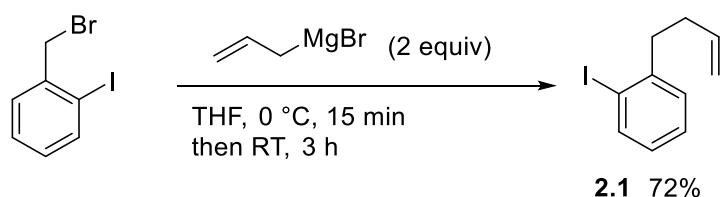
Following the optimisation and mechanistic study of the previously mentioned hydrodeiodination in Section 1.2.3, a radical mechanism was proposed.<sup>48</sup> Interestingly, the reaction showed selectivity for iodides over other halides, suggesting a new and selective radical initiation procedure. Many new reactions were hypothesised to make use of the radical intermediate, one of which is the 5-exo-trig cyclisation of 4-(2-iodobenzene)but-1-ene (**2.1**), in which the aromatic ring is deiodinated forming an aryl radical complex (**2.1a**). The aryl radical and tethered alkene then form the 5-membered ring, 1-methylindane (**2.2**, Scheme 2.2 A). As well as providing evidence for the proposed radical mechanism, modification of the catalyst cyclopentadienyl ligand provides the opportunity to introduce enantiomeric control of the chiral product. Previous studies have shown that binding racemic 1-methylindane in  $\eta^6$ -coordination to  $[\text{RuCp}]^+$  leads to a slight (3:2) facial preference as a result of steric effects from cyclopentadienyl and the methyl group of the indane (Scheme 2.2 B). It would be expected that this preference is enhanced if a bulkier cyclopentadienyl analogue was used, such as pentamethylcyclopentadienyl.



**Scheme 2.2** **A** Reaction pathway of 5-*exo-trig* cyclisation from 4-(2-iodobenzene)but-1-ene via  $\eta^6$ -coordination. **B** Formation of  $[RuCp(\eta^6\text{-1-methylindane})]^+$  complex.

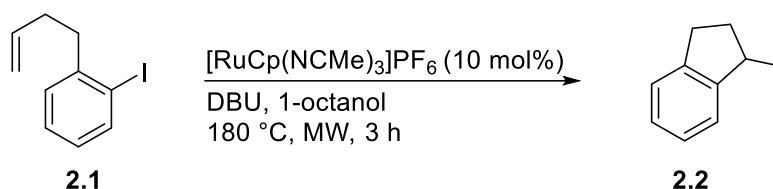
## 2.2 Results and Discussion

### 2.2.1 Initial Results



**Scheme 2.3** Synthesis of 4-(2-iodobenzene)but-1-ene.

To begin testing, 4-(2-iodobenzene)but-1-ene (**2.1**) was synthesised according to Scheme 2.3. The Grignard reacted smoothly at the benzylic bromide to give the desired compound after purification by chromatography (eluent: hexane). Under standard hydrodeiodination conditions as shown in Scheme 2.4, a reaction was attempted with **2.1** in attempts to observe the formation of cyclised product. The resulting reaction mixtures proved difficult to analyse as a result of 1-octanol overlapping with product signals in crude  $^1\text{H-NMR}$  spectrum. To overcome this issue, other solvents were looked at. An advantage of using a microwave reactor is that solvents can safely be elevated far above their boiling points, meaning alcohols with lower boiling points could be tested as a substitute to 1-octanol. Investigation of reaction conditions found 2-propanol as a suitable solvent alternative for the hydrodeiodination of 4-iodotoluene, with conversions of 70% achieved using 5% catalyst loading at 165 °C in just one hour. The use of 2-propanol allows easy removal of solvent and thus easy analysis of  $^1\text{H-NMR}$ , especially in the aliphatic region of the spectrum following cyclisation reactions. With the new conditions, hydrodeiodination conditions were applied as shown in Figure 2.1. After extraction and without further purification, the cyclised product signals were clearly visible at 1.3 ppm, 2.9 ppm, and 3.2 ppm in the  $^1\text{H-NMR}$  spectrum (Figure 2.1). Moreover, the sextet at 3.2 ppm provides an isolated signal to compare against DMF as an internal standard during reaction optimisations.



**Scheme 2.4** Reaction of 4-(2-iodobenzene)but-1-ene to form cyclised product 1-methylindane.

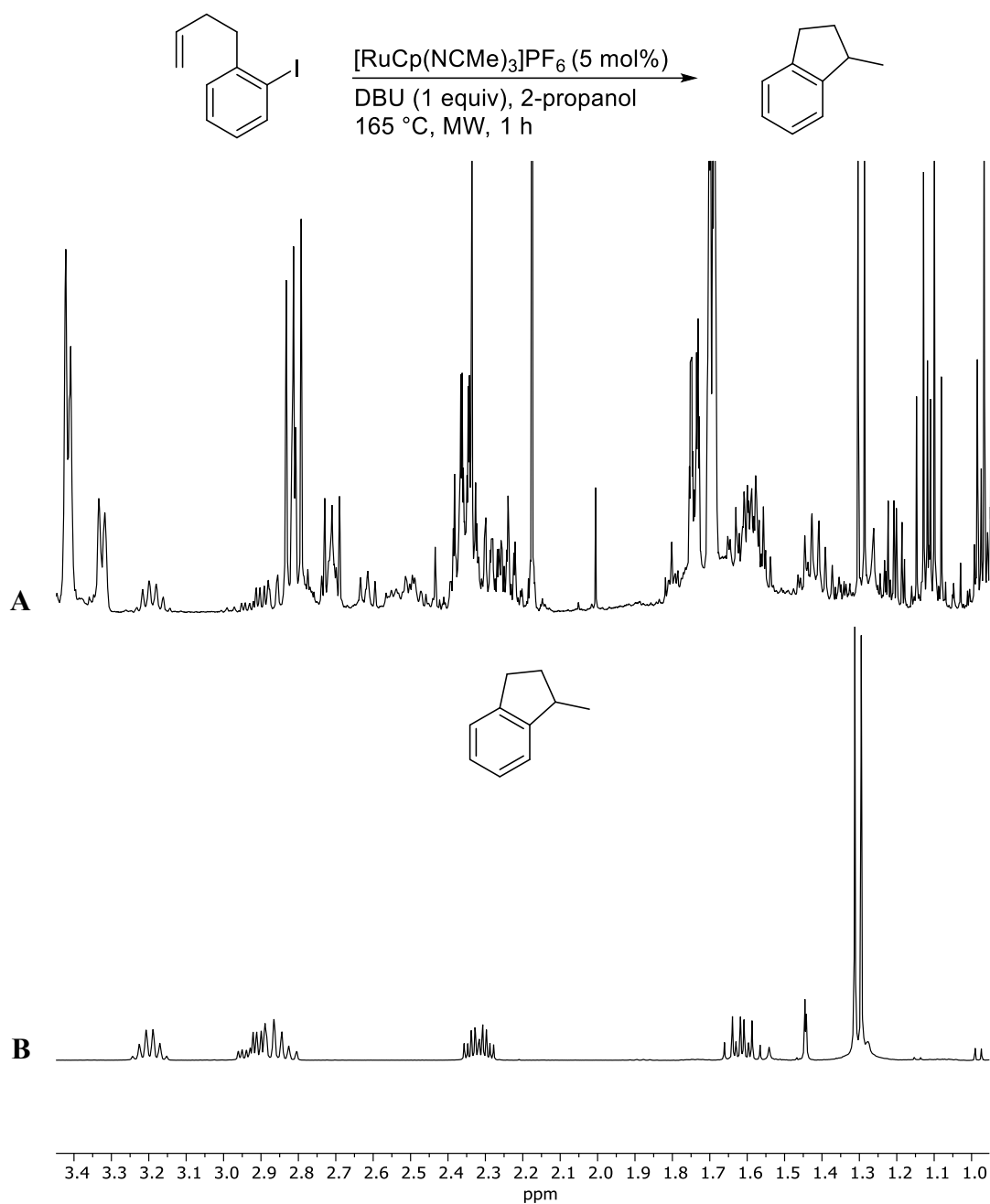


**Figure 2.1** Reaction of 4-(2-iodobenzene)but-1-ene under specified conditions with  $^1H$ -NMR spectra ( $CDCl_3$ , 298 K, 400 MHz) showing: **A** crude aliquot taken from the reaction mixture, **B** 1-methylindane ( $CDCl_3$ , 298 K, 400 MHz).

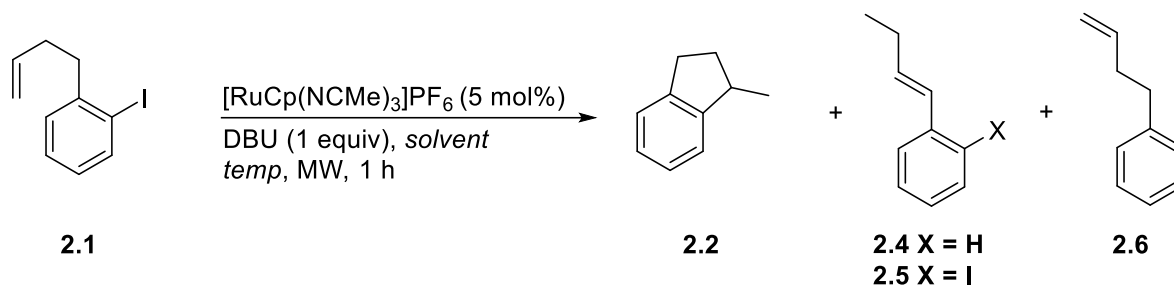
While the cyclised product could be seen in the NMR spectrum of the reaction mixture, several other species were also present. These species included alkene isomerisation products with and without deiodination. These species will be discussed in more detail in Section 2.2.2. Their yields are reported in optimisation Tables 2.1-2.3 for reference in later sections. Some additional species were present but unidentifiable. With the new standard reaction conditions, other parameters were investigated in an attempt to increase the yield of

the cyclised product. Initial efforts focussed around the optimisation of base and time (Table 2.1). Under the standard conditions (entry 2) a very small yield of 2% was recorded, measured by <sup>1</sup>H-NMR integral comparisons of DMF and product signal at 3.2 ppm. Other bases were tested to clarify whether DBU was hindering the cyclisation but proved even less successful (entry 7 and 8). Increasing the amount of DBU (relative to 4-(2-iodobenzene)but-1-ene) from 1 to 2 equivalents resulted in a slight increase of yield to 3% but increasing it further to three equivalents did not provide any benefit (entries 5 and 6). Conversely, using only 0.5 equivalents of DBU decreased the yield significantly (entry 1). Increasing the reaction time from one to three hours resulted in a lower yield, however no significant increase in yield should be expected as minimal starting material remains after just one hour.



point solvent, also had comparable yields at 165 °C to those of 2-propanol (entry 11). In order to explore higher temperatures, DMA (b.p 165 °C), 1,4-butanediol (b.p 230 °C) and DMF (b.p 153 °C) were also tested at 165 °C as a comparison. Each of these solvents performed better than 2-propanol, with 1,4-butanediol giving the highest yield of 8% (entries 4, 7 and 9). Strangely, reactions with these solvents at 180 °C provided increased yields for DMA and DMF but a lower yield in 1,4-butanediol (entries 5, 8 and 10). A possible explanation for these differences is that 1,4-butanediol is significantly more viscous than DMA and DMF and this could favour intramolecular cyclisation against intermolecular hydrodeiodinations.

**Table 2.2** Catalytic radical cyclisation by varying temperature and solvent. <sup>a</sup>2.1 and 2.6 were indistinguishable by <sup>1</sup>H-NMR, so a combined yield is given.

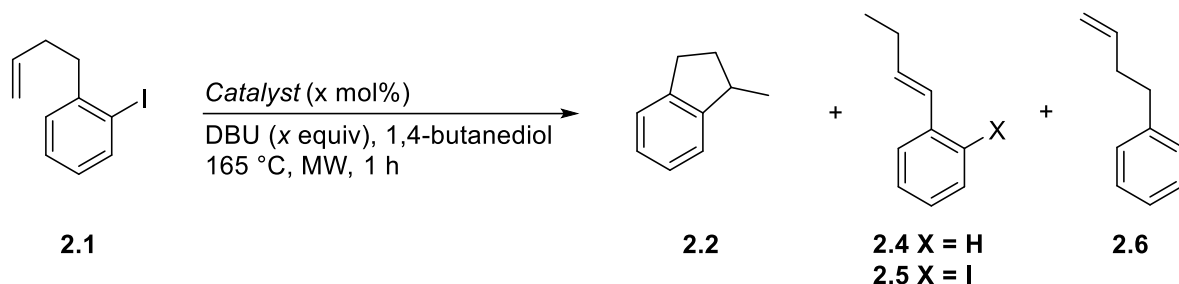


Entry	Solvent	Temperature (°C)	Yield (%)			
			2.2	2.4	2.5	2.1 and 2.6 <sup>a</sup>
1	2-propanol	120	2	2	2	43
2	2-propanol	150	2	4	4	19
3	2-propanol	165	2	14	6	1
4	DMA	165	4	1	5	44
5	DMA	180	5	2	7	34
6	1,4-butanediol	150	4	4	1	7
7	1,4-butanediol	165	8	11	0	3
8	1,4-butanediol	180	7	14	0	1
9	DMF	165	4	1	4	48
10	DMF	180	6	2	6	33
11	MeCN	165	2	1	11	52

Lastly, the ruthenium catalyst and loading were varied in conjunction with the previously optimised conditions to determine their impact on the cyclised yield (Table 2.3).



**Table 2.3** Catalytic radical cyclisation by varying catalyst and catalyst loadings. <sup>a</sup>2.1 and 2.6 were indistinguishable by <sup>1</sup>H-NMR, so a combined yield is given.

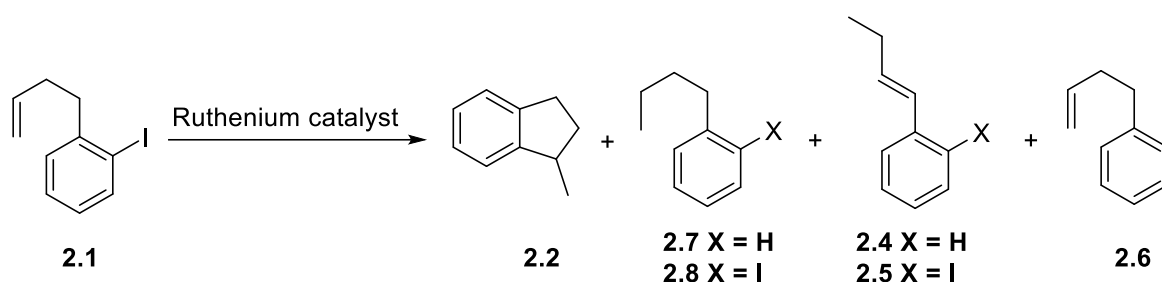


Entry	DBU equiv.	Catalyst	Catalyst loading (%)	Yield (%)			
				2.2	2.4	2.5	2.1 and 2.6 <sup>a</sup>
1	2	[RuCp(NCMe) <sub>3</sub> ]PF <sub>6</sub>	1	2	1	3	34
2	1	[RuCp(NCMe) <sub>3</sub> ]PF <sub>6</sub>	5	8	11	0	3
3	2	[RuCp(NCMe) <sub>3</sub> ]PF <sub>6</sub>	5	7	5	0	1
4	1	[RuCp(NCMe) <sub>3</sub> ]PF <sub>6</sub>	10	7	13	0	2
5	2	[RuCp(NCMe) <sub>3</sub> ]PF <sub>6</sub>	10	8	11	0	1
6	2	[RuCp*(NCMe) <sub>3</sub> ]PF <sub>6</sub>	5	4	5	1	2

Entry 2 shows the current highest yield of 8% with 5 mol% loading of [RuCp(NCMe)<sub>3</sub>]PF<sub>6</sub> (relative to 4-(2-iodobenzene)but-1-ene) and 1 equivalent of DBU. In 2-propanol, increasing the base equivalents from 1 to 2 led to a slight increase in yield. However, using 2 equivalents with 1,4-butanediol had no such benefit, and instead decreased the yield by 1% (entry 3). A more electron rich catalyst, [RuCp\*(NCMe)<sub>3</sub>]PF<sub>6</sub>, was tested to determine if the pentamethylcyclopentadienyl ligand would provide a favourable difference but the recorded yield was only 4% (entry 6). Pentamethylcyclopentadienyl, while more electron donating than cyclopentadienyl, is larger and could be sterically hindering the 5-exo-trig cyclisation step. Using 10 mol% of [RuCp(NCMe)<sub>3</sub>]PF<sub>6</sub> provided a slight increase of yield whilst using 2 DBU equivalents (entry 5) but less with 1 equivalent (entry 4) when compared to entry 2. These anomalies, combined with low yields, suggested that there were probably multiple reactions happening that were being catalysed at different rates.

## 2.2.2 Alkene Hydrogenation and Isomerism

Upon further investigation of  $^1\text{H-NMR}$  spectra, it became clear that multiple products were forming and deactivating the starting material for cyclisation. When comparing the  $^1\text{H-NMR}$  (Figure 2.2) of starting material and reaction mixture after extraction, only a trace of starting material remains. A new group of signals appear at 6.42 ppm to 6.24 ppm which have the characteristic chemical shift and splitting pattern for alkenes. A GCMS spectrum shows a significant amount of compound with an  $m/z = 132$ , which correlates to the hydrodeiodinated 4-phenylbut-1-ene (**2.6**) product. However, if only hydrodeiodination occurred it would be expected that the alkene signals would not change by so much. The splitting patterns and integrations of these signals were no longer that of a terminal alkene, and instead suggests an internal alkene. The  $^1\text{H-NMR}$  spectrum of *trans* 1-phenylbut-1-ene (**2.4**) was compared to the reaction  $^1\text{H-NMR}$  spectrum and they show similarities of in the alkene region.<sup>54</sup> Furthermore, GCMS also reveals a compound with  $m/z = 134$ , which indicates that hydrogenation is also occurring. The combination of all these products creates complicated spectra and it can be assumed that there is a lot of competition between reactions. The range of reaction products is summarised in Scheme 2.5.



**Scheme 2.5** Potential products from the attempted cyclisation of 4-(2-iodobenzene)but-1-ene

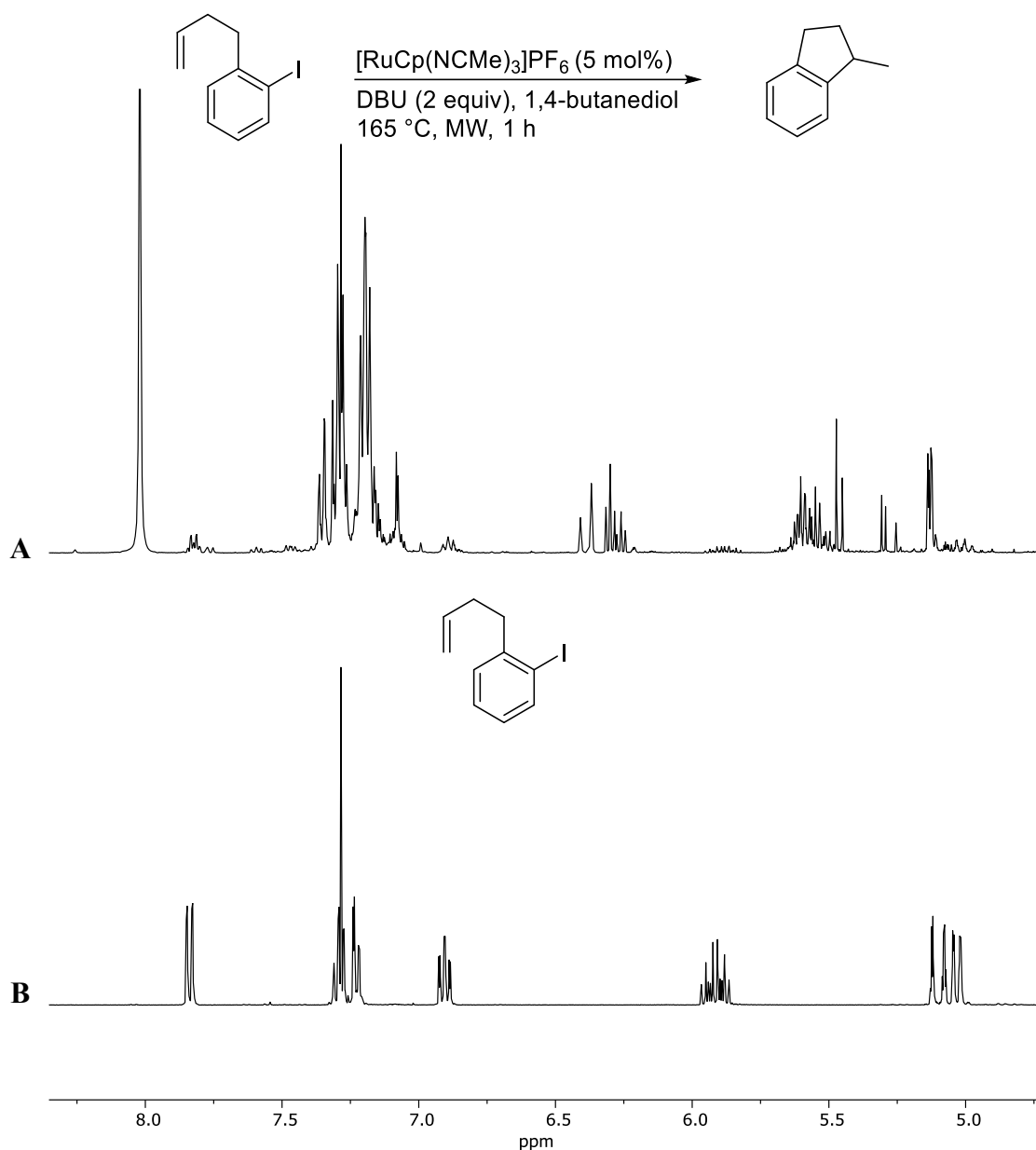


**Figure 2.2** Reaction of 4-(2-iodobenzene)but-1-ene under specified conditions with  $^1\text{H-NMR}$  spectra ( $\text{CDCl}_3$ , 298 K, 400 MHz) showing: **A** crude aliquot taken from the reaction mixture. **B** 4-(2-iodobenzene)but-1-ene.

Ruthenium catalysts are known to react with alkenes, with the 2005 Nobel Prize in Chemistry awarded for contributions towards olefin metathesis. Notably, Grubbs catalysts based on a ruthenium-carbene catalytic species catalyse cross-metathesis according to the mechanism in Figure 2.3.<sup>55</sup> In addition, ruthenium complexes have been extensively explored as catalysts for asymmetric hydrogenation of ketones to alcohols, imines to amines, and olefins to alkanes.<sup>56,57</sup> Transfer hydrogenation, typically using solvents such as 2-propanol as H-sources, provides obvious advantages over traditional  $\text{H}_2$  reductions. While use of  $\text{H}_2$  gas offers higher atom economies than transfer hydrogenations, the latter has fewer

associated safety hazards making its use more accessible, as well as being cheaper than H<sub>2</sub> gas.

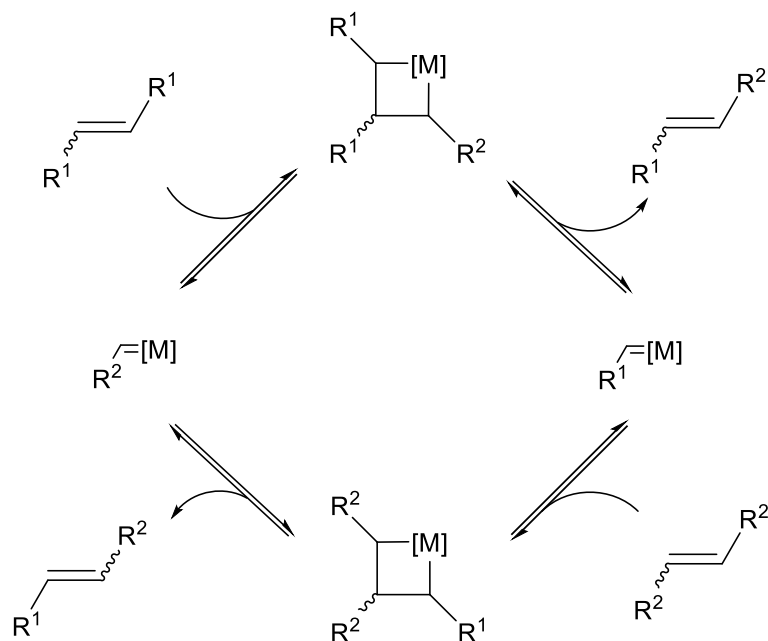
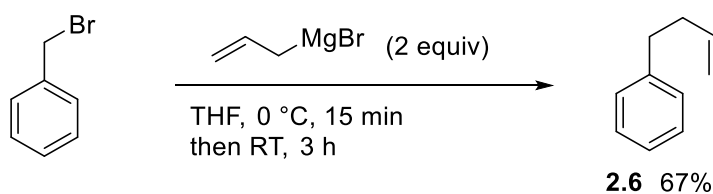


**Figure 2.3** Olefin metathesis mechanism.

The yields of isomerised (iodinated and deiodinated) products (Tables 2.1 – 2.3) were calculated by <sup>1</sup>H-NMR integral comparison of DMF internal standard and alkene signals. Yields of 0 – 14.4% were measured for hydrodeiodinated and isomerised compound (**2.4**) and 0 – 10.8% for iodinated and isomerised product (**2.5**). By-products still containing a terminal alkene (iodinated (**2.1**) and hydrodeiodinated (**2.6**)) were indistinguishable by <sup>1</sup>H-NMR due to overlapping alkene signals at 5.90 ppm and 5.05 ppm. These compounds combined account for 1 – 57% of the yield. Hydrogenated products (**2.7** and **2.8**) could not be quantified by <sup>1</sup>H-NMR as, despite extraction, the aliphatic region remains too complicated to measure accurate integrations. The unquantifiable hydrogenated products are possibly the reason that total conversions do not get close to 100%, and an investigation into the speed at which hydrogenation occurs should be carried out. The large number of potential products makes investigating hydrogenation and isomerisation independently of any hydrodeiodination-type reactions difficult.

In order to simplify the hydrogenation and isomerisation investigation, 4-phenylbut-1-ene (**2.6**) was synthesised according to Scheme 2.6. Removing iodide from the starting material eliminates the potential of cyclised product and combinations of iodinated or deiodinated products. Arylalkene **2.6** was reacted according to the conditions in Table 2.4 and

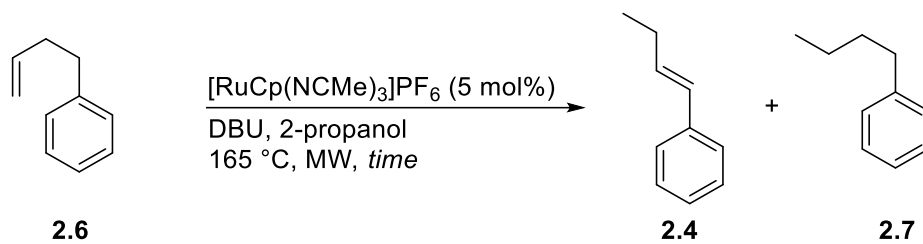
conversions were calculated by  $^1\text{H-NMR}$  integral comparison between total aromatic signals and alkene (or alkane for hydrogenated product). The duration of the reaction seems to have little effect on the conversion to isomerised product (entries 1 – 3). The conversion to hydrogenated compound (**2.7**) is favoured by longer reaction times, going from 45% in 5 minutes to 61% in 60 minutes (entries 1 – 3). No starting material remains even after 5 minutes. Considering isomerised conversions are 30 – 33% at every reaction time, it is unlikely that the isomerised 1-phenylbut-1-ene (**2.4**) is quickly hydrogenated to 1-butylbenzene. When reacting in absence of DBU (entry 4), only minimal hydrogenated compound is formed, and a large excess of isomerised product is formed. Base is usually required in 2-propanol transfer hydrogenations to deprotonate the alcohol, rendering the alpha-hydrogen more labile.<sup>57</sup> Interestingly, no significant amount of 4-phenyl-2-butene is formed at any reaction time. Figure 2.4 shows that after a simple extraction with  $\text{CH}_2\text{Cl}_2$  and water a relatively clean  $^1\text{H-NMR}$  spectrum can be obtained containing a mixture of the hydrogenated and isomerised products. Product signals were assigned using 2D experiments such as COSY, HSQC and HMBC.



**Scheme 2.6** Synthesis of 4-phenylbut-1-ene.

**Table 2.4** Catalytic isomerisation and hydrogenation of 4-phenylbut-1-ene by varying time.

<sup>a</sup>Reaction without DBU. <sup>b</sup>Reaction in absence of  $[\text{RuCp}(\text{NCMe})_3]\text{PF}_6$ .



Entry	Time (min)	Conversion to isomerised 2.4 (%)	Conversion to hydrogenated 2.7 (%)
1	60	30	61
2	15	33	51
3	5	33	45
4 <sup>a</sup>	60	79	3
5 <sup>b</sup>	60	0	0

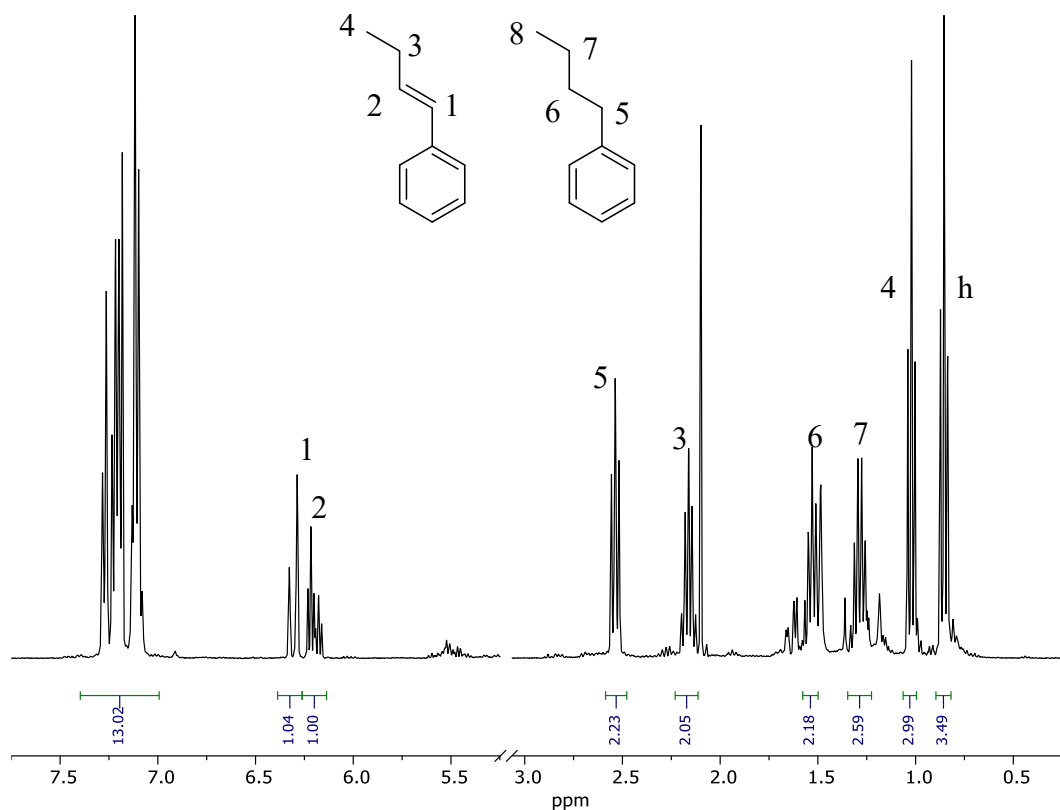
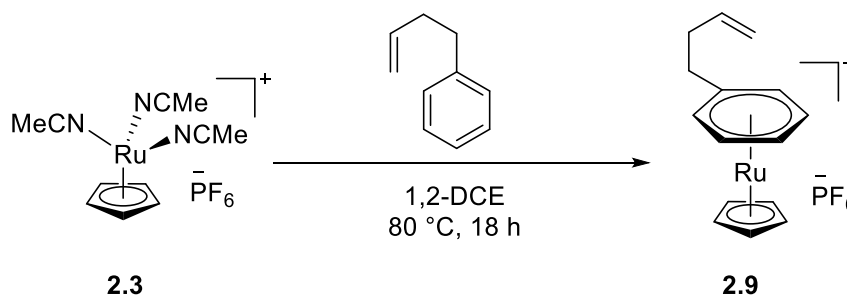


**Figure 2.4**  $^1\text{H-NMR}$  spectrum of reaction mixture after extraction in  $\text{CH}_2\text{Cl}_2$  and water ( $\text{CDCl}_3$ , 298 K, 400 MHz).

To determine if isomerisation and hydrogenation of 4-phenylbut-1-ene was occurring via an  $\eta^6$ -coordination mechanism, its complex with ruthenium was synthesised according to Scheme 2.7. Elemental analysis should be carried out in future to determine the purity of the complex.



**Scheme 2.7** Synthesis of  $[\text{RuCp}(\eta^6\text{-4-phenylbut-1-ene})]\text{PF}_6$ .

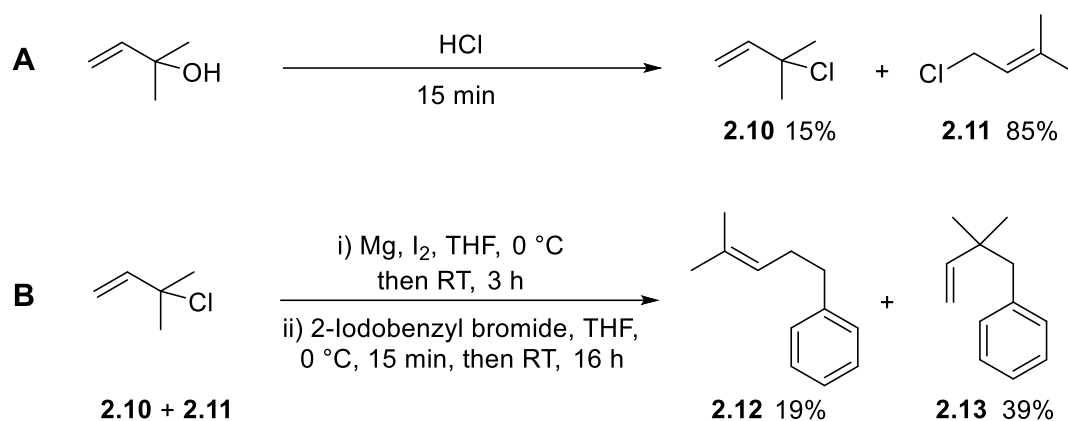
When complex **2.9** was reacted at 140 °C in 2-propanol for 1 hour, it was apparent that hydrogenation had occurred to give  $\eta^6$ -butylbenzene complex, as shown by  $^1\text{H-NMR}$ . In addition, no alkene signals could be found, suggesting that no isomerisation was happening. ESI-MS showed a peak for  $m/z = 301$  which corresponds to the same hydrogenated complex

(**2.9**-PF<sub>6</sub>). Under the same conditions but with 2-methyl-2-propanol instead of 2-propanol as reaction solvent, no hydrogenated product could be found, and only isomerised compound was evident. A peak with  $m/z = 299$  was found in ESI-MS which corresponds to the isomerised product and no signal for hydrogenated product could be identified. This information suggests that transfer hydrogenation is dependent on the solvent used and that arene  $\pi$ -coordination could potentially accelerate the reaction.

### 2.2.3 Synthesis of a Hindered Alkene

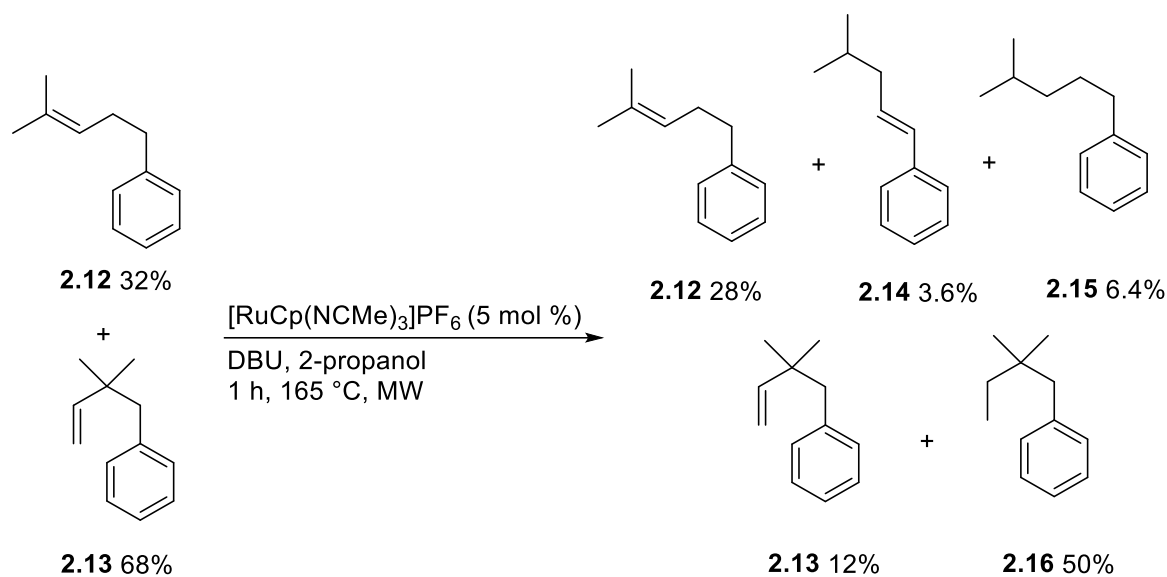
Suppressing or controlling these hydrogenation and isomerisation reactions could prove beneficial for radical cyclisations, also structurally modifying the starting material could provide mechanistic detail about the reactions. (2,2-Dimethylbut-3-en-1-yl)benzene (**2.13**) was synthesised according to Scheme 2.8, the idea being that dimethyl groups will prevent isomerisation of the alkene all the way to the styrene position. According to the Thorpe-Ingold effect, two methyl groups should also encourage the cyclisation reaction.<sup>58</sup> Reacting 2-methyl-3-buten-2-ol with HCl forms the chloro-substituted alkene as two isomers, with 85% being the more stable primary alkyl chloride (**2.11**) and 15% being the tertiary alkyl chloride (**2.10**). Despite a high formation of primary alkyl chloride, which is undesirable, formation of the Grignard reagent allows both chlorides to react preferentially through the tertiary isomer. This is evidenced in the reaction of crude alkyl chlorides with 2-iodobenzyl bromide where the tri-substituted alkene (**2.12**) is formed in a 19% yield and the monosubstituted in a 39% yield (**2.13**). The <sup>1</sup>H-NMR spectrum showed that the iodide was lost in the reaction, possibly because unreacted magnesium in the reaction flask forms the aromatic Grignard of 2-iodobenzyl bromide, which is then protonated after acidic workup. This was confirmed by GCMS which showed two products with  $m/z = 160$ . However, the aryl iodide is not needed to assess the reactivity of the alkenes towards hydrogenation and isomerisation. The isomers were difficult to separate by column chromatography and so were used as a mixture in hydrogenation/isomerisation reactions.





**Scheme 2.8** **A** Synthesis of 3-chloro-3-methylbut-1-ene. **B** synthesis of (2,2-dimethylbut-3-en-1-yl)benzene.

The sterically crowded alkenes were then subject to hydrogenation/isomerisation conditions as described in Scheme 2.9. The starting reaction mixture consisted of a mixture of 32% **2.12** and 68% **2.13**. Following extraction with dichloromethane and water the resulting compounds were analysed by  $^1\text{H-NMR}$  and GCMS. The  $^1\text{H-NMR}$  showed a significant decrease in alkene signals arising from compound **2.13** (relative to compound **2.12**), suggesting that it reacts much faster than **2.12**. GCMS peaks were assigned using predicted fragmentation patterns of the compounds (Figure 2.5). Three peaks (**2.13**, **2.14** and **2.12**) contained  $m/z = 160$  corresponding to the three un-hydrogenated compounds. **2.14** fragmented into the diagnostic signal  $m/z = 117$  which arises from the loss of the terminal isopropyl group. The retention times of the starting mixture of **2.12** and **2.13** were compared to those of the product mixture in Scheme 2.6 B and assigned accordingly. Peak **2.16** and **2.15** both contained  $m/z = 162$  signals, where **2.16** was assigned to 3.35 minutes (see Figure 2.5) as it contained a fragment signal at  $m/z = 71$  which corresponds to the relatively stable tertiary 2-methylbutane cation.



**Scheme 2.9** Potential products from hydrogenation and isomerisation of sterically hindered alkenes.

Integration analysis of the GCMS signals allows comparisons between compounds, revealing that of the total areas, **2.12** remains in 28% (starting material contained 32% **2.12**). The relative concentration of **2.13** dropped from 68% to 12%, which agrees with the  $^1\text{H-NMR}$  spectrum. The two possible products from either hydrogenation or isomerisation of compound **2.12** are **2.15** and **2.14**, which, when combined with remaining **2.12**, account for 38% of total products. A 38% concentration is higher than the amount of **A** that was initially put in. The reason for this could be that the peaks at 3.33 minutes and 3.35 minutes have a slight overlap near the baseline, possibly causing some inaccuracies in integral calculation. The proposed product from the hydrogenation reaction of **2.13** is **2.16** and this accounts for 50% of the resulting mixture. In conclusion, this investigation confirms that alkenes with greater substitution are more resistant to hydrogenation/isomerisation and that isomerisation can be prevented by implementing a dimethyl substitution on the aliphatic tether.

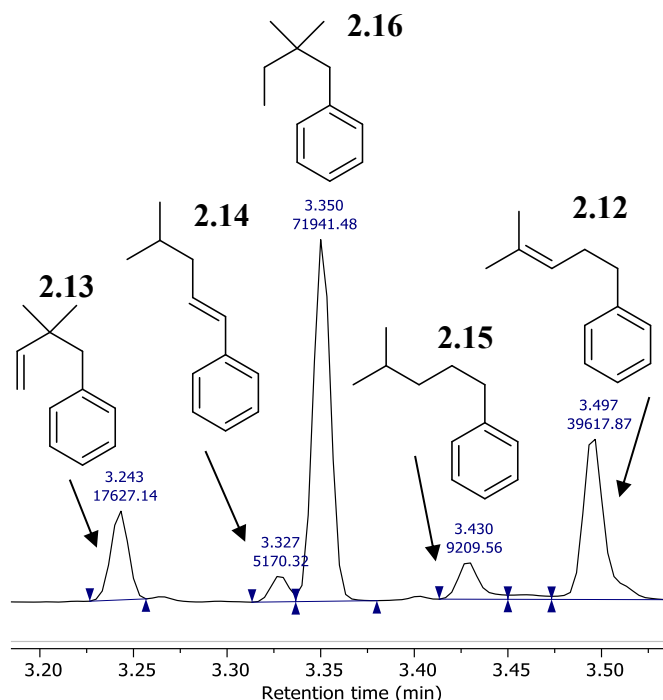


**Figure 2.5** GCMS of reaction mixture (Scheme 2.8) after purification by extraction in  $\text{CH}_2\text{Cl}_2$  and water.

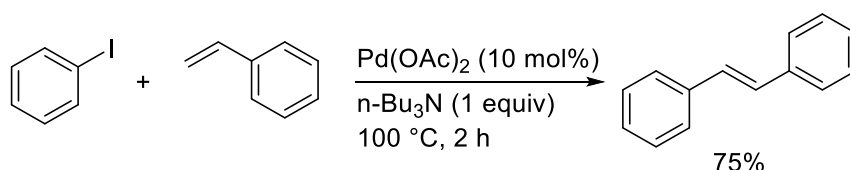
## 2.3 Conclusions and Future Work

In summary, clear evidence was found for the radical cyclisation product, which adds support to a radical intermediate in the catalytic hydrodeiodination. The yields of this reaction were very low and so the use of this system to generate more elaborate cyclisation products was not attempted. One reason for the low cyclisation yield was found to be that  $[\text{RuCp}]^+$  catalyses alkene hydrogenation and isomerisation in very short reaction times and leads to deactivated compounds that are unable to cyclise. Early studies show that introducing methyl groups on the tethered alkene can modify reactivity significantly, with trisubstituted alkenes being comparatively more unreactive than monosubstituted analogues. This is likely a combination of greater stability in more-substituted alkenes arising from hyperconjugation and steric effects. The use of trisubstituted alkenes possibly provides a better alternative starting material for this type of hydrodeiodination-cyclisation reaction. Iodinated analogues of these alkenes should be synthesised to establish whether the yield of cyclisation is significantly increased.

# 3. Ruthenium-Catalysed Aromatic Halogen Exchange

## 3.1 Introduction

Aryl halides are among the most useful compounds in synthetic chemistry. Their ability to undergo transformations at the carbon-halogen bond means they are ubiquitous synthetic intermediates for carbon-carbon and carbon-heteroatom bond formation. Notably, cross-coupling reactions such as the palladium catalysed Sonogoshira, Heck (Scheme 3.1), Ullman and Suzuki reactions are used routinely in academic and industrial laboratories.<sup>59</sup> Aryl halides have also found use in pharmaceuticals and as radionuclide carriers for molecular imaging.<sup>60,61</sup> Therefore, the development of methods that allow introduction of aryl halides and interchange between halogens offer widespread impacts.



**Scheme 3.1.** Palladium-catalysed Heck reaction.<sup>62</sup>

Simple halogenation of aromatics is typically done *via* the Sandmeyer reaction<sup>63</sup> (Figure 3.1 A) or electrophilic aromatic substitution with molecular halogens and Lewis acid catalysts (Figure 3.1 B), however these methods suffer from poor functional group tolerance and regioselectivity issues.<sup>64</sup> More recently, halogenation has been achieved using transition metal catalysts, such as the palladium-catalysed conversion of aryl triflates to halides by Buchwald and co-workers (Figure 3.1 C).<sup>65</sup> Aryl iodides are typically more reactive than bromides and chlorides in cross-coupling reactions, and nucleophilic aromatic substitutions show the reverse reactivity.<sup>66</sup> Therefore, selectively exchanging the halogen in the aryl halide can allow reactivity to be enhanced or suppressed.

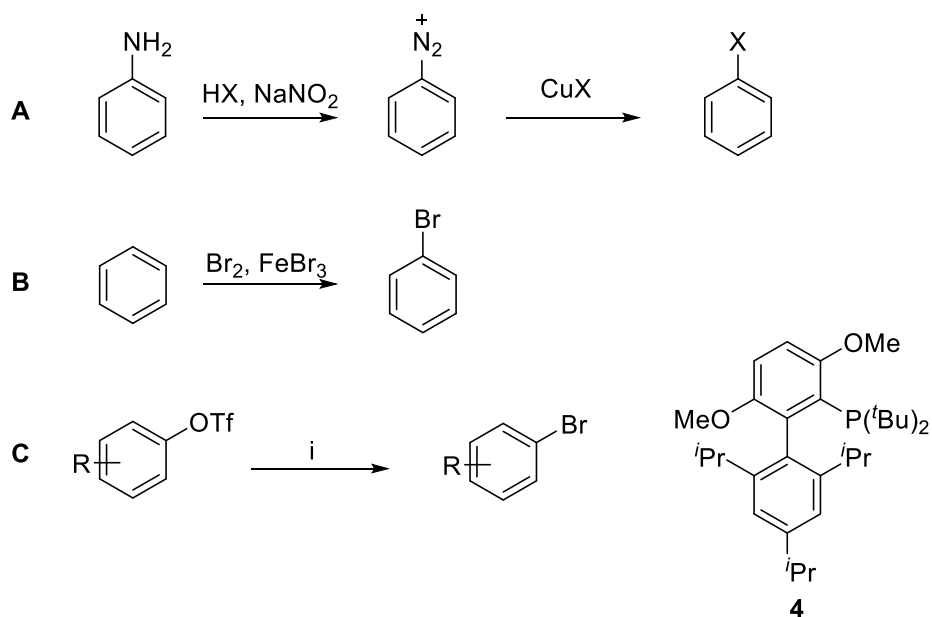


**Figure 3.1.** **A** Sandmeyer reaction. **B** Bromination via electrophilic aromatic substitution. **C** Palladium-catalysed conversion of triflates to bromides. Reagents and conditions: (i)  $Pd_2(dba)_3$  (1.5 – 2.5 mol%) / **4** (3.75 – 6.25 mol%) /  $KBr$  (1.5 equiv) / PEG3400 / 2-butanone (1.5 equiv) /  $iBu_3Al$  (1.5 equiv) /  $PhCH_3$  / 100 °C.

### 3.1.1 Transition Metal-Catalysed Halogen Exchange

The conversion of heavier aryl halides to lighter ones typically proceed *via* transition metal catalysts, by which a variety of mechanisms are proposed. A classical approach would involve the oxidative addition of the aryl halide to a metal catalyst, followed by ligand exchange and then reductive elimination (Figure 3.2).

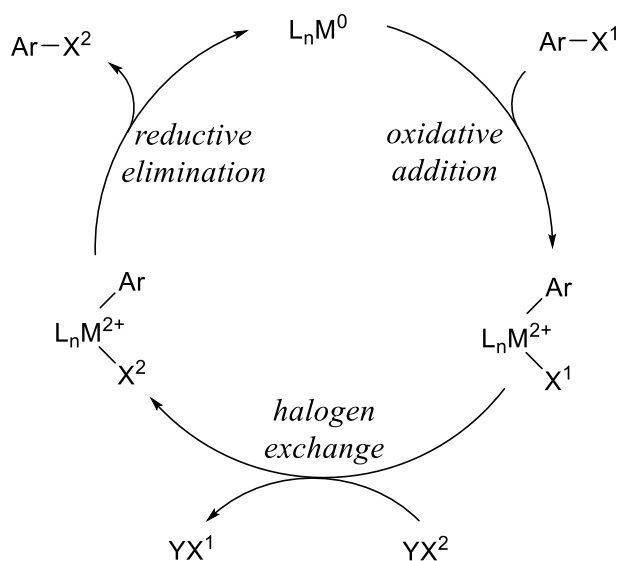
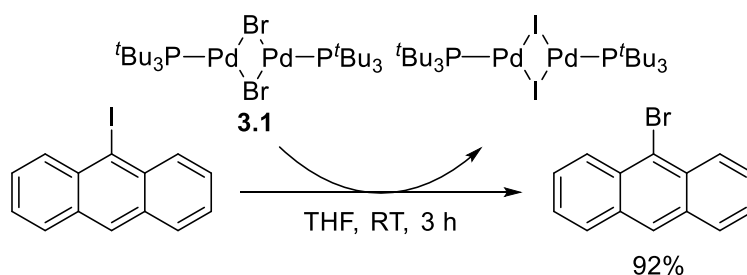


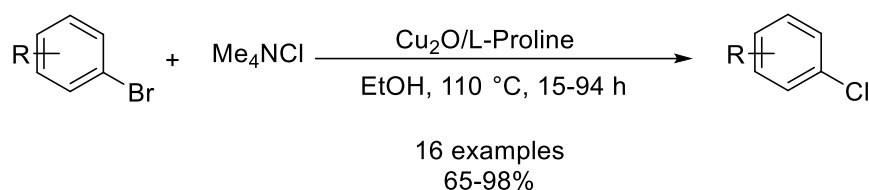
**Figure 3.2.** General metal catalyzed oxidative addition-reductive elimination type halogen exchange.

Aromatic retro-Finkelstein reactions exchange less for more electronegative halides, and are catalysed by many metals.<sup>67,68</sup> In 1975, Cramer and Coulson developed a process in which bromobenzene can be converted to chlorobenzene using a  $\text{NiCl}_2$  catalyst and stoichiometric  $\text{LiCl}$ , albeit with high temperatures of  $210\text{ }^\circ\text{C}$ .<sup>69</sup> An improvement upon this came in 1980 when Kochi and Tsou reported  $(o\text{-tolyl})\text{NiBr}(\text{PET}_3)_2$  as an effective catalyst for the formation of aryl bromides from aryl iodides.<sup>70</sup> Using tetrabutylammonium bromide as the bromine source, they achieved yields of 64-76% at  $80\text{ }^\circ\text{C}$  in benzene for 20 hours. Moreover, upon the addition of quinones and nitroarenes the halogen exchange was suppressed, suggesting a radical process. Subsequently, Burrows reported chlorination of aryl iodides *via* the same mechanism but with chlorine radicals generated from  $\text{NaOCl}$ .<sup>71</sup> Palladium catalysts, while less used than nickel, can also catalyse halogen exchanges. A dinuclear palladium (I) complex (**3.1**) was found to convert aryl iodides to bromides *via* a proposed oxidative addition mechanism, evidenced by a low activation barrier for the oxidative addition step of aryl iodides through calculations (Scheme 3.2).<sup>72</sup>



**Scheme 3.2** Halogen exchange by a Pd(I) complex.

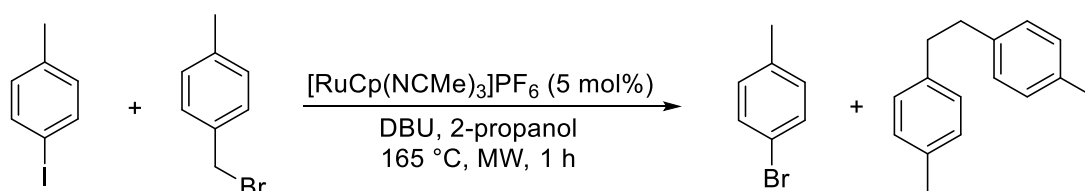
Copper can offer cheaper alternatives to the palladium catalysts discussed above. Reported in 2012 was a copper-catalysed conversion of aryl and heteroaryl bromides to chlorides by Feng (Scheme 3.3).<sup>73</sup> Using copper oxide as a precatalyst with L-proline ligand, yields of 65-98% are reported for 16 examples of aryl halides and with excellent functional group tolerance. The same conditions catalyse the bromide to chloride halogen exchange of 7 examples of heteroaryls, such as 2-chloropyridine and 2-chloro-5-nitropyridine with yields of 93% and 52% respectively. In addition, the source of chlorine, tetramethylammonium chloride, is cheap and reaction conditions are mild which represents a significant improvement over previous methods in copper catalysed halogen exchange.



**Scheme 3.3** Copper-catalysed aromatic retro-Finkelstein reaction of aryl bromides to aryl chlorides.

### 3.1.2 Ruthenium-Catalysed Halogen Exchange

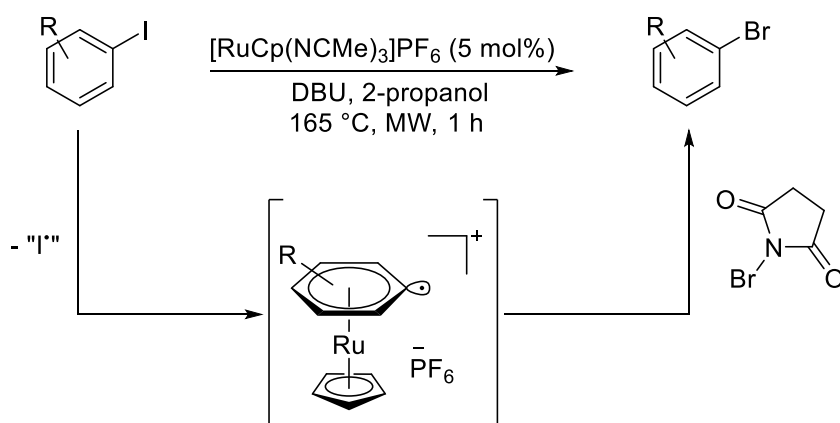
Another approach for halogen exchange would be one in which the aryl halide  $\eta^6$ -coordinates to a transition metal, further activating the carbon-halogen bond, to undergo nucleophilic aromatic substitution by another halide. In 2015, Grushin reported a regio- and chemo-selective fluorination of aryl chlorides, facilitated by transient  $\eta^6$ -coordination to a Ru(II) catalyst (see Section 1.2.2).<sup>47</sup> Aryl radicals are another possibility, in which the starting aryl halide is reduced, triggering the cleavage of the carbon-halogen bond and subsequent recombination with another halide. As discussed in Section 1.2.3, previous unpublished work from the Walton group suggests that  $\eta^6$ -coordination to ruthenium may catalyse the formation of aryl radicals from aryl iodides, leading to hydrodeiodination.<sup>48</sup>



**Scheme 3.4** Reaction of 4-iodotoluene with 4-methylbenzyl bromide and the observed products.

The ruthenium-catalysed hydrodeiodination of aryl iodides, discussed in Section 1.2.3 was initially considered to be proceeding *via* an aromatic carbanion. To help provide evidence

for this proposal, 4-methylbenzyl bromide was added to the reaction mixture to trap the carbanion (Scheme 3.4). Rather than seeing the expected substitution product (tolyl addition), the formation of 4-bromotoluene was observed. This signified that the mechanism was probably occurring through an aryl radical intermediate, which abstracts bromine from 4-methylbenzyl bromide. A second unexpected product was the formation of 1,2-*para*-ditolyethane in an apparent  $sp^3$  carbon homocoupling reaction. Should the bromination reaction proceed *via* a radical mechanism, it would be expected that this radical intermediate can react with a source of radical halogen, such as NBS. NBS, an inexpensive brominating agent, also has the advantage that its byproduct, succinimide, can easily be recovered and rebrominated.<sup>74</sup> The proposed radical intermediate and bromination are shown in Scheme 3.5. Moreover, Houk has shown that  $\eta^6$ -coordination to chromium stabilises radical formation by up to  $10^5$  fold, and similar a similar stabilisation should be likely with ruthenium.<sup>49</sup>



**Scheme 3.5** Proposed pathway for the radical halogen exchange of aryl iodides to aryl bromides.

## 3.2 Results and Discussion

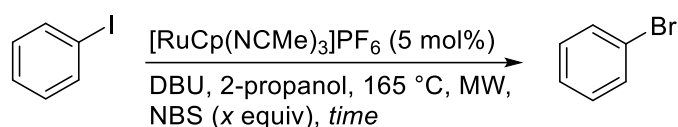
### 3.2.1 Initial Optimisations

We set out to investigate the ruthenium-catalysed conversion of iodobenzene into bromobenzene. Initial optimisations focused on NBS equivalents and reaction time, using the previously discussed hydrodeiodination conditions with 2-propanol as the standard conditions (Table 3.1). Under standard conditions with 1 equivalent of NBS, bromobenzene was being formed albeit in a low conversion of 8% (entry 1). Increasing the equivalents of NBS to 2 provided no benefit and increasing to 3 was detrimental (entries 2 and 3). With 1 equivalent of NBS, the reaction time was doubled to 2 hours providing an increase to 14%



conversion and increasing the reaction further to 5 hours resulted in a 17% conversion (entries 4 and 5). A conversion increase of 3% from an additional 3 hours of reaction time was deemed inefficient and so further optimisations were carried out using 2 hours reaction time. An expected by-product of this reaction is benzene, arising from the hydrodeiodination of iodobenzene. Conversions to bromobenzene were calculated from integral comparisons of product to starting material, accounting for any benzene formed.

**Table 3.1** Catalytic halogen exchange of iodobenzene with varying time and NBS equivalents.

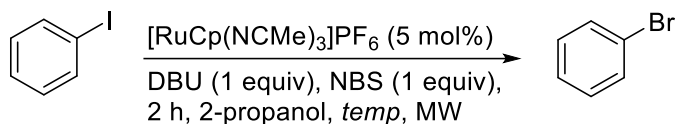


Entry	NBS equiv.	Time (h)	Conv. (%)
1	1	1	8
2	2	1	8
3	3	1	2
4	1	2	14
5	1	5	17

Next, the reaction temperature was investigated (Table 3.2). Should the reaction proceed *via*  $\eta^6$ -coordination, a higher temperature should increase conversions as arene exchange would be the expected rate determining step.<sup>38</sup> The reaction was tested at 120 °C and minimal amounts of bromobenzene were formed, which, if proceeding *via* a similar mechanism to hydrodeiodination, is expected (entry 1). Similarly, reaction at 140 °C resulted in only 2% conversion. In order to explore higher temperatures, a higher boiling point solvent was required. Unlike in Chapter 2, 1-octanol is acceptable for halogen exchange as aliphatic signals are not required to be analysed and so it was used as an alcohol substitute. The reaction was carried out at 165 °C in 1-octanol to establish a comparison between 2-propanol, however an insignificant conversion of 3% was observed (entry 4). Nonetheless, 180 °C was tested but conversions were still low (entry 5). 1-Octanol is significantly less polar than 2-propanol as a result of its long hydrophobic alkyl chain, and this could possibly be causing

solubility issues. It could also provide information regarding the mechanism, as linear alcohols are less coordinating towards metals.<sup>75</sup>

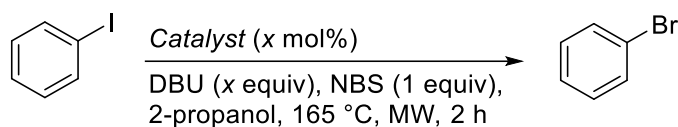
**Table 3.2** Catalytic halogen exchange of iodobenzene at varying temperatures. <sup>a</sup>1-octanol as solvent. <sup>b</sup>Reaction for 5 hours using 1-octanol as solvent.



Entry	Temperature (°C)	Conv. (%)
1	120	1
2	140	2
3	165	14
4	165	3 <sup>a</sup>
5	180	2 <sup>b</sup>

Retaining the 165 °C reaction temperature, the effect of catalyst and catalyst loading was investigated (Table 3.3). The reaction was tested in the absence of ruthenium catalyst to prove that it was catalytic, with a 0% conversion. (entry 1). When reacting with 1 mol% of  $[\text{RuCp}(\text{NCMe})_3]\text{PF}_6$ , no bromobenzene was observed in the <sup>1</sup>H-NMR spectrum and doubling the standard catalyst loading to 10% was unfruitful (entries 2 and 4). Due to low conversions with  $[\text{RuCp}(\text{NCMe})_3]\text{PF}_6$ , the more electron rich  $[\text{RuCp}^*(\text{NCMe})_3]\text{PF}_6$  was tested for its halogen exchange ability. Remarkably, the conversion more than doubled to 31% (entry 5). The pentamethylcyclopentadienyl ligand is more electron rich than cyclopentadienyl, suggesting that arene dissociation could be limiting when using the standard  $[\text{RuCp}]^+$  fragment. Lastly, halogen exchange was tested in the absence of any base (entry 6). In ruthenium catalysed hydrodeiodinations, stoichiometric base is required to attain high conversions. In halogen exchange the role of the base is unclear, as there appears to be no transfer of proton to the product. In addition, the absence of base should suppress any benzene formation, which was commonly observed in the previous optimisations. It was found that reaction without DBU offered a slight increase in conversion to 37%.

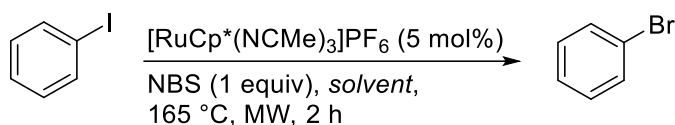
**Table 3.3** Catalytic halogen exchange of iodobenzene under various DBU equivalents and catalyst loadings.



Entry	DBU equiv.	Catalyst	Catalyst loading (mol%)	Conv. (%)
1	1	None	0	0
2	1	[RuCp(NCMe) <sub>3</sub> ]PF <sub>6</sub>	1	0
3	1	[RuCp(NCMe) <sub>3</sub> ]PF <sub>6</sub>	5	14
4	1	[RuCp(NCMe) <sub>3</sub> ]PF <sub>6</sub>	10	12
5	1	[RuCp*(NCMe) <sub>3</sub> ]PF <sub>6</sub>	5	31
6	0	[RuCp*(NCMe) <sub>3</sub> ]PF <sub>6</sub>	5	37

In the temperature investigation (Table 3.2), it was observed that alcohol solvents, despite having the same functional group, afford different conversions. Table 3.4 focuses on solvent and concentration optimisations with varying degrees of success. To determine if the reaction was dependent on concentration, half and double concentration halogen exchanges were tested (entries 1 – 3). The results suggested that concentration did not have a significant effect on conversion. While conversion was observed in all solvents tested, MeCN and EtOAc performed the worst (entries 7 – 8). Bromobenzene was formed in 51% conversion with 1-octanol as a solvent, which is an interesting result as when using [RuCp]<sup>+</sup> instead of [RuCp\*]<sup>+</sup> 1-octanol is outperformed significantly by 2-propanol (entry 5). Ethanol was also tested and afforded lower conversions than both 1-octanol and 2-propanol (entry 6). THF and 2-MeTHF were tested and the latter performed almost twice as well as the former (entries 4 and 9).

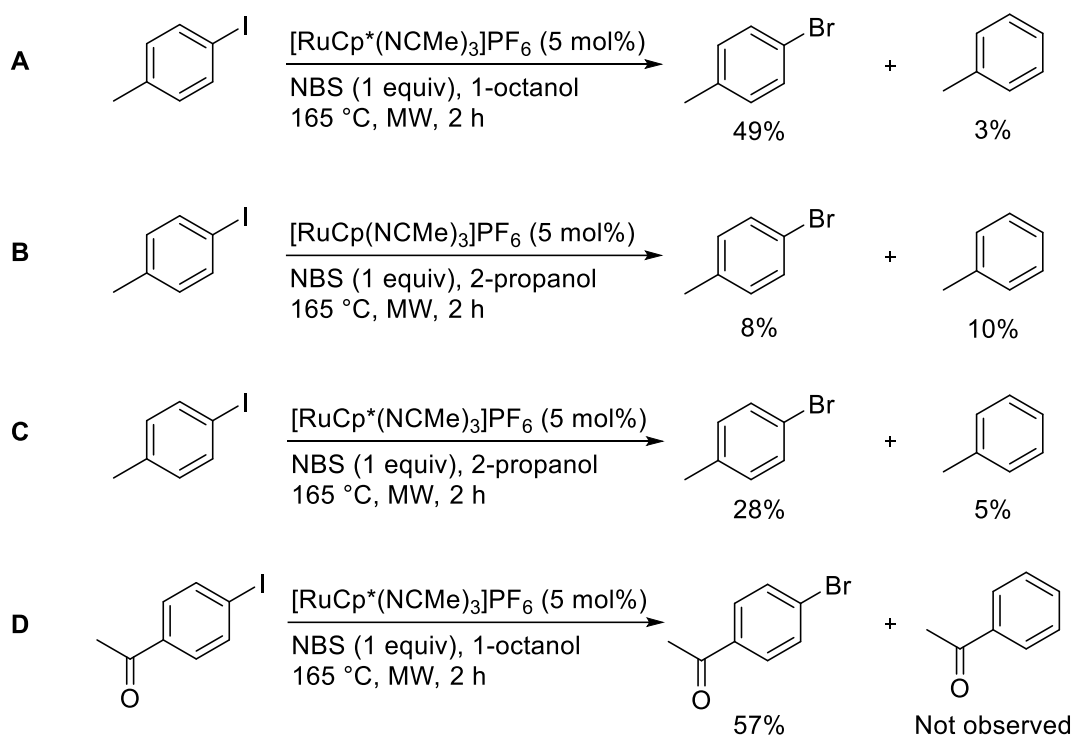
**Table 3.4** Catalytic halogen exchange of iodobenzene with varying solvents and concentrations.



Entry	Solvent	Concentration (mol dm <sup>-3</sup> )	Conv. (%)
1	2-propanol	0.346	37
2	2-propanol	0.173	35
3	2-propanol	0.692	36
4	THF	0.346	21
5	1-octanol	0.346	51
6	EtOH	0.346	25
7	EtOAc	0.346	2
8	MeCN	0.346	6
9	2-MeTHF	0.346	39

The previously stated differences between catalysts in 1-octanol and 2-propanol could provide valuable mechanistic insight to this ruthenium catalysed halogen exchange. Higher conversions are observed in 2-propanol only when using  $[\text{RuCp}]^+$  whereas the reverse is true for  $[\text{RuCp}^*]^+$  and 1-octanol. It is expected that pentamethylcyclopentadienyl would be harder to solubilise with polar solvents, but this was not an issue with the previously discussed hydrodeiodination and cyclisation. When using  $[\text{RuCp}^*]^+$ , bromobenzene formation seems to favour solvents which are less coordinating, evidenced by the higher conversions in 2-MeTHF and 1-octanol. However, 2-propanol and EtOAc would be anomalies with this theory, as their conversions are opposite to what would be expected. Lower conversions in polar solvents could be due them favouring heterolytic cleavage of the NBS Br-N bond, forming bromonium ions that could react *via* electrophilic aromatic substitution.<sup>76</sup> Ultimately, mechanistic detail cannot be confirmed solely from relative conversions in different solvents.

With 51% conversion being the highest observed so far, it was necessary to investigate aryl iodides of a different electronic nature. Firstly, 4-iodotoluene was subjected to halogen exchange conditions as described in Scheme 3.6. A conversion of 49% to 4-bromotoluene was observed under the current best conditions, which is comparable to the 51% conversion observed when reacting iodobenzene under the same conditions (Scheme 3.6 A). To determine if, like iodobenzene, conversions show significant variation depending on solvent, 4-iodotoluene was reaction in 2-propanol. With  $[\text{RuCp}]^+$  as catalyst, 8% conversion was observed which confirmed the importance of the  $[\text{RuCp}^*]^+$  catalyst (Scheme 3.6 B). When using  $[\text{RuCp}^*]^+$ , 4-bromotoluene was formed in 28% conversion which is slightly less than the 37% conversion when reacting iodobenzene under identical conditions (Scheme 3.6 C). Interestingly the amount of toluene formed, which is thought to be formed by a radical mechanism, is slightly different between conditions. Next, the electron-deficient iodoarene 4-iodoacetophenone was reacted under halogen exchange conditions and 4-bromoacetophenone was formed in 57% conversion, a markedly increase over electron richer arenes (Scheme 3.6 D). The hydrodeiodinated by-product acetophenone was not observed by  $^1\text{H-NMR}$ , evidenced by the absence of any triplet signals in the aromatic region. This increase in yield over electronically neutral arenes could be due to electron deficient substrates binding weaker to ruthenium, facilitating faster arene exchange. However, further investigations need to be carried out to elucidate the reaction mechanism.

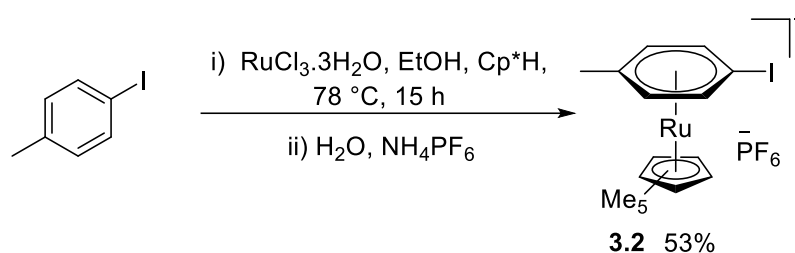


**Scheme 3.6** Reactions of 4-iodotoluene under various conditions. **A** best halogen exchange conditions. **B**  $[\text{RuCp}]^+$  catalyst with 2-propanol. **C**  $[\text{RuCp}^*]^+$  catalyst with 2-propanol. **D** Reaction of 4-iodoacetophenone under halogen exchange conditions.

### 3.2.2 Mechanistic Studies

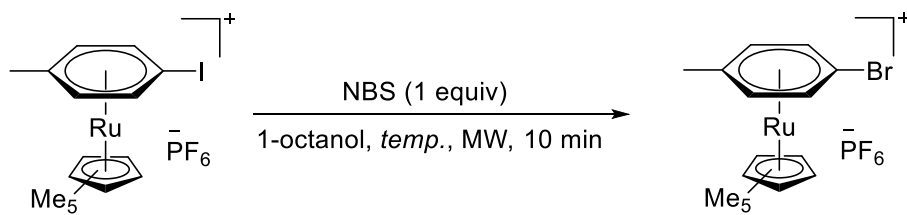
The result that  $[\text{RuCp}^*]^+$  provides much greater conversions than  $[\text{RuCp}]^+$  indicates that the strong electron donating character and/or the increased sterics of  $\text{Cp}^*$  plays a significant role in the catalytic mechanism. With the evidence that electron-deficient arenes (4-iodoacetophenone) react better than electron rich (4-iodotoluene) and electron neutral (iodobenzene), tests were carried out to determine if iodoarenes are reacting *via* an  $\eta^6$ -coordination mechanism.  $[\text{RuCp}^*(\eta^6\text{-4-iodotoluene})]\text{PF}_6$  (**3.2**) was synthesised according to Scheme 3.7 and fully characterised by multinuclear NMR and mass spectrometry. During the reaction, ethanol acts as a mild reducing agent, reducing the ruthenium species from a 3+ to the 2+ oxidation state.<sup>77</sup> Following the addition of 4-iodotoluene and pentamethylcyclopentadiene, the sandwich complex is formed over 15 hours of reflux. Salt metathesis with ammonium hexafluorophosphate results in precipitation of the product from water after aqueous workup of the reaction solution. Despite recrystallising and washing the complex with diethyl ether, elemental analysis was 1.42% out on carbon.  $^1\text{H-NMR}$  showed multiple small signals between 2.05 ppm and 1.66 ppm, suggesting the complex was slightly

impure. However, the diagnostic region between 8 ppm and 5 ppm contained no impurities, so the complex was used without further purification. As future work, a different purification technique should be used to attain clean spectra and elemental analysis.



**Scheme 3.7** Synthesis of  $[\text{RuCp}^*(\eta^6\text{-4-iodotoluene})]\text{PF}_6$

Complex **3.2** was then reacted under halogen exchange conditions at 140 °C and 165 °C (Scheme 3.8). 140 °C was chosen as a test temperature as in optimisations only minimal conversions were recorded at this temperature, presumably because arene exchange is inefficient. The  $^1\text{H-NMR}$  spectrum of the reaction at 140 °C after 10 minutes showed that minimal 4-bromotoluene complex had formed (9% conversion), but nonetheless product was observed. At 165 °C for 10 minutes the  $^1\text{H-NMR}$  spectrum showed significantly more signals than that of the reaction at 140 °C (Figure 3.3 B). On binding arenes to ruthenium, aromatic signals experience a decrease in chemical shift. The arene rings of three main complexes are visible in the spectrum in the chemical shift range 5.5 ppm to 6.5 ppm: hydrodeiodinated arene, brominated product and starting material. The peak that appears as a triplet at 6.4 ppm arises from overlap of starting material and brominated product, as confirmed by a COSY spectrum. Along with the  $\pi$ -coordinated species, there were also significant amounts of uncoordinated arenes: both 4-bromotoluene and 4-iodotoluene. Using integration, the relative amounts of the various bound and unbound compounds were calculated. The combined integral of iodinated compounds (bound and unbound) account for 26% of the reaction mixture, while brominated compounds (bound and unbound) account for 38% and toluene complex accounts for 36%. When correlating these relative values to the conversions in Scheme 3.6 A, significantly more hydrodeiodinated compound and less brominated product is observed. The signal at 5.8 ppm, together with one at 5.0 ppm, appears to be that of a terminal alkene, possibly from the dehydration of 1-octanol.



**Scheme 3.8** Reaction of  $[\text{RuCp}^*(\eta^6\text{-4-iodotoluene})]\text{PF}_6$  with NBS at 140 °C and 165 °C.

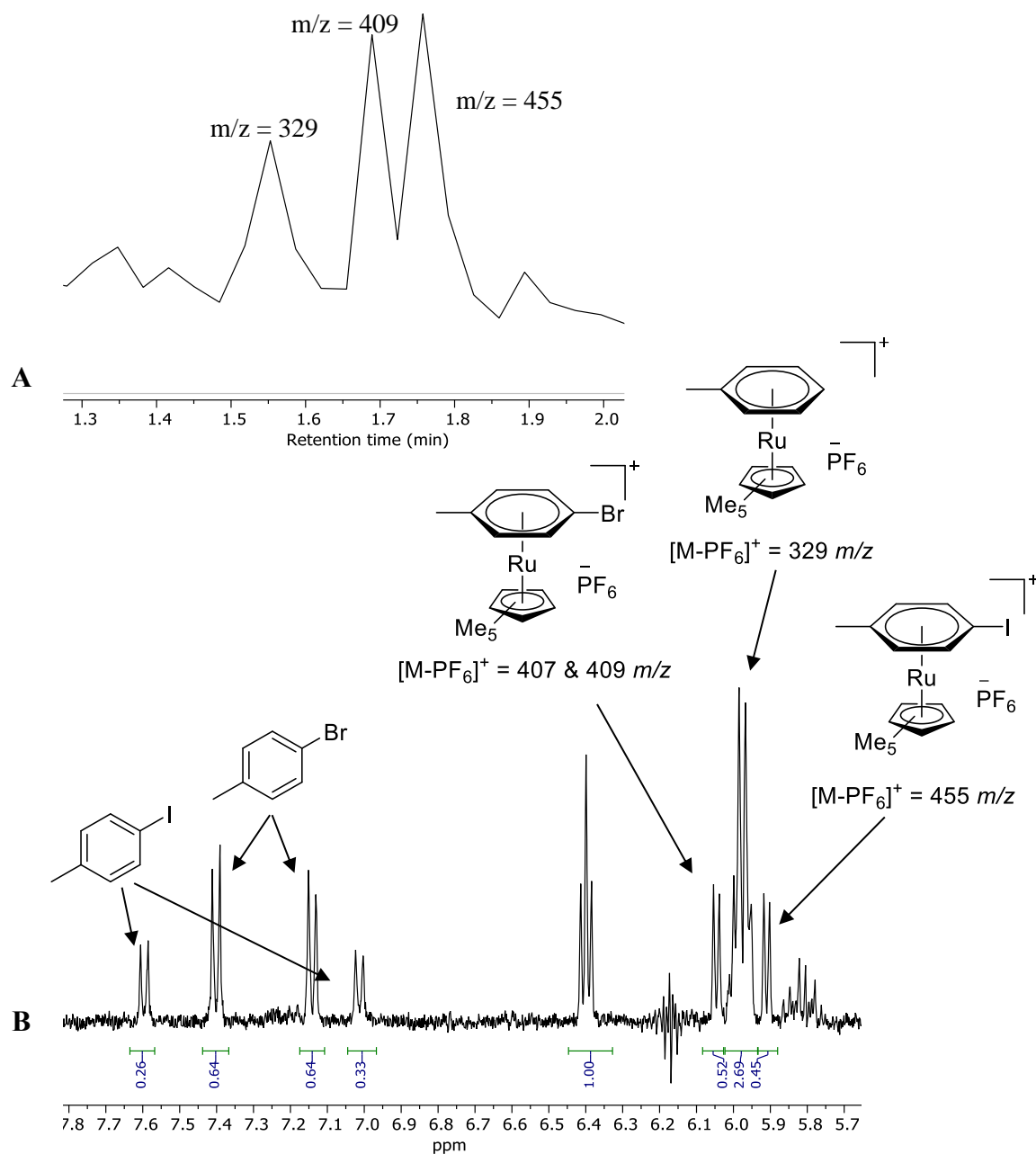
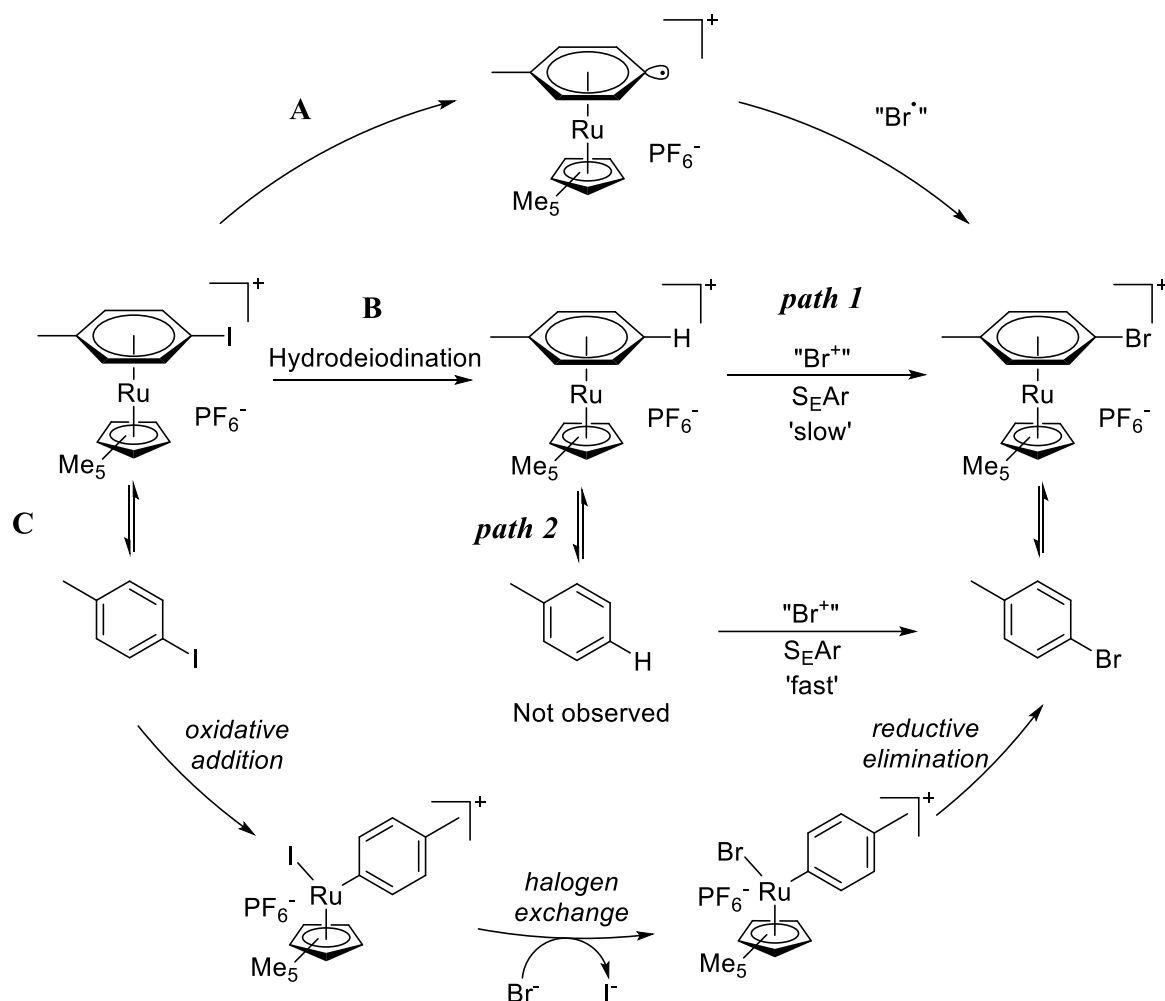


**Figure 3.3** Spectra of reaction mixture after reacting complex 3.2 under halogen exchange conditions at 165 °C for 10 minutes. **A** ESI<sup>+</sup> mass spectrum. **B** <sup>1</sup>H-NMR spectrum ( $\text{CO}(\text{CD}_3)_2$ , 298 K, 400 MHz).



Drawing conclusions about the reaction mechanism remains difficult. Hydrodeiodination appears to occur *via*  $\pi$ -coordination to ruthenium, as evidenced the absence of free toluene in the  $^1\text{H-NMR}$  spectrum, but hydrodeiodination typically requires basic conditions so a 36% conversion suggests there is a base present. Succinimide, a by-product of NBS brominations, is basic and could potentially allow the formation of toluene. Potential pathways for halogen exchange are summarised in Scheme 3.9. The observed free 4-bromotoluene can arise from two mechanisms: 4-bromotoluene forms while  $\eta^6$ -coordinated to ruthenium and then decomplexes from ruthenium (Scheme 3.9 A and B path 1) or 4-iodotoluene decomplexes from ruthenium and then bromination proceeds *via* a different mechanism (Scheme 3.9 C). Another possibility is an electrophilic aromatic substitution reaction of toluene with NBS, either bound to ruthenium or unbound (Scheme 3.9 B path 1 or 2). It would be expected that free toluene, which is not observed in the  $^1\text{H-NMR}$  spectrum, is more activated towards  $\text{S}_{\text{EAr}}$  than  $\pi$ -coordinated toluene due to the absence of the electron withdrawing  $[\text{RuCp}^*]^+$ . Moreover, *ortho*-bromotoluene would be expected to form in addition to *para*-bromotoluene, but the *ortho* product is not seen in the  $^1\text{H-NMR}$ . This suggests that an  $\text{S}_{\text{EAr}}$  reaction from toluene (bound or unbound) is not occurring. This was confirmed upon reacting toluene under the conditions in Scheme 3.8 at 165 °C, in which no brominated product was observed by  $^1\text{H-NMR}$  in the absence of ruthenium catalyst.

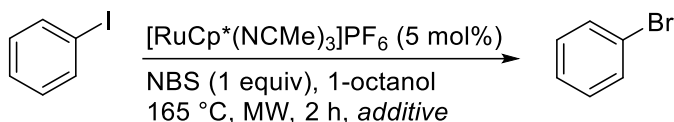


**Scheme 3.9** Possible pathways for [RuCp\*]<sup>+</sup>-catalysed halogen exchange.

As a final investigation, some additives were tested for their effect on halogen exchange. Due to the low optimised conversion of 51%, it was speculated that the starting material and product might be in equilibrium. Finkelstein reactions exploit relative solubilities of halide salts to drive the equilibrium towards the products so a similar approach was attempted with this halogen exchange.<sup>67</sup> Silver hexafluorophosphate was added to the reaction to determine if a less soluble silver iodide would precipitate, however the conversion was lower with the silver addition (Table 3.5, entry 2). Finally, a reaction was attempted with lithium bromide instead of N-bromosuccinimide and interestingly bromobenzene was formed in 52% conversion (entry 3). The fact that iodine is being exchanged by bromide suggests an S<sub>N</sub>Ar or oxidative addition/reductive elimination type reaction (Scheme 3.9 C). However, it is unknown if it is the same mechanism as when using N-bromosuccinimide, which was hypothesised to react as a bromine radical. If they are proceeding *via* the same mechanism, a source of bromide must be available when using NBS. Moreover, oxidative addition type catalysis are known for ruthenium (II), which has been used in the catalytic arylation of

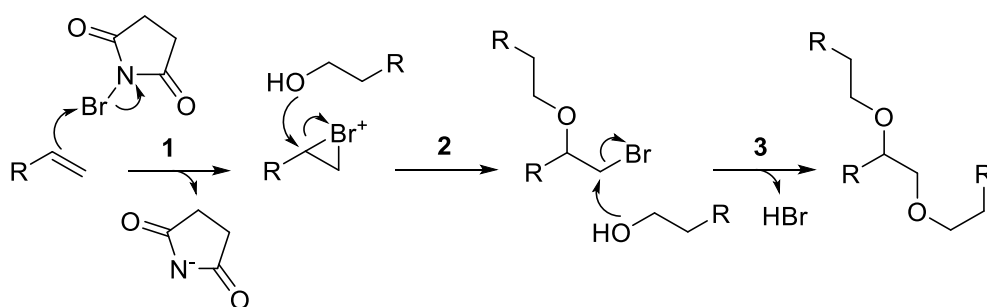
aromatics.<sup>78-80</sup> Specifically, in 2012, Hayashi and co-workers reported a ruthenium-catalysed aryl triflate to halide reaction, which is proposed to be *via* an oxidative addition mechanism.<sup>81</sup>

**Table 3.5** Catalytic halogen exchange of iodobenzene with different additives. <sup>a</sup>Reaction without NBS.



Entry	Additive	Conv. (%)
1	None	51
2	AgPF <sub>6</sub>	34
3	LiBr	52 <sup>a</sup>

An interesting observation from <sup>1</sup>H-NMR is that small amounts of a terminal alkene appear to be forming in the reaction, presumably from dehydration of 1-octanol. NBS is known to react with alkenes to form bromohydrins, which could be a source of bromide.<sup>82</sup> A potential mechanism for the formation of bromide is shown in Scheme 3.10. In step 1, a bromonium ion is formed due to the electrophilic nature of the NBS bromide. This is followed by addition from a solvent molecule in step 2. Step 3 shows nucleophilic substitution of the bromide by another solvent molecule, forming HBr and a diether. However, no evidence of these compounds was found using <sup>1</sup>H-NMR spectroscopy or in mass spectrometry. It is also unknown as to what forms the initial alkene, as alcohol dehydrations are typically catalysed by acids, although it is possible that coordination of solvent to the ruthenium catalyst catalyses its dehydration. This theory does not explain conversions to bromobenzene in solvents which are not known to create bromide in this way, such as THF and 2-MeTHF.

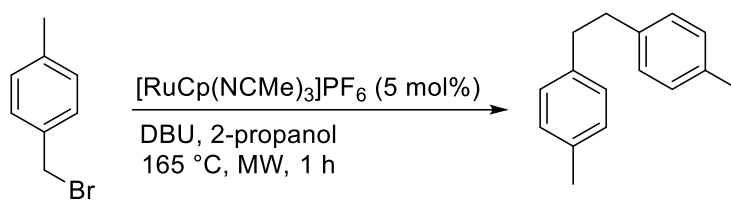


**Scheme 3.10** Potential mechanism for the formation of a bromide species.

### 3.3 Conclusions and Future Work

In summary,  $[\text{RuCp}^*]^+$  was found to catalyse halogen exchange of aryl iodides to aryl bromides in moderate conversions. Although it was initially thought to proceed *via* aryl radical intermediates as a result of deiodination, later evidence suggests it might in react in an  $\text{S}_{\text{N}}\text{Ar}$  or oxidative addition/reductive elimination fashion. Optimisation studies show that electron deficient arenes react with higher conversions than those that are electron rich, supporting this theory. Studies to determine whether aryl bromides were formed *via*  $\eta^6$ -coordinated intermediates showed that this type of coordination probably favours hydrodeiodination, evidenced by the 36% conversion to  $[\text{RuCp}^*(\eta^6\text{-toluene})]\text{PF}_6$ . Future work should focus on investigating the reaction mechanism, which will allow better design of reaction conditions. Following this, the reaction scope should be extended to cover a larger range of substrates, such as those that are more electron-donating, sterically hindered, and positional isomers of withdrawing/donating groups. The conditions should also be replicated in the presence of radical chlorine sources, to determine if this halogen exchange is compatible with other halogens.

Another project that should be explored is the ruthenium-catalysed homocoupling reaction shown in Scheme 3.11. Preliminary results show that base is required for the formation of product, however nucleophilic bases result in large amounts of nucleophilic substitution product at the benzylic position. As a result, conversions to homocoupled product are ~10%. It is possible that this reaction proceeds *via* an  $[(\eta^6\text{-4-methylbenzylbromide})\text{RuCp}^*]^+$  complex and the mechanism should be investigated.

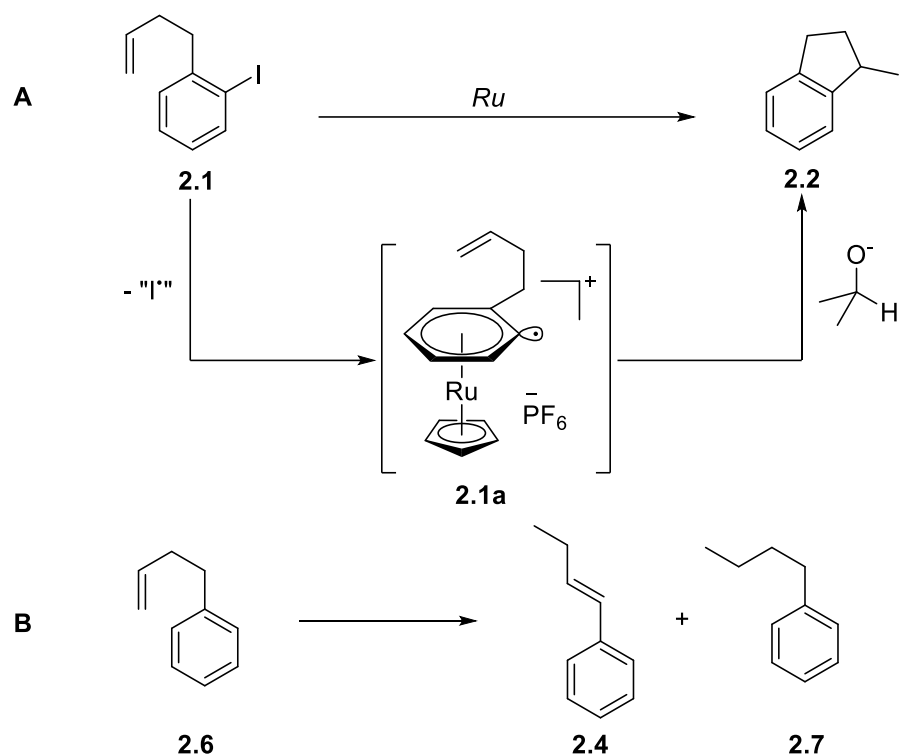


**Scheme 3.11** Ruthenium-catalysed  $C(sp^3)$ - $C(sp^3)$  homocoupling.

## 4. Conclusions and Future Work

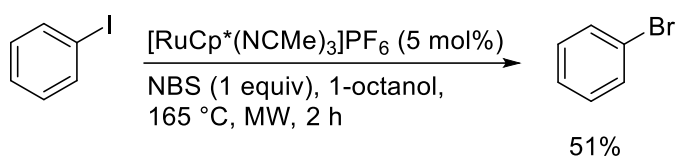
The overall aims of this project were to investigate the synthetic applicability of ruthenium  $\pi$ -arene complexes. The scarcity of reactions proceeding *via* arene exchange means that development of new processes offers significant advancements in synthetic chemistry, but an understanding of the mechanisms involved is important to help develop this area.

The project was initiated with the development of an intramolecular radical cyclisation reaction in Chapter 2 (Scheme 4.1 A). Subjecting aryl iodide **2.1** to hydrodeiodination conditions resulted in the formation of cyclised product **2.2**, albeit in low yield. Further optimisations, namely with 1,4-butanediol as solvent, resulted in a maximum yield of just 8%. While this result did indicate the possibility of radical intermediates, investigations into the by-products revealed that significant amounts of alkene isomerisation and hydrogenation was also occurring. Synthesis of 4-phenylbut-1-ene (**2.6**) and reaction under cyclisation conditions resulted in a 33% conversion to isomerised product (**2.4**), in which the alkene shifts to the most thermodynamically stable position next to the arene, and 45% conversion to hydrogenated product (**2.7**) in 5 minutes (Scheme 4.2 B). This indicates a significant deactivation of starting material towards cyclisation. Preliminary data suggests that incorporating dimethyl substitutions on the aliphatic tether reduces isomerisation, but has no effect on hydrogenation, whereas trisubstituted alkenes are relatively resistant to both processes. Future work of this project should focus on suppressing these side reactions, allowing radical cyclisation to be the dominant process.



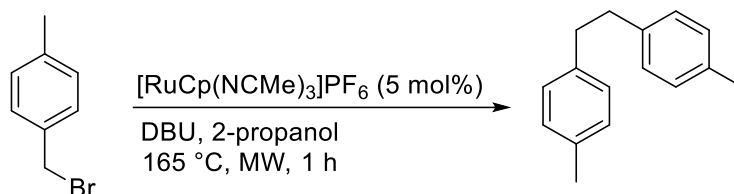
**Scheme 4.1** *A* Ruthenium-catalysed intramolecular radical cyclisation. *B* Ruthenium-catalysed alkene isomerisation and hydrogenation.

Chapter 3 focused on the exploration of a ruthenium-catalysed halogen exchange reaction. N-bromosuccinimide, which is a source of bromine for radical bromination, was hypothesised to react with the proposed aryl radical intermediates that are produced in hydrodeiodination reactions. Optimisations were carried out, with 1-octanol and  $[\text{RuCp}^*]^+$  catalyst at 165 °C returning the best conversions, resulting in a moderate yield of 51% (Scheme 4.2). Initially believed to be proceeding *via* an arene exchange mechanism similar to hydrodeiodination, mechanistic investigation revealed the possibility of an oxidative addition/reductive elimination or  $\text{S}_{\text{N}}\text{Ar}$  type-reaction. Further work of this project should focus on determining the reaction mechanism, and potentially designing a catalyst that allows halogen exchange at lower temperatures. For example, a dramatic increase in reaction conversion was observed in going from a Cp ligand to a Cp\* ligand at Ru. It is feasible that further changes to the sterics and electronics of this ligand could lead to improved reactivity.



**Scheme 4.2** *Optimised conditions for the halogen exchange of iodobenzene to bromobenzene.*

The potential for  $\pi$ -arene complexes to undergo reactions at benzylic positions has previously been discussed in Section 1.1.1. An unexpected result from halogen exchange experiments was the formation of 1,2-di-*p*-tolylethane as shown in Scheme 4.3. Further study is required to achieve considerable yields, as the required presence of base also reacts at the benzylic position. Although mechanistic detail is unknown, if the reaction proceeds *via*  $\eta^6$ -coordinated intermediates it would offer another entry to the relatively empty library of  $\pi$ -arene intermediate reactions.



**Scheme 4.3** Ruthenium-catalyzed homocoupling of 4-methylbenzyl bromide.

The alteration of arene properties on binding to ruthenium presents exciting opportunities to exploit arene-exchange-type mechanisms. The vast majority of literature procedures rely on stoichiometric metal activator. However, if catalytic reactions can be developed then the efficiency of these reactions would be greatly improved. To achieve this, a better understanding of the factors that lead to catalytic processes is needed. This study has shown some development in new catalytic reactions potentially occurring *via*  $\pi$ -arene complexes, however mechanistic details of the reactions discussed remain somewhat unclear. With further development in this area there is a great opportunity to produce efficient and novel transformations in the future.



# 5. Experimental

## 5.1 Experimental Procedures

### 5.1.1 General Procedures

Commercially available reagents were purchased from Sigma Aldrich UK and Fluorochem and were used without further purification. Solvents were laboratory grade or dried by the Durham University SPS service. Dried solvents were stored over activated 3 Å molecular sieves. Reactions requiring anhydrous conditions were carried out under an atmosphere of dry argon or nitrogen using Schlenk-line techniques. Where appropriate, solvents were sparged with argon or degassed using the freeze-pump-thaw cycle method. Thin-layer chromatography was carried out on silica plates (Merck 5554) and visualised under UV (254/365 nm).

NMR spectra (<sup>1</sup>H, <sup>13</sup>C, <sup>19</sup>F, <sup>31</sup>P) were recorded on a Varian VXR-400 spectrometer (<sup>1</sup>H at 399.97 Hz, <sup>13</sup>C at 100.57 MHz, <sup>19</sup>F at 76.50 MHz, <sup>31</sup>P at 164.98 MHz) or a Varian VNMRs-700 spectrometer (<sup>1</sup>H at 699.73 MHz, <sup>13</sup>C at 175.95 MHz, <sup>31</sup>P at 150.50 MHz). Spectra were recorded at 295 K in commercially available deuterated solvents and referenced internally to the residual solvent proton resonances.

Electrospray and high-resolution mass spectrometry were performed on a TQD with Acquity UPLC (Waters Ltd, UK) using MeCN as the carrier solvent. GCMS was performed on a Shimadzu QP2010-Ultra with MeOH or CH<sub>2</sub>Cl<sub>2</sub> as the carrier solvent.

## 5.2 Synthetic Procedures

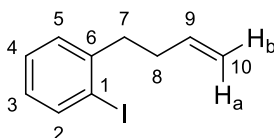
### *General Procedure for the cyclisation of 4-(2-iodobenzene)but-1-ene*

A 0.5 – 2 mL microwave vial purged under argon/nitrogen atmosphere was charged with 4-(2-iodobenzene)but-1-ene (44.5 mg, 0.172 mmol) and *ruthenium catalyst*. To this was added dry, degassed *solvent* (1 mL) and *base* and the vial was sealed and further purged with argon/nitrogen for 5 minutes before. The vial was transferred to the microwave reactor and heated at the specified temperature for the specified time. The reaction mixture was then dropped into diethyl ether (15 mL) and washed with water (3 x 10 mL). The organic layer was dried over magnesium sulphate and filtered before removing solvent under vacuum. To the residue was added DMF (10 µL) and CDCl<sub>3</sub> (0.8 mL) and the solution was transferred

to an NMR tube for analysis. Yields were calculated by integral comparison of DMF and product.

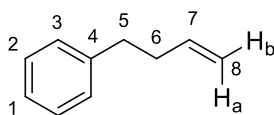
#### *General Procedure for the halogen exchange optimisation of iodobenzene*

A 0.5 – 2 mL microwave vial purged under argon/nitrogen atmosphere was charged with iodobenzene (38.7  $\mu$ L, 70.8 mg, 0.347 mmol), N-bromosuccinimide and *ruthenium* catalyst. To this was added dry, degassed *solvent* (1 mL) and DBU and the vial was sealed and further purged with argon/nitrogen. The vial was transferred to the microwave reactor and heated at the specified temperature for the specified time. Conversions were calculated by integral comparison of starting material and product, accounting for any by-products formed.



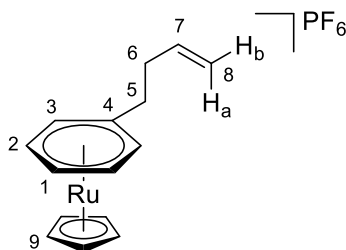
#### *4-(2-iodobenzene)but-1-ene 2.1*

A solution of allylmagnesium bromide in Et<sub>2</sub>O (6.7 mL, 1.0 M, 6.7 mmol) was added slowly to a stirred solution of 2-iodobenzyl bromide (0.9906 g, 3.39 mmol) in dry THF (6.7 mL) at 0 °C. After 15 minutes, the reaction was warmed to room temperature and stirred for an additional 3 hours. The reaction was quenched with sat. NH<sub>4</sub>Cl solution and extracted with CH<sub>2</sub>Cl<sub>2</sub>, dried over MgSO<sub>4</sub>, filtered, concentrated and purified over silica gel chromatography (hexanes, R<sub>f</sub> = 0.55) to yield *title compound* as a colourless oil (0.6227 g, 2.41 mmol). The product is spectroscopically identical to the known 2-(3'-butenyl)-1-iodobenzene.<sup>83</sup>  $\delta_{\text{H}}$  (CDCl<sub>3</sub>) 7.81 (dd,  $J$  = 7.9, 1.3 Hz, 1H, H<sup>2</sup>), 7.29 – 7.23 (m, 1H, H<sup>4</sup>), 7.20 (dd,  $J$  = 7.6, 1.7 Hz, 1H, H<sup>5</sup>), 6.89 – 6.85 (m, 1H, H<sup>3</sup>), 5.89 (ddt,  $J$  = 17.0, 10.2, 6.6 Hz, 1H, H<sup>9</sup>), 5.07 (dq,  $J$  = 17.0, 1.7 Hz, 1H, H<sup>10a</sup>), 5.00 (ddt,  $J$  = 10.2, 1.7, 1.3 Hz, H<sup>10b</sup>), 2.86–2.76 (m, 2H, H<sup>7</sup>), 2.34 (dt,  $J$  = 9.4, 6.6, 1.3 Hz, 2H, H<sup>8</sup>).



#### 4-phenylbut-1-ene **2.6**

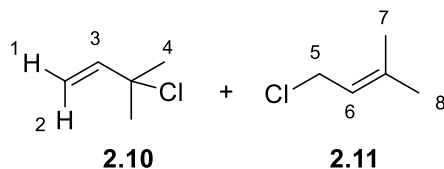
A solution of allylmagnesium bromide in Et<sub>2</sub>O (7.6 mL, 1.0 M, 7.6 mmol) was added slowly to a stirred solution of 2-iodobenzyl bromide (0.6386g, 3.73 mmol) in dry THF (7.6 mL) at 0 °C. After 15 minutes, the reaction was warmed to room temperature and stirred for an additional 3 hours. The reaction was quenched with sat. NH<sub>4</sub>Cl solution and extracted with CH<sub>2</sub>Cl<sub>2</sub>, dried over MgSO<sub>4</sub>, filtered, concentrated and purified over silica gel chromatography (hexanes, R<sub>f</sub> = 0.56) to yield *title compound* as a colourless oil (350.7 mg, 71%). The product is spectroscopically identical to the known 4-phenylbut-1-ene.<sup>84</sup>  $\delta_{\text{H}}$  (CDCl<sub>3</sub>) 7.31 – 7.27 (m, 2H, H<sup>2</sup>), 7.22 – 7.18 (m, 3H, H<sup>1,3</sup>), 5.88 (ddt,  $J = 17.0, 10.2, 6.6$  Hz, 1H, H<sup>7</sup>), 5.06 (dq,  $J = 17.0, 2.0$  Hz, 1H, H<sup>8a</sup>), 4.99 (ddt,  $J = 10.2, 2.0, 1.3$  Hz, H<sup>8b</sup>), 2.72 (d,  $J = 8.9, 6.8$  2H, H<sup>5</sup>), 2.43 – 2.34 (m, 2H, H<sup>6</sup>).



#### [Ru(η<sup>6</sup>-4-phenylbut-1-ene)(η<sup>5</sup>-cyclopentadienyl)]PF<sub>6</sub> **2.9**

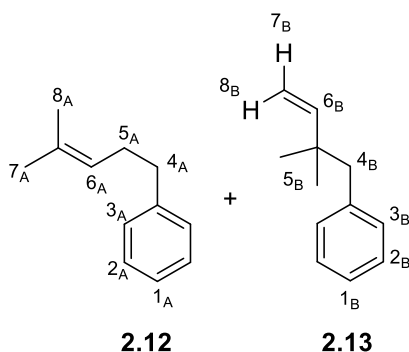
An oven-dried Schlenk tube charged with 4-phenylbut-1-ene (18.3 mg, 0.139 mmol) and [RuCp(NCMe)<sub>3</sub>]PF<sub>6</sub> (49.3 mg, 0.114 mmol) was purged with argon for 10 minutes. To this was added 1,2-dichloroethane (3 mL) and the resulting solution was heated to reflux for 18 hours, allowed to cool to room temperature and filtered. The filtrate was concentrated in vacuo to yield a dark brown residue which was dissolved in minimal MeCN and added dropwise to Et<sub>2</sub>O. The precipitate was triturated in Et<sub>2</sub>O, solvent removed and dried under vacuum to give *title compound* as an off-white solid (44.8 mg, 89%).  $\delta_{\text{H}}$  (acetone-D<sub>6</sub>) 6.38 – 6.34 (m, 2H, H<sup>3</sup>), 6.32 – 6.28 (m, 2H, H<sup>2</sup>), 6.28 – 6.24 (m, 1H, H<sup>1</sup>), 5.87 (ddt,  $J = 17.1, 10.3, 6.6$  Hz, 1H, H<sup>7</sup>), 5.51 (s, 5H), 5.06 (dq,  $J = 17.1, 1.8$  Hz, 1H, H<sup>8a</sup>), 5.01 (ddt,  $J = 10.2, 1.8, 1.3$  Hz, 1H, H<sup>8b</sup>), 2.74 – 2.69 (m, 2H, H<sup>5</sup>), 2.42 (tdt,  $J = 7.9, 6.6, 1.3$  Hz, 2H, H<sup>6</sup>);  $\delta_{\text{C}}$  (acetone-D<sub>6</sub>) 136.60 (s, 1C, C<sup>7</sup>), 115.66 (s, 1C, C<sup>8</sup>), 106.21 (s, 1C, C<sup>4</sup>), 86.77 (s, 2C, C<sup>3</sup>),

85.48 (s, 2C, C<sup>2</sup>), 84.93 (s, 1C, C<sup>1</sup>), 80.47 (s, 5C, C<sup>9</sup>), 34.91 (s, 1C, C<sup>6</sup>), 33.45 (s, 1C, C<sup>5</sup>);  $\delta_P$  (acetone-D<sub>6</sub>) -144.3 (sept.,  $J = 709$  Hz);  $\delta_F$  (acetone-D<sub>6</sub>) -71.6 (d,  $J = 709$  Hz);  $m/z$  (HR-ESI<sup>+</sup>) 293.0417 [M-PF<sub>6</sub>]<sup>+</sup> (C<sub>15</sub>H<sub>16</sub>I<sup>96</sup>Ru requires 293.0406).



*3-chloro-3-methyl-but-1-ene* **2.10** and *3,3-dimethylallylchloride* **2.11**

To a solution of hydrochloric acid (10 mL, 9.2 M) was added 2-methyl-3-buten-2-ol (2 mL) and stirred for 15 minutes. The mixture was then transferred to a separatory funnel and the lower acidic layer was separated. The organic phase was washed with water (3 x 5 mL), sat. NaHCO<sub>3</sub> solution (5 mL) and finally brine (5 mL). The compound was collected and stored over 3 Å molecular sieves without further purification. The product is spectroscopically identical to the known 3-chloro-3-methyl-but-1-ene and 3,3-dimethylallylchloride.<sup>85</sup> **2.10**  $\delta_H$  (CDCl<sub>3</sub>) 6.11 (dd,  $J = 17.2, 10.5$  Hz, 1H, H<sup>3</sup>), 5.24 (d,  $J = 17.2$  Hz, 1H, H<sup>2</sup>), 5.05 (d,  $J = 10.5$  Hz, 1H, H<sup>1</sup>), 1.71 (s, 6H, H<sup>4</sup>). **2.11**  $\delta_H$  (CDCl<sub>3</sub>) 5.46 (tt,  $J = 8.0, 1.4$  Hz, 1H, H<sup>6</sup>), 4.10 (d,  $J = 8.0$  Hz, 2H, H<sup>5</sup>), 1.79 (s, 3H, H<sup>7</sup>), 1.74 (d,  $J = 1.4$  Hz, 3H, H<sup>8</sup>).

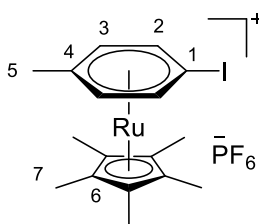


(2,2-Dimethylbut-3-en-1-yl)benzene **2.13** and (4-methylpent-3-en-1-yl)benzene **2.12**

A two-neck round-bottom flask was charged with magnesium turnings (0.275 g, 11.3 mmol) and dried under vacuum with a heat gun. Dry THF (5 mL) was added to the round-bottom flask and the mixture was cooled to 0 °C. A solution of a mixture of 3-chloro-3-methyl-but-1-ene **2.10** and 3,3-dimethylallylchloride **2.11** (1.314 g, 12.6 mmol) in dry THF (2.5 mL)

was added dropwise over 20 minutes and the resulting solution was warmed to room temperature and stirred for 3 hours. A solution of 2-iodobenzyl bromide (1.042 g, 3.51 mmol) in dry THF (6.5 mL) was added slowly to the solution at 0 °C and then the solution was warmed to room temperature and stirred for 18 hours. The reaction was quenched with sat. NH<sub>4</sub>Cl solution and extracted with CH<sub>2</sub>Cl<sub>2</sub>, dried over MgSO<sub>4</sub>, filtered, concentrated and purified over silica gel chromatography (hexanes, R<sub>f</sub> = 0.57) to yield a mixture of compounds **2.12** and **2.13** as a colourless oil (0.327 g, 58%). The product is spectroscopically identical to the known (4-methylpent-3-en-1-yl)benzene and (2,2-dimethylbut-3-en-1-yl)benzene.<sup>86</sup>

**2.12** δ<sub>H</sub> (CDCl<sub>3</sub>) 7.33 – 7.11 (m, 5H, H<sup>1A-3A</sup>), 5.20 (tdt, *J* = 7.1, 2.8, 1.4 Hz, 1H, H<sup>6A</sup>), 2.70 – 2.62 (m, 2H, H<sup>4A</sup>), 2.32 (q, *J* = 7.6 Hz, 2H, H<sup>5A</sup>), 1.72 (s, 3H, H<sup>8A</sup>), 1.59 (s, 3H, H<sup>7A</sup>). **2.13** δ<sub>H</sub> (CDCl<sub>3</sub>) 7.33 – 7.11 (m, 5H, H<sup>1B-3B</sup>), 5.89 (dd, *J* = 17.5, 10.7 Hz, 1H, H<sup>6B</sup>), 4.94 (dd, *J* = 10.7, 1.4 Hz, 1H, H<sup>7B</sup>), 4.88 (dd, *J* = 17.5, 1.4 Hz, 1H, H<sup>8B</sup>), 2.61 (s, 2H, H<sup>4B</sup>), 1.02 (s, 6H, H<sup>5B</sup>).



*[Ru(η<sup>6</sup>-4-iodotoluene)(η<sup>5</sup>-pentamethylcyclopentadienyl)]PF<sub>6</sub> 3.2*

RuCl<sub>3</sub>·3H<sub>2</sub>O (0.2507 g, 0.959 mmol) was added to a Schlenk flask containing degassed EtOH (10 mL) and heated to reflux for 30 minutes. 4-iodotoluene (0.4285 g, 1.97 mmol) and 1,2,3,4,5-pentamethylcyclopentadiene (0.3 mL, 0.261 g, 1.92 mmol) were added to the solution and refluxed for 15 hours. The reaction solution was cooled to room temperature and then a 1:1 mixture of Et<sub>2</sub>O and water was added to the Schlenk flask and then transferred to a separatory funnel. The aqueous layer was extracted and washed with Et<sub>2</sub>O (3 x 5 mL) and the organic layer was washed with water (3 x 5 mL). To the combined aqueous layers, an aqueous 0.3M solution of NH<sub>4</sub>PF<sub>6</sub> was added slowly, giving a brown precipitate which was collected by filtration. The precipitate was dried under vacuum and dissolved in minimal MeCN. The MeCN solution was added dropwise to Et<sub>2</sub>O and a brown precipitate formed. The precipitate was washed 3 times with Et<sub>2</sub>O and then dried under vacuum leaving a brown solid (0.3027 g, 0.505 mmol, 53%). δ<sub>H</sub> (acetone-D<sub>6</sub>) 6.40 (d, *J* = 6.2 Hz, 2H, H<sup>2</sup>), 5.90 (d, *J* = 6.2 Hz, 2H, H<sup>3</sup>), 2.27 (s, 3H, H<sup>5</sup>), 1.99 (s, 15H, H<sup>7</sup>) ; δ<sub>C</sub> (acetone-D<sub>6</sub>) 100.77 (s, 1C, C<sup>4</sup>),

96.83 (s, 5C, C<sup>6</sup>), 95.35 (s, 2C, C<sup>2</sup>), 89.09 (s, 2C, C<sup>3</sup>), 57.00 (s, 1C, C<sup>1</sup>), 17.18 (s, 1C, C<sup>5</sup>), 8.91 (s, 5C, C<sup>7</sup>);  $\delta_{\text{P}}$  (acetone-D<sub>6</sub>) -144.3 (sept., J = 709 Hz);  $\delta_{\text{F}}$  (acetone-D<sub>6</sub>) -71.6 (d, J = 708 Hz);  $m/z$  (HR-ESI<sup>+</sup>) 448.9851 [M-PF<sub>6</sub>]<sup>+</sup> (C<sub>17</sub>H<sub>22</sub>I<sup>96</sup>RuI requires 448.9842); Anal. Found (Expected): C 35.49 (34.07); H 3.87 (3.70); N -0.01 (0.00).

## 6. References

- 1 J. Okuda, *Eur. J. Inorg. Chem.*, 2017, **2017**, 217–219.
- 2 G. Wilkinson, M. Rosenblum, M. C. Whiting and R. B. Woodward, *J. Am. Chem. Soc.*, 1952, **74**, 2125–2126.
- 3 E. O. Fischer and W. Pfab, *Zeitschrift für Naturforsch. - Sect. B J. Chem. Sci.*, 1952, **7**, 377–379.
- 4 T. J. Kealy and P. L. Pauson, *Nature*, 1951, **168**, 1039–1040.
- 5 A. Miller, J. A. Tebboth and F. Tremaine, *J. Chem. Soc.*, 1952, 632–635.
- 6 T. J. Colacot and N. S. Hosmane, *Zeitschrift für Anorg. und Allg. Chemie*, 2005, **631**, 2659–2668.
- 7 A. R. Pape, K. P. Kaliappan and E. P. Kündig, *Chem. Rev.*, 2000, **100**, 2917–2940.
- 8 E. O. Fischer and W. Hafner, *Zeitschrift für Naturforsch. - Sect. B J. Chem. Sci.*, 1955, **10**, 665–668.
- 9 E. P. Kundig, in *Transition Metal Arene  $\pi$ -Complexes in Organic Synthesis and Catalysis*, 2004.
- 10 D. A. Brown, *J. Chem. Soc.*, 1966, 4455–4460.
- 11 G. I. McGrew, J. Temaismithi, P. J. Carroll and P. J. Walsh, *Angew. Chem. Int. Ed.*, 2010, **49**, 5541–5544.
- 12 G. I. McGrew, C. Stanciu, J. Zhang, P. J. Carroll, S. D. Dreher and P. J. Walsh, *Angew. Chem. Int. Ed.*, 2012, **51**, 11510–11513.
- 13 M. Lafrance, C. N. Rowley, T. K. Woo and K. Fagnou, *J. Am. Chem. Soc.*, 2006, **128**, 8754–8756.
- 14 P. Ricci, K. Krämer, X. C. Cambeiro and I. Larrosa, *J. Am. Chem. Soc.*, 2013, **135**, 13258–13261.
- 15 P. Ricci, K. Krämer and I. Larrosa, *J. Am. Chem. Soc.*, 2014, **136**, 18082–18086.
- 16 A. J. Pearson and K. Lee, *J. Org. Chem.*, 1994, **59**, 2304–2313.
- 17 L. A. Wilkinson, J. A. Pike and J. W. Walton, *Organometallics*, 2017, **36**, 4376–4381.
- 18 E. M. D'Amato, C. N. Neumann and T. Ritter, *Organometallics*, 2015, **34**, 4626–4631.
- 19 M. Rosillo, G. Domínguez and J. Pérez-Castells, *Chem. Soc. Rev.*, 2007, **36**, 1589–1604.
- 20 M. F. Semmelhack, H. T. Hall, R. Farina, M. Yoshifuji, G. Clark, T. Bargar, K. Hirotsu and J. Clardy, *J. Am. Chem. Soc.*, 1979, **101**, 3535–3544.

- 21 D. Whitaker, M. Batuecas, P. Ricci and I. Larrosa, *Chem. Eur. J.*, 2017, **23**, 12763–12766.
- 22 J. A. Pike and J. W. Walton, *Chem. Commun.*, 2017, **53**, 9858–9861.
- 23 M. H. Beyzavi, D. Mandal, M. G. Strebl, C. N. Neumann, E. M. D’Amato, J. Chen, J. M. Hooker and T. Ritter, *ACS Cent. Sci.*, 2017, **3**, 944–948.
- 24 J. S. Fowler and A. P. Wolf, *Acc. Chem. Res.*, 1997, **30**, 181–188.
- 25 F. Rose-Munch, R. Chavignon, J. P. Tranchier, V. Gagliardini and E. Rose, *Inorganica Chim. Acta*, 2000, **300–302**, 693–697.
- 26 M. F. Semmelhack, J. Bisaha and M. Czarny, *J. Am. Chem. Soc.*, 1979, **101**, 768–770.
- 27 G. R. Knox, D. G. Leppard, P. L. Pauson and W. E. Watts, *J. Organomet. Chem.*, 1971, **34**, 347–352.
- 28 M. F. Semmelhack, W. Seufert and L. Keller, *J. Am. Chem. Soc.*, 1980, **102**, 6584–6586.
- 29 A. J. Pearson, J. G. Park, S. H. Yang and Y.-H. Chuang, *J. Chem. Soc. Chem. Commun.*, 1989, **2**, 1363–1364.
- 30 R. G. Sutherland, A. Piorko, U. S. Gill and C. C. Lee, *J. Heterocycl. Chem.*, 1982, **19**, 801–803.
- 31 J. W. Janetka and D. H. Rich, *J. Am. Chem. Soc.*, 1997, **119**, 6488–6495.
- 32 Y. K. Chung, H. S. Choi, D. A. Sweigart and N. G. Connelly, *J. Am. Chem. Soc.*, 1982, **104**, 4245–4247.
- 33 W. H. Miles, P. M. Smiley and H. R. Brinkman, *J. Chem. Soc. Chem. Commun.*, 1989, **1897**, 1897–1899.
- 34 J. P. Djukic, P. Geysmans, F. Rose-Munch and E. Rose, *Tetrahedron Lett.*, 1991, **32**, 6703–6704.
- 35 J. P. Djukic, F. Rose-Munch, E. Rose, F. Simon and Y. Dromzee, *Organometallics*, 1995, **14**, 2027–2038.
- 36 M. F. Semmelhack, A. Chlenov and D. M. Ho, *J. Am. Chem. Soc.*, 2005, **127**, 7759–7773.
- 37 T. G. Traylor and K. Stewart, *Organometallics*, 1984, **3**, 325–327.
- 38 T. G. Traylor, K. J. Stewart and M. J. Goldberg, *J. Am. Chem. Soc.*, 1984, **106**, 4445–4454.
- 39 T. G. Traylor, K. J. Stewart and M. J. Goldberg, *Organometallics*, 1986, **5**, 2062–2067.
- 40 J. W. Walton and J. M. J. Williams, *Chem. Commun.*, 2015, **51**, 2786–2789.
- 41 C. A. L. Mahaffy and P. L. Pauson, *J. Chem. Res. Synopsys*, 1979, **126**, 1752–1775.



- 42 R. P. Houghton and M. Voyle, *J. Chem. Soc. Chem. Commun.*, 1980, 884–885.
- 43 R. P. Houghton, M. Voyle and R. Price, *J. Chem. Soc. Perkin Trans. 1*, 1984, 925–931.
- 44 M. Otsuka, K. Endo and T. Shibata, *Chem. Commun.*, 2010, **46**, 336–338.
- 45 M. Otsuka, H. Yokoyama, K. Endo and T. Shibata, *Synlett*, 2010, 2601–2606.
- 46 T. M. Koenig and D. Mitchell, *Tetrahedron Lett.*, 1994, **35**, 1339–1342.
- 47 A. I. Konovalov, E. O. Gorbacheva, F. M. Miloserdov and V. V. Grushin, *Chem. Commun.*, 2015, **51**, 13527–13530.
- 48 J. A. Pike, D. Bradley, A. W. Mcneillis, N. O. Driscoll, A. Wilkinson and J. W. Walton, *Catalysis via  $\pi$ -Arene Intermediates: a Radical Hydrodeiodination*, 2019.
- 49 C. A. Merlic, M. M. Miller, B. N. Hietbrink and K. N. Houk, *J. Am. Chem. Soc.*, 2001, **123**, 4904–4918.
- 50 D. P. Curran and D. M. Rakiewicz, *J. Am. Chem. Soc.*, 1985, **107**, 1448–1449.
- 51 H. Zhang, S. Ma, Z. Xing, L. Liu, B. Fang, X. Xie and X. She, *Org. Chem. Front.*, 2017, **4**, 2211–2215.
- 52 K. J. Romero, M. S. Galliher, D. A. Pratt and C. R. J. Stephenson, *Chem. Soc. Rev.*, 2018, **47**, 7851–7866.
- 53 A. Székely and M. Klussmann, *Asian J. Chem.*, 2019, **14**, 105–115.
- 54 X. L. Tang, Z. Wu, M. B. Li, Y. Gu and S. K. Tian, *Eur. J. Org. Chem.*, 2012, 4107–4109.
- 55 S. J. Connon and S. Blechert, *Angew. Chem. Int. Ed.*, 2003, **42**, 1900–1923.
- 56 C. S. G. Seo and R. H. Morris, *Organometallics*, 2019, **38**, 47–65.
- 57 R. Noyori and S. Hashiguchi, *Acc. Chem. Res.*, 1997, **30**, 97–102.
- 58 J. Field, C. K. Ingold and R. M. Beesley, *J. Chem. Soc.*, 1915, **105**, 1080–1106.
- 59 J. Hassan, M. Sévignon, C. Gozzi, E. Schulz and M. Lemaire, *Chem. Rev.*, 2002, **102**, 1359–1469.
- 60 S. M. Ametamey, M. Honer and P. A. Schubiger, *Chem. Rev.*, 2008, **108**, 1501–1516.
- 61 R. H. Seevers and R. E. Counsell, *Chem. Rev.*, 1982, **82**, 575–590.
- 62 K. F. Heck and J. P. Nolley, *J. Org. Chem.*, 1972, **37**, 2320–2322.
- 63 H. H. Hodgson, *Chem. Rev.*, 1947, **40**, 251–277.
- 64 G. A. Olah, *Acc. Chem. Res.*, 1971, **4**, 240–248.
- 65 J. Pan, X. Wang, Y. Zhang and S. L. Buchwald, *Org. Lett.*, 2011, **13**, 4974–4976.

- 66 N. Miyaura and A. Suzuki, *Chem. Rev.*, 1995, **95**, 2457–2483.
- 67 G. Evano, A. Nitelet, P. Thilmany and D. F. Dewez, *Front. Chem.*, 2018, **6**, 1–18.
- 68 T. D. Sheppard, *Org. Biomol. Chem.*, 2009, **7**, 1043–1052.
- 69 R. Cramer and D. R. Coulson, *J. Org. Chem.*, 1975, **40**, 2267–2273.
- 70 T. T. Tsou and J. K. Kochi, *J. Org. Chem.*, 1980, **45**, 1930–1937.
- 71 K. J. O'Connor and C. J. Burrows, *J. Org. Chem.*, 1991, **56**, 1344–1346.
- 72 K. J. Bonney, F. Proutiere and F. Schoenebeck, *Chem. Sci.*, 2013, **4**, 4434–4439.
- 73 X. Feng, Y. Qu, Y. Han, X. Yu, M. Bao and Y. Yamamoto, *Chem. Commun.*, 2012, **48**, 9468–9470.
- 74 J. S. Yadav, B. V. S. Reddy, P. S. R. Reddy, A. K. Basak and A. V. Narsaiah, *Adv. Synth. Catal.*, 2004, **346**, 77–82.
- 75 N. R. Champness, *Dalton Trans.*, 2011, **40**, 10311–10315.
- 76 M. C. Carreño, J. L. G. Ruano, G. Sanz, M. A. Toledo and A. Urbano, *J. Org. Chem.*, 1995, **60**, 5328–5331.
- 77 B. T. Loughrey, B. V. Cuning, P. C. Healy, C. L. Brown, P. G. Parsons and M. L. Williams, *Asian J. Chem.*, 2012, **7**, 112–121.
- 78 L. Ackermann, A. Althammer and R. Born, *Angew. Chem. Int. Ed.*, 2006, **45**, 2619–2622.
- 79 S. Oi, R. Funayama, T. Hattori and Y. Inoue, *Tetrahedron*, 2008, **64**, 6051–6059.
- 80 F. Kakiuchi, Y. Matsuura, S. Kan and N. Chatani, *J. Am. Chem. Soc.*, 2005, **127**, 5936–5945.
- 81 Y. Imazaki, E. Shirakawa, R. Ueno and T. Hayashi, *J. Am. Chem. Soc.*, 2012, **134**, 14760–14763.
- 82 A. Chandra, K. N. Parida and J. N. Moorthy, *Tetrahedron*, 2017, **73**, 5827–5832.
- 83 H. X. Zheng, X. H. Shan, J. P. Qu and Y. B. Kang, *Org. Lett.*, 2017, **19**, 5114–5117.
- 84 F. Weber, A. Schmidt, P. Röse, M. Fischer, O. Burghaus and G. Hilt, *Org. Lett.*, 2015, **17**, 2952–2955.
- 85 P. Schneider, R. Cloux, K. Foti and E. sz. Kovats, *Synthesis*, 1990, **1990**, 1027–1031.
- 86 Y. L. Lai and J. M. Huang, *Org. Lett.*, 2017, **19**, 2022–2025.